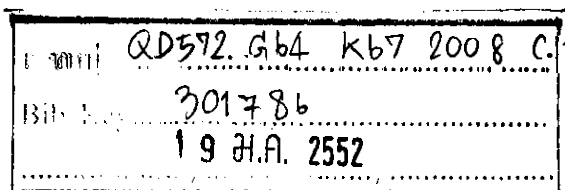**Development of Electrode for Biosensor**

Kosin Teeparuksapun

A Thesis Submitted in Partial Fulfillment of the Requirements

for the Degree of Master of Science in Analytical Chemistry

Prince of Songkla University

2008

Copyright of Prince of Songkla University

Thesis Title   Development of Electrode for Biosensor

Author   Mr. Kosin Teeparuksapun

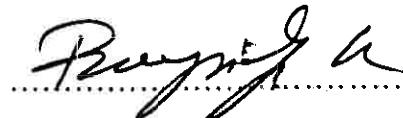**Major Program**   Analytical Chemistry

---

Major Advisor

....
(Assoc. Prof. Dr. Panote Thavarungkul)

Co-advisor

....
(Assoc. Prof. Dr. Proespichaya Kanatharana)

Examining Committee
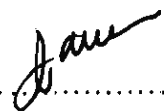
....Chairperson
(Assoc. Prof. Dr. Nongporn Towatana)

....Committee
(Assoc. Prof. Dr. Panote Thavarungkul)

....Committee
(Assoc. Prof. Dr. Proespichaya Kanatharana)

....Committee
(Miss Jaruwan Limsajjasakul)

       The Graduate School, Prince of Songkla University, has approved this thesis as partial fulfillment of the requirements for the Master of Science Degree in Analytical Chemistry

....
(Assoc. Prof. Dr. Krerkchai Thongnoo)
Dean of Graduate School

ชื่อวิทยานิพนธ์	การพัฒนาอิเล็กโทรคสำหรับไบโอเซนเซอร์
ผู้เขียน	นายโกสินทร์ ทีปรักษพันธ์
สาขาวิชา	เคมีวิเคราะห์
ปีการศึกษา	2550

บทคัดย่อ

งานวิจัยนี้ศึกษาการพัฒนาขั้วไฟฟ้าทอง (gold electrode) แบบฟิล์มบางโดยใช้ เทคนิค สปัตเตอริง (sputtering) และกระเหยด้วยความร้อน (thermal evaporation) เคลือบ โครเมียมและทองบนแผ่นสไลด์ขนาด 25.4 × 76.2 × 2.0 มิลลิเมตร สามารถใช้ขั้วไฟฟ้าที่พัฒนาขึ้น เป็นขั้วไฟฟ้าทำงานแบบใช้แล้วทิ้ง (disposable) โดยไม่ต้องมีขั้นตอนของการขัด ขั้วไฟฟ้าที่ได้จาก การพัฒนาด้วยเทคนิค สปัตเตอริงถูกตรึง (immobilized) ด้วยแอนติ โฮส เซลล์ โปรตีน (anti-host cell protein) โดยใช้เซลฟ- แอสเซมเบิลโมโนเลเยอร์ (Self-assembled monolayer) ของกรดไธออก ติก (thioctic acid) และนำไปทดสอบในระบบคาพาซิทีฟ อิมมูโนเซนเซอร์เบบไม่ติดฉลาก (label-free capacitive immunosensor) ได้ช่วงความเป็นเส้นตรง (linear dynamic range) 1.0×10^{-17} - 1.0×10^{-13} โมลาร์ โดยมีขีดจำกัดการตรวจวัด (detection limit) 8.0×10^{-18} โมลาร์ และใช้เวลาในการ วิเคราะห์ (analysis time) 15 นาที ขั้วไฟฟ้าทำงานนี้สามารถใช้งานได้ 25 ครั้งโดยมีค่าเบี่ยงเบน มาตรฐาน 4.9 เปอร์เซ็นต์ ระบบที่พัฒนาขึ้นให้ประสิทธิภาพในการนำไปวิเคราะห์หาปริมาณของ โฮส เซลล์ โปรตีน (host cell protein) ที่ตกค้างในกระบวนการผลิตเอนไซม์แลกเทท ดี ไฮโรจีเนส (Lactate Dehydrogenase) จากอีโคไล *(E coli)*.

ทดสอบขั้วไฟฟ้าทำงนที่พัฒนาขึ้น โดยใช้เทคนิคการระเหยด้วยความร้อนใน ระบบคาพาซิทีฟ อิมมูโนเซนเซอร์เบไม่ติดฉลากโดยใช้ แอนติ ฮิวแมน ซีรัม อัลบูมิน (anti-human serum albumin) และอัลบูมิน (albumin) เป็นคู่ทดสอบ ตรึงแอนติ ฮิวแมน ซีรัม อัลบูมินบน ชั้นฟิล์มบางที่ไม่นำไฟฟ้าของออร์โท-ฟีนิลีนไดเอมีน (o-phenylenediamine) ที่ได้จากการอิเล็กโทร โพลีเมอไรซ์เซชั่น (electropolymerization) โดยใช้พันธะ โควาเลนซ์ จากนั้นศึกษาสภาวะที่ เหมาะสมของระบบโฟลว์อินเจ็กชั่น ภายใต้ สภาวะที่เหมาะสมช่วงความเป็นเส้นตรงของระบบคือ 1.0×10^{-14} - 1.0×10^{-9} โมลาร์ โดยมีขีดจำกัดการตรวจวัดที่ 8.0×10^{-15} โมลาร์ และใช้เวลาในการ วิเคราะห์ 15 นาที ขั้วไฟฟ้าทำงน สมรถ ใช้งานได้ถึง 30 ครั้งโดยมีค่าเบี่ยงเบนมาตรฐาน 3.5 เปอร์เซนต์ ระบบที่พัฒนาขึ้นนี้สามารถนำไปใช้ในภาวิเคราะห์ปริมาณของอัลบูมินในตัวอย่าง ซีรัมคนเปรียบเทียบกับวิธีอัลบูมิน บีซีจี (albumin BCG method) จากการวิเคราะห์ พบว่า

ปริมาณของอัลบูมิน ในตัวอย่างที่ได้ จากการวิเคราะห์ด้วยเทคนิคคาพาซิทีฟอิมมูโนเซนเซอร์ ต่ำกว่าการวิเคราะห์ด้วยเทคนัค อิลบูมีน บีซีจ โดยมีเปอร์เซ็นตความตกต่างของการวิเคราะห์ 0.4 – 15.7 เปอร์เซนต์

Thesis Title   Development of Electrode for Biosensor

Author   Mr. Kosin Teeparuksapun

Major Program   Analytical chemistry

Academic year   2007

Abstract

Thin gold film electrodes were fabricated using sputtering and thermal evaporation techniques to coat chromium and gold on glass microscope slide (25.4 × 76.2 × 2.0 mm). These electrodes were used as disposable working electrodes in a label-free capacitive immunosensor system without any pretreatment steps. Sputtered gold electrode was immobilized with anti host cell protein (anti-HCP) via self-assembled thioctic acid monolyer and then tested in a label-free capacitive immunosensor system. A linear dynamic range was between 1.0×10^{-17} and 1.0×10^{-13} M with a detection limit of 8.0×10^{-18} M. Analysis time was 15 min. The regeneration of the binding capacity of the working electrode can be performed with good reproducibility (% RSD = 4.9) enabled the electrode to be reused up to 25 times. The system show good performance for the investigation of residual HCP impurity in the purification process of Lactate dehydrogenase (LDH) from *Escherichia coli (E. coli)*.

Thermally evaporated gold electrode was also tested in a label-free capacitive immunosensor system using anti human serum albumin (anti-HSA) and human serum albumin (HSA) as a model system. A thin layer of non-conducting *o*-phenylenediamine was electropolymerized onto the gold surface and was used for the immobilization of anti-HSA by covalent binding. In the flow injection mode, the parameter affecting to the performance of the system were optimized. Under optimum conditions, a linear dynamic range was between 1.0×10^{-14} to 1.0×10^{-9} M with the limit of detection 8.0×10^{-15} M. The analysis time was 15 min. The electrode can be reused up to 30 times (% RSD = 3.5). The developed system was applied for the determination of albumin in human serum samples. Concentration of albumin determine by capacitive immunosessor is lower than those obtained from Albumin BCG method. The difference between the two methods is 0.4-15.7 %.

Acknowledgements

The completion of this thesis would be impossible without the help of many people, whom I would like to thank.

I express my sincere thank to my advisors, Assoc. Prof. Dr. Panote Thavarungkul and Assoc. Prof. Dr. Proespichaya Kanatharana for their kindness, support, encouragement, advice and suggestions throughout the course of this work.

I would like to thank Prof. Bo Mattiasson, Dr. Martin Hedström, Dr. Marika Murto for their advice, help and support during my research at the Department of Biotechnology, Center for Chemistry and Chemical Engineering, Lund University, Lund, Sweden.

I would also like to thank Asst. Prof. Punnee Asawatreratanakul for her help and suggestion about the biochemistry knowledges.

Thanks are also sincerely express to:

The examination committee members of this thesis, for their valuable time;

Staffs of Clinical clinic Songklanakarind Hospital for their kind suggestions and for the human serum samples.

Staffs of the Department of Chemistry and the Department of Physics for their help in some technical aspects of this thesis;

Staffs of the Department of Biotechnology, Center for Chemistry and Chemical Engineering, Lund University, Lund, Sweden for their help;

The Development and Promotion of Science and Technology Talents Project (DPST), The Center for Innovation in Chemistry: Postgraduate Education and Research Program in Chemistry (PERCH-CIC), Commission on Higher Education, Ministry of Education for the scholarship;

PERCH-CIC and Graduate School, Prince of Songkla University for the partial support of the research fund;

The Swedish Research Council (VR) and The Swedish International Development and Cooperating Agency (SIDA) under the Asian-Swedish Research Links Programme for a grant supporting my research visit at the Department of Biotechnology, Lund University, Lund, Sweden;

My friends in the Trace Analysis and Biosensor Research Center who helped me in many ways;

My parents, family and Mr. Erich Steiner for all their love, understanding, support and encouragement.

Kosin Teeparuksapun

CONTENTS

CONTENTS (CONTINUED)

CONTENTS (CONTINUED)

CONTENTS (CONTINUED)

LIST OF TABLES

LIST OF FIGURES

LIST OF FIGURES (CONTINUED)

LIST OF FIGURES (CONTINUED)

LIST OF FIGURES (CONTINUED)

LIST OF FIGURES (CONTINUED)

CHAPTER 1

INTRODUCTION

1.1 Background and Rationale

Solid gold electrodes are currently in widespread use in both electro –
and bioanalysis (Bechera and Raj, 2007; Limbut *et al.*, 2006; Liu *et al.*, 2007;
Thavarungkul *et al.*, 2007), primarily because of its broad potential window, rich
surface chemistry and suitability for various sensing and detection application (Chen
and Li, 2006). It is also generally used as working electrode in the development of
electrochemical biosensors (Bechera and Raj, 2007; Limbut *et al.*, 2006; Liu *et al.*,
2007; Thavarungkul *et al.*, 2007).

To construct biosensors, before immobilization procedures of
biomolecules, the transducer surfaces must be carefully cleaned and pre-treated for
the coupling chemistries of immobilization. The properties of the gold electrode
substrate, especially surface topography and roughness, play an important role in the
properties of the resulting immobilization. Cleaning solid gold electrode surface is
frequently accomplished by repeated polishing with different particle sizes of alumina
slurry subsequently cleaned through sonication to remove any physisorbed multilayer
(Limbut *et al.*, 2006; Yang *et al.*, 1995), sometime subjected to electrochemical
treatment with H_2SO_4 and mounted in a Teflon electrode holder which restricted a
certain exposed area (Limbut *et al.*, 2006; Thavarungkul *et al.*, 2007). Once the
electrode with immobilized biomolecules has lost its activity, to be able to reuse,
these electrodes need to be oxidized with Piranha solution, followed by the
pretreatment steps as described previously. This sequence of treatments is
cumbersome. Moreover, even though alumina can be used successfully for the
polishing of gold surface, but there are problems created by additives in the alumina
preparations (Xu *et al.*, 2007) and it was reported that alumina can be caused of
cancer (Myoshi *et al.*, 2007). Therefore the use of alumina should be avoided. Due to
these drawbacks, an alternative inexpensive strategy to obtain a smooth surface
without polishing is of interest. One such strategy is to obtain a smooth thin gold film.

The fabrication of thin gold film has been proposed by several methods. Sputtering and thermal evaporation are two examples (Abdelmalek, 2002; Townsend *et al.*, 1976). These methods are based on the coating of gold on the surface of substrates. The thin gold film can be used as an electrode in both electroanalysis and biosensor. Because the thickness of the gold coated on the substrate is very thin, normally varies from micrometer (μm) to nanometer (nm). Therefore after used, the surface of electrode can't be polished. However, several electrodes can be fabricated at one time, and the film does not require a large amount of gold therefore the fabrication cost is not expensive. The electrodes can then be used as disposable electrodes and hence do not require any treatment steps neither before nor after the analysis. In this work electrodes fabricated by sputtering and thermal evaporation techniques will be tested in a capacitive immunosensor system that has been successfully applied for the determination of affinity binding in direct immunosensor (label-free) (Hedström *et al.*, 2005; Limbut *et al.*, 2006).

To construct a capacitive sensor the electrode surface with immobilized biomolecules needs to be totally insulated (Hedström *et al.*, 2005; Limbut *et al.*, 2006). Although immobilization via the formation of a self-assembled monolayer (SAM) of alkanethiol, such as thioctic acid, on the electrode surface can generally fulfill this requirement (Berggren and Johansson, 1997; Berggren *et al.*, 1998; Hedström *et al.*, 2005; Limbut *et al.*, 2006), the method is time-consuming since the completed adsorption of such compound on gold electrodes need several hours (Hedström *et al.*, 2006; Limbut *et al.*, 2006; Lu *et al.*, 2005). Therefore, another strategy to obtain an insulated layer such as electropolymerization of non-conducting polymer, that requires much less time, needs to be considered.

Ortho-phenylenediamines (*o*-PD) is a non-conducting polymer which has been widely used for the immobilization of biological element in biosensor technique (Garjonyte *et al.*, 2000; Yin *et al.*, 2002). The electropolymerization of *o*-PD will form a 1,4 substituted benzonoid-quinoid with free amino group expose on the backbone of the poly *o*-PD (Yano and Nagaoka, 1996). These free amino groups can be crossed-linking with glutaraldehyde (Curulli *et al.*, 1998; Myler *et al.*, 1997; Karalemas *et al.*, 2000) and provides biosensor with more stable performance and possible to apply for the immobilization of antibody in the capacitive immunosensor.

In this work thin gold film electrodes were fabricated using sputtering and thermal evaporation techniques. These electrodes were tested in a capacitive immunosensor system. Immobilization of biological molecules on the electrode surface was performed by the most often use method of self assembled monolayer (SAM). Electropolymerization of *o*-PD was also tested as an alternative technique for immobilization. Antibody to host cell protein (anti-HCP) and its antigen (HCP) was used as a model study to test the performance of sputtered gold electrodes and antibody to human serum albumin (anti-HSA) and its antigen (HSA) was used for thermally evaporated gold electrode.

1.2 Thin gold film electrodes

Two methods are generally applied to fabricate thin gold film electrodes, i.e. sputtering (Kelly and Arnell, 2000; Pierson *et al.*, 2005; Sangpour *et al.*, 2007; Townsend *et al.*, 1976) and thermal evaporation (Gizeli *et al.*, 2003; Lund *et al.*, 2006; Spadavecchia *et al.*, 2005; Xu *et al.*, 2006).

1.2.1 Sputtering

Sputtering is a vacuum evaporation process which physically removes portions of a coating material called target, and deposits a thin film, firmly bound onto an adjacent surface call the substrate (Figure 1.1). The process occurs by bombarding the surface of the sputtering target with gaseous ions under high voltage acceleration. As these ions collide with the target, atoms or occasionally entire molecules of the target material are ejected and propelled against the substrate, where they form a very tight bond (Behrisch, 1981; Rossnagel, 1995; Townsend *et al.*, 1976).

Sputtering has proven to be a successful method of coating a variety of substrates with thin film of electrically conductive or non-conductive materials (Odeh, 2008; Vanderstraeten, 1998). One of the most striking characteristics of sputtering is its universality. Since the coating material is passed into the vapor phase by mechanical rather than a chemical or thermal process, virtually any material can be deposited (Chung-Lee *et al.*, 2007; Delong, 2000). The coating of gold on substrate by this technique needs an adhesion layer. This is because a thin gold film when directly coated on a substrate can very easily be peeled off during immobilization or

electrochemical measurement. Ti and Pd have been used as the adhesion layer
(Rehacek *et al.*, 1998), but Cr was the most use since it provides strong bond to gold
(Ghalichechian *et al.*, 2007; Wang *et al.*, 2005).
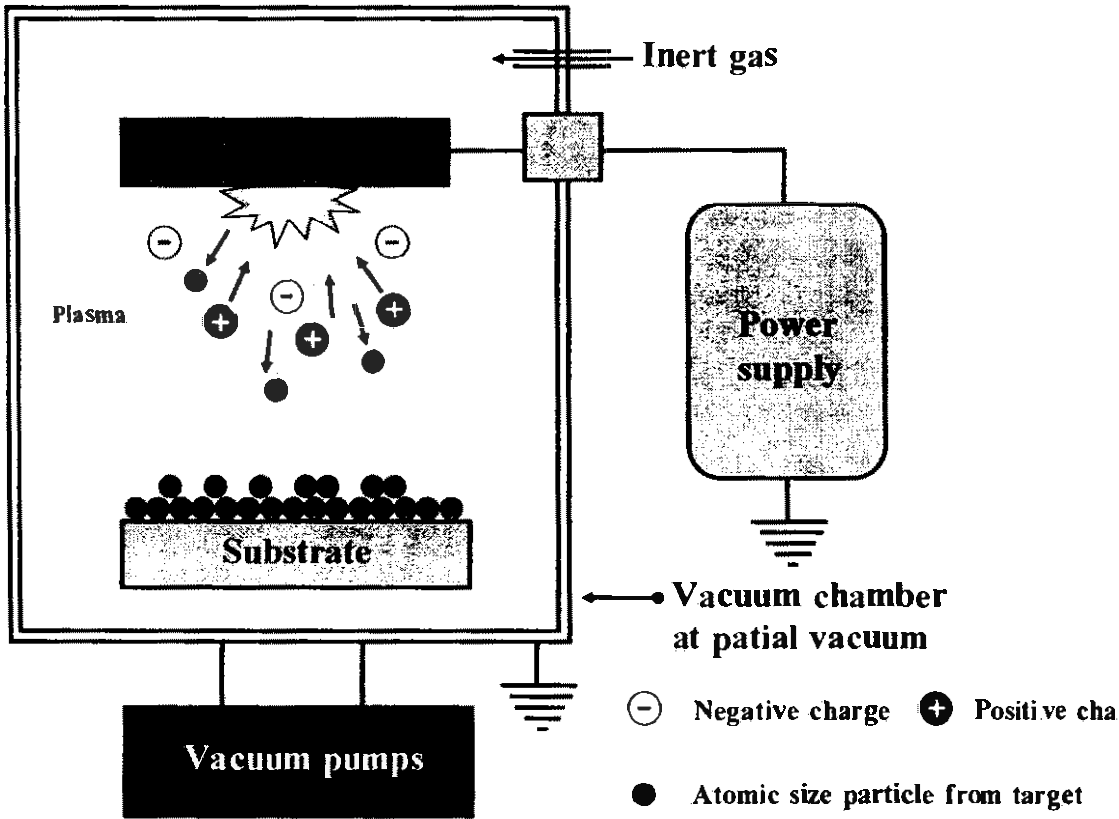
Figure 1.1 Shematic diagram showing a sputtering process. Substrates are placed into
the vacuum chamber, and is pumped down to the process pressure.
Negative charge is applied to the target material causing plasma. Positive
charged gas ions generated in the plasma region are attracted to the
negative biased target plate at a very high speed. This collision creates a
momentum transfer and ejects atomic size particles from the target. These
particles traverse the chamber and are deposited as a thin film onto the
surface of the substrates.

1.2.2 Thermal evaporation

Thermal evaporation consists of vaporising a solid material (pure metal, eutectic or compound) by heating it to a sufficiently high temperature and recondensing it onto a cooler substrate to form a thin film (Basha, 1998; Dai *et al.*, 2003; Nemetschek *et al.*, 2002) (Figure 1.2). As the name implies, the heating is carried out by passing a large current through a filament container (usually in the shape of a basket, boat or crucible) which has a finite electrical resistance. The choice of this filament material is dictated by the evaporation temperature and its inertness to alloying/chemical reaction with the evaporant. Usually, the chamber is pumped to 10^{-6} mB background pressure (Jedrzejewska-Szczerska *et al.*, 2008; Zhang *et al.*, 2007). During deposition, the distance between the sources and the substrate which is in the range of several ten centimeters sets the scale for the required mean free path. To control the film composition the evaporation rates have to be online monitored individually by some kind of sensor heads (Barsha, 1998).

The fabrication of thin gold film electrode is always performed by coating chromium (Cr) as a first layer and then gold is deposited. Different thickness of chromium layer have been applied such as 2 nm (Spadavecchia *et al.*, 2005; Xu *et al.*, 2006), 5 nm (Lund *et al.*, 2006) and 10 nm (Gizeli *et al.*, 2003) and different thickness of gold, 35 nm (Lund *et al.*, 2006), 50 nm (Spadavecchia *et al.*, 2005; Xu *et al.*, 2006) and 200 nm (Gizeli *et al.*, 2003). The appropriate thickness of gold film depends on its applications. As an electrode, 200 nm have been proposed (Choi *et al.*, 2004; Zhang *et al.*, 2000).

Glass bell jar

Substrate table

Crystal detector

Substrate holder
and sample

Path of vapour

Clamps connected to
high current source

Filament boat filled
with evaporant

High vacuum created by
diffusion pump back by rotary pump
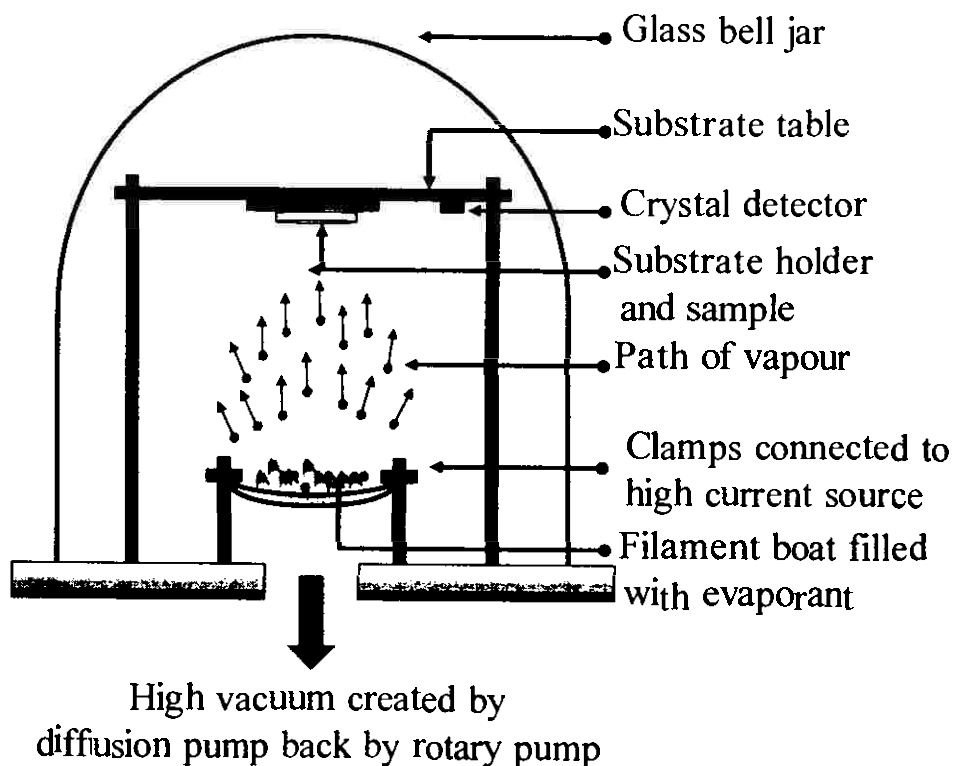
Figure 1.2 Schematic diagram of a thermal evaporation system. Solid material is heated to a sufficiently high temperature and recondensed onto a cooler substrate to form a thin film.

1.2.3 Application of thin gold film electrodes

Thin gold film electrodes have been applied in several applications. Sputtering technique has been used for the coating of gold film on silicon wafer (Hurley and Gamble, 2003; Rehacek et al., 1998) and glass (Pierson et al., 2005). Thin gold film fabricated by this technique have been widely used in biosensor development such as an electrode for electrochemical biosensor (Gil et al., 1999; Kase and Muguruma, 2004; Rho et al., 2008) and surface plasmon resonance (SPR) (Koukarenko et al., 2004; Lamarre et al., 2005; Sangpour et al., 2007).

Thermal evaporation is a technique that has also been widely used for the fabrication of thin gold film (Gizeli et al., 2003; Levlin et al., 1997; Lund et al., 2006; Zhang et al., 2007). The different literature surveys reported the use of this technique to fabricated a thin gold film which can be used as a part of transducers in

biosensor design such as, a sensor for surface plasmon resonance (SPR) (Abdelmalek, 2002; Zhang *et al.*, 2007), electrodes for conductivity measurement (Limbut *et al.*, 2007), and quartz crystal microbalance (QCM) (Feng *et al.*, 2007).

1.3 Biosensor

Biosensor is an analytical technique that has been developed since 1962 by Clark and Lyons (Clark and Lyons, 1962). It is a device combining a biological recognition element and suitable transducers. The International Union of Pure and Applied Chemistry (IUPAC) defined a biosensor as "a self-contained integrated device which is capable of providing specific quantitative analytical information using a biorecognition element (biochemical receptor) which is in direct contact with a transducer element". The biological recognition element of a biosensor interacts selectively with the target analytes, assuring the selectivity of the sensors (Figure 1.3).
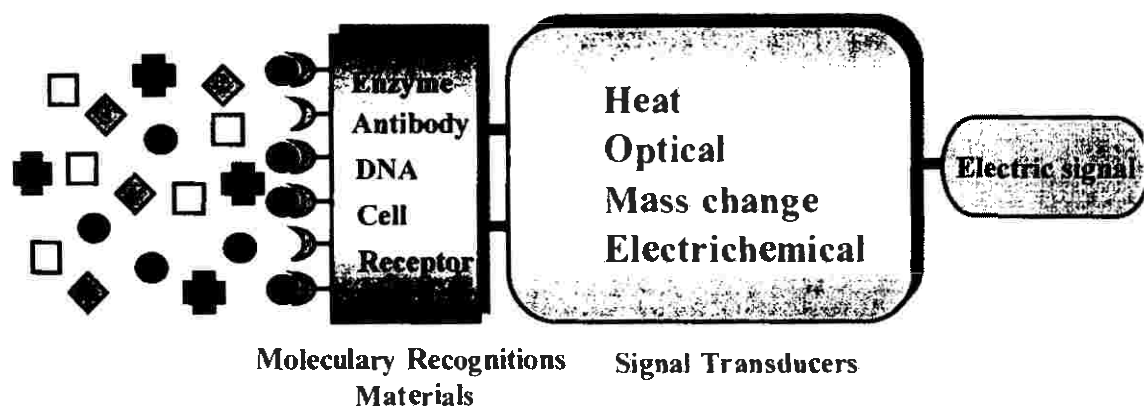
Figure 1.3 Schematic illustrations of the components of a biosensor. The specific interaction between analyte and biological element can be detected with appropriate transducers.

Biosensor can be subdivided into two classes based on the type of biorecognition molecules (Turner *et al.*, 1995). Catalytic biosensors employ enzymes and microorganisms as the biorecognition molecule which catalyses a reaction involving the analyte to give a product (Figure 1.4-a). The other category of biosensors is affinity biosensors. Biorecognition molecules commonly used in affinity biosensors include antibodies, DNA, peptides, and lectins. Affinity biosensors are

characterised by a binding event between the biorecognition molecule and the analyte (the affinity reaction) often with no further reaction (Figure 1.4-b). In the literatures, the popular affinity-based ligands are anibodies and the resulting sensor is known as immunosensor which are now the subject of increasing interest mainly because of their potential application as an alternative immunoassay technique (Engström *et al.*, 2006).

a.) Catalytic biosensor

b.) Affinity biosensor
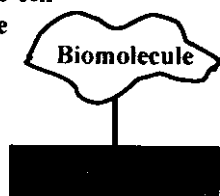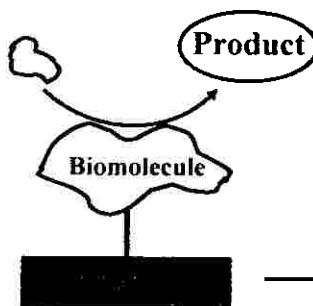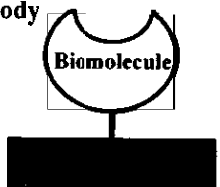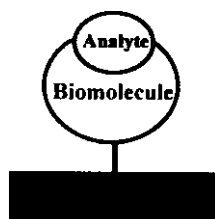
Figure 1.4 Major types of biosensor. (a) Catalytic biosensor involves the biochemical interaction between biomolecules and the analyte is detected by an appropriate transducer.(b) Affinity biosensors, the binding interaction between biomolecules and the analyte is detected by a transducer.

1.4 Immunosensor

Immunosensor belongs to biosensors because an essential component, the antibody (Ab), is derived from a biological process. The antibody conveys selectivity and sensitivity to the sensor. The Ab binds the analyte (antigen) with high affinity and is therefore able to detect the analyte in the presence of other substances. The merits of immunosensors are cleary related to the selectivity and affinity of the Ab-analyte binding reaction. There are several possibilities to derive a measurable signal from Ab binding. (Hock, 1997). They can be related to two basic approaches: labeled (indirect) and label free (direct) immunosensors (Luppa *et al.*, 2001).

1.4.1 Labeled immunosensor

Labeled or indirect sensors rely on labels conjugated to either the antibody or antigen to visualize the binding event. High sensitivity can be induced by incorporation of enzymes such as peroxidase and glucose oxidase, electroactive compounds such as ferrocene and a series of fluorescent labels (rhodamine, fluorescene, ruthenium) (Luppa *et al.*, 2001). An immunocomplex may be formed in a variety of ways, but the final step must include incorporation of a label, which is then determined by potentiometric, amperometric, or optical measurements.

The indirect method provides an advantage since the signal generation is significantly facilitated and amplified. However, indirect detection requires labeling of the detecting molecules and this make this type of immunosensor associates with other problems such as, expensive, time consuming and seriously compromising a real-time analysis (Berggren *et al.*, 2001; Luppa *et al.*, 2001; Van der Voort *et al.*, 2005; Yaguida *et al.*, 1996)

1.4.2 Label free immunosensor

Label free or direct sensors are designed so that formation of the antibody-antigen complex induces physical changes in the signal. Electrodes, piezoelectric material, or optically active material surfaces are sensitive enough to construct direct immunosensors. The target analyte presents in the solution and reacts with the complementary antibody or antigen bound on the sensing matrix. Formation

of the immunocomplex alters the physical properties of the surface, such as electrode potential, the intrinsic piezofrequency, or the optical properties allowing for target measurement (Aizawa, 1994). The concept of a direct sensor device represents a true alternative development to immunoassay systems (Luppa *et al.*, 2001).

Transducers that are often employed can be broadly divided into optical, electrochemical and mass sensitive (Table 1.1). Among these, optical immunosensors are the most studied, but the detection limits are expected to be better for electrochemical sensors and the instrumentation is less complicated (Berggren *et al.*, 2001).

Electrochemical detection is the measurements of electrical properties such as current, potential, or charge, and their relationship to chemical or biological compounds. The technique of electrochemical detection provides a sensitive method for trace analysis of chemical and biological material. Thus, electrochemical immunosensor is of great interest and have been widely used for label-free immunosensor (Berggren *et al.*, 1998; 2001; Bontidean *et al.*, 1998; Fu *et al.*, 2004; Hu *et al.*, 2002; Hedström *et al.*, 2005; Limbut *et al.*, 2006; Thavarungkul *et al.*, 2007; Zhang *et al.*, 2005). Electrochemical detection for label-free immunosensor employs several transduction principles, i.e. amperometric (Ramanaviviene *et al.*, 2004; Tang *et al.*, 2005; Yuan *et al.*, 2005), voltammetric (Liang *et al.*, 2007), potentiometric (Fu *et al.*, 2004; Yuan *et al.*, 2004), conductimetric (Kanugo *et al.*, 2002; Yaguida *et al.*, 1996) and capacitive (Berggren *et al.*, 1998, 2001; Bontidean *et al.*, 1998; Hedström *et al.*, 2005; Hu *et al.*, 2005; Limbut *et al.*, 2006). Capacitive immunosensor has been investigated as a highly sensitive approach and this is the subject of further reviews.

Table 1.1 Catagories of recently reported label-free immunosensor according to different physical principles.

Transducers	Reference
1. Optical immunosensor	
Surface plasmon resonance (SPR)	Gobi *et al.*, 2005
	Gobi *et al.*, 2007
Optical fiber	Lepesheva *et al.*, 2000
	Yang et al., 2007
2. Electrochemical immunosensor	
Potentiometric	Liang *et al.*, 2008
	Campanella *et al.*, 2008
Capacitive	Limbut *et al.*, 2006
	Hedström *et al.*, 2005
Impedimetric	Fu *et al.*, 2004
	Li *et al.*, 2005
Amperometric	O' Regan *et al.*, 2002
	Yuan *et al.*, 2005
Voltammetric	Fu, 2008
	Liang *et al.*, 2008
3. Mass sensitive immunosensor	
Quartz crystal microbalance (QCM)	Park *et al.*, 2007
Saw technique (acoustic surface wave)	Freudeberg *et al.*, 2001

1.5 Capacitive immunosensor

Recently, capacitive immunosensor has attracted considerable interest due to its high sensitivity, specificity, label-free, and simple instrumentation (Berggren *et al.*, 1998, 2001; Betty *et al.*, 2004; Hu *et al.*, 2002, 2005; Li *et al.*, 2005; Limbut *et al.*, 2006; Mirsky *et al.*, 1997). The principle of the capacitance transducer is based on the theory of the electrical double layer. A metal electrode immersed in an electrolyte solution can generally be described as resembling a capacitor in its ability

to store charge. The principle of capacitance measurement is based on changes in dielectric properties or charge distribution when an antibody-antigen complex forms on the surface (Berggren *et al.*, 2001; Gebbert *et al.*, 1992). This measurement can be made in several ways such as measuring the change in capacitance between two metal conductors in close proximity with each other with biorecognition element immobilized between them (interdigitated electrodes) (Gebbert *et al.*, 1992), measuring capacitance through impedance (Ho *et al.*, 1999) and measuring the capacitance potentiostatically at the electrode/solution interface with an recognition element immobilized on the surface of working electrode (Berggren *et al.*, 1998; Hedström *et al.*, 2005; Limbut *et al.*, 2006).

1.5.1 Interdigitated electrode

A normal electrical plate capacitor consists of two parallel metal plates separated by a certain distance and with a dielectric in between. The capacitance can be described by Equation 1.1:

$$C = \frac{\varepsilon_0 \, A}{d} \tag{1.1}$$

Where, ε is the dielectric constant of the material between the plates, ε_0 the dielectric constant for vacuum, A the area of the plates and d the distance between them. According to the equation the capacitance will increase when the distance between the two plates decreases. If the recognition element is immobilized on the electrodes, the sensitivity will increase when distance decreases (Figure 1.5 (a)) (Berggren *et al.*, 1998). In the case of interdigitated electrodes, with antibody (or antigen) immobilized in between, the forming of antibody-antigen complex will change the dielectric properties between electrode causing the change in capacitance (Figure 1.5 (b)). There will be a mechanical limitation to produce a short and reproducible distance between the two plates. Another limitation associated with this approach is that this method is very sensitive to change in bulk solution.

(a)

(b)
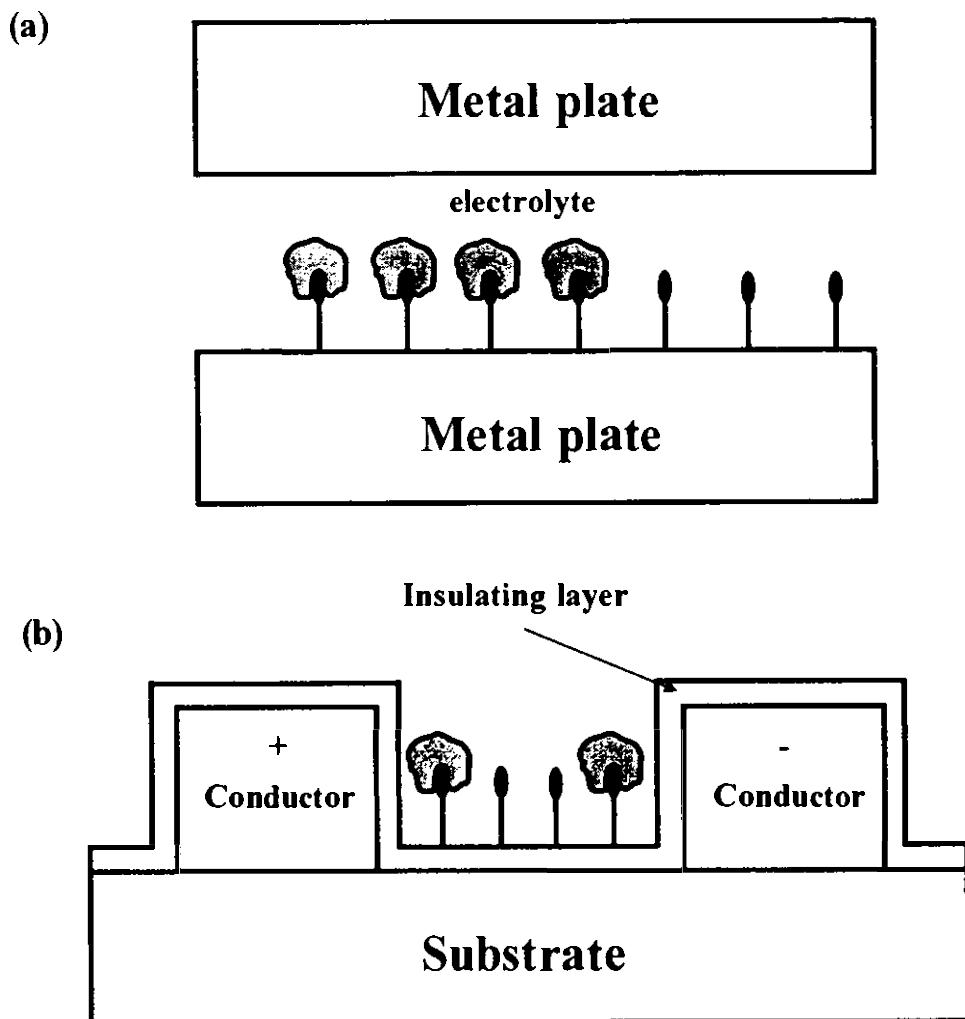
Figure 1.5 (a) A schematic diagram of the capacitive immunosensor measures the capacitance change due to the change in the distance between two plates and/or change in dielectric constant (b) due to the change in dielectric constant using interdigitated electrode (Modified from Gebbert *et al.*, 1992; Berggren *et al.*, 2001).

1.5.2 Impedance measurement

Another way to evaluate the capacitance is to measure with an the impedance. Impedance is a totally complex resistance encountered when a current flows through a circuit made of resisters, capacitors, or inductor, or any combination of these. In electrochemistry, the inductive effect is not usually encountered, therefore

only simple equivalent circuit which no inductor is present (Figure 1.6) (Park and Yoo, 2003).
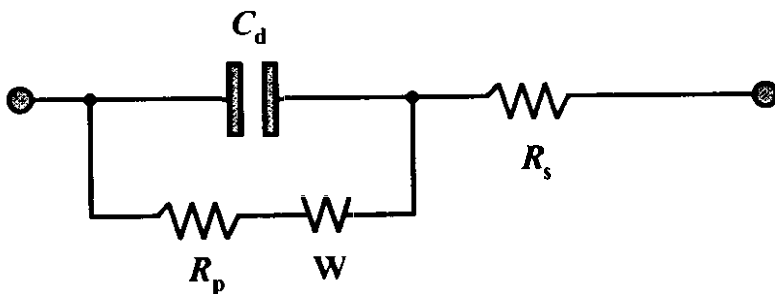
Figure 1.6 An equivalent circuit representing each component at the interface and in the solution during an electrochemical reaction is shown for comparison with the physical component. C_d, double layer capacitor; R_p, polarization resister; W, Warburg resister; R_s, solution resistor (Redrawn from Park et al., 2003).

A straightforward impedance expression of an equivalent circuit can be derived by applying Ohm's law to two components connected in parallel. One of these is R_p, and the other is $1/(j\omega C_d)$, in which C_d is the double layer capacitance.

$$Z(\omega) = R_s + \frac{R_p}{1+j\omega R_p C_d} = R_s + \frac{R_p}{1+\omega^2 R_p^2 C_d^2} - \frac{j\omega R_p^2 C_d}{1+\omega^2 R_p^2 C_d^2} = Z' + jZ'' \qquad (1.2)$$

The Warburg component is neglected in order to make the derivation of the equation and its interpretation straightforward. Thus, the impedance of the interface consists of two parts, a real number Z' and imaginary Z" with a complex representation, $Z(\omega) = Z'(\omega) + jZ''(\omega)$.

Nyquist plot, in which imaginary numbers $Z''(\omega)$ are plotted against real numbers $Z'(\omega)$ (Figure 1.7) can be used for the treating impedance data according to equation 1.2. At high frequency, the frequency dependent term of equation 1.2 vanishes, resulting in $Z(\omega) = Z'(\omega) = R_s$, which is intercept on the $Z'(\omega)$ axis on the high-frequency side ($Z''(\omega) = 0$). Equation 1.2 becomes $Z(\omega) = R_s + R_p$ for $\omega \rightarrow$ 0

which is an intercept on the $Z'(\omega)$ axis on the low frequency side. At the frequency where the maximum $Z''(\omega)$ is observed, $R_p \cdot C_d = 1/\omega_{max} = 1/(2\pi f_{max}) = \tau_{rxn}$, which is the time constant of the electrochemical reaction, can be shown and indicates how fast the reaction takes place. The double layer capacitance (C_d) can be calculated if $R_p \cdot C_d$ is known and R_p is already obtained from the low frequency intercept on the $Z''(\omega)$ axis.

Similar information can be obtained by examining the Bode diagram (Figure 1.8) using equation 1.2. In this case the logs of amplitudes (absolutes) of the impedance or phase angles are plotted against the log of frequency. Log R_s and log (R_s + R_p) are obtained straightforwardly from the log $Z(\omega)$ vesus log (ω) plot at high and low frequencies (Figure 1.8 (a)) from the same argument as the Nyquist plot. In the intermediate frequency region, an almost straight line with a slope of ~ -1 can be seen.
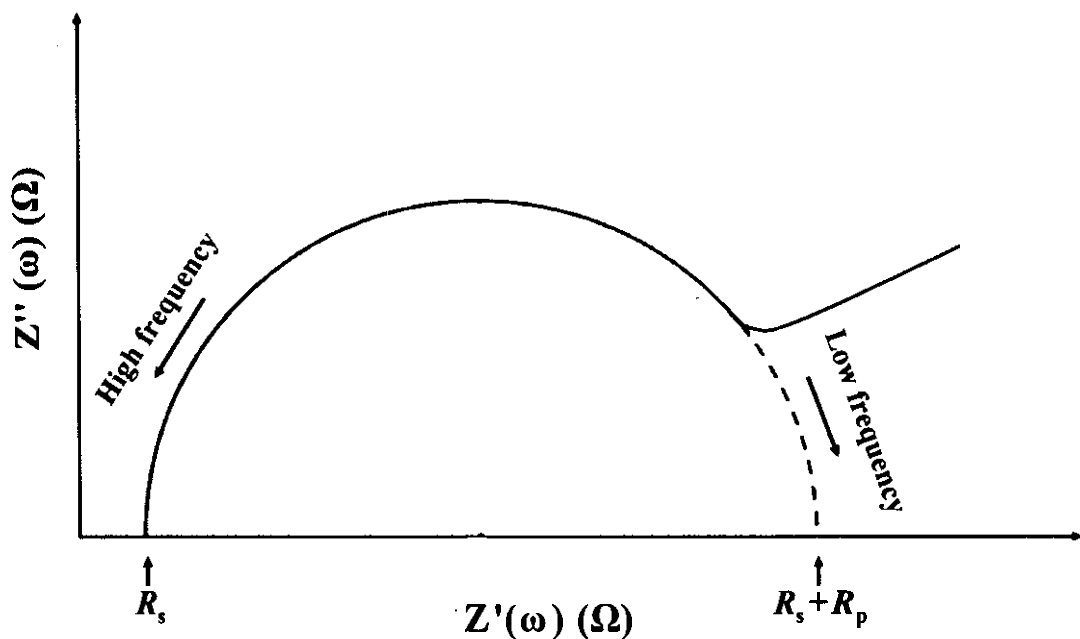
Figure 1.7 Nyquist plot; Z' = real part of impedance, Z'' = imaginary part of impedance, ω = the radial frequency, R_s = solution resistance, R_p= polarization resistor electron-transfer resistance and C_d = couble layer capacitance.

The equation of this line obtained by ignoring the frequency-independent terms, R_s and 1 in the denominator, of equation 1.2 to yield

$$Z(\omega) = R_s + \frac{R_p}{1 + j\omega R_p C_d} \qquad (1.3)$$

Taking the logarithm on both sides of the resulting equation yield log $Z(\omega)$ = - log ω - log C_d, which say that log $|Z(\omega)|$ versus log ω would have a slope of -1, and C_d can be obtained from the intercept of this line with the $Z(\omega)$ axis when $-\log \omega = 0$ at $\omega = 1$. Thus, the Bode plot provides the same information as the Nyquist plot. The Φ (phase angle) versus log ω plot (Figure 1.8 (b)) shows that the impedance responses are resistive primary at high and low frequencies as indicated by practically no phase shifts, whereas at intermediate frequencies, they are mostly capacitive as their phase shifts, get closer to 90° (Park and Yoo, 2003; Wu *et al.*, 2005)

Although the evaluation of capacitance through the measurement of impedance was an effective method to prove the electron-transfer resistance features of surface-modified electrodes and evaluate capacitance value. However, the recording of a full impedance spectrum within a broad region of frequencies required a long time, which made the method impractical (Katz *et al.*, 2001). Moreover the data of this measurement is difficult to interpret and it is not suitable for real-time measurement (Berggren *et al*, 2001; Guiducci *et al.*, 2004).
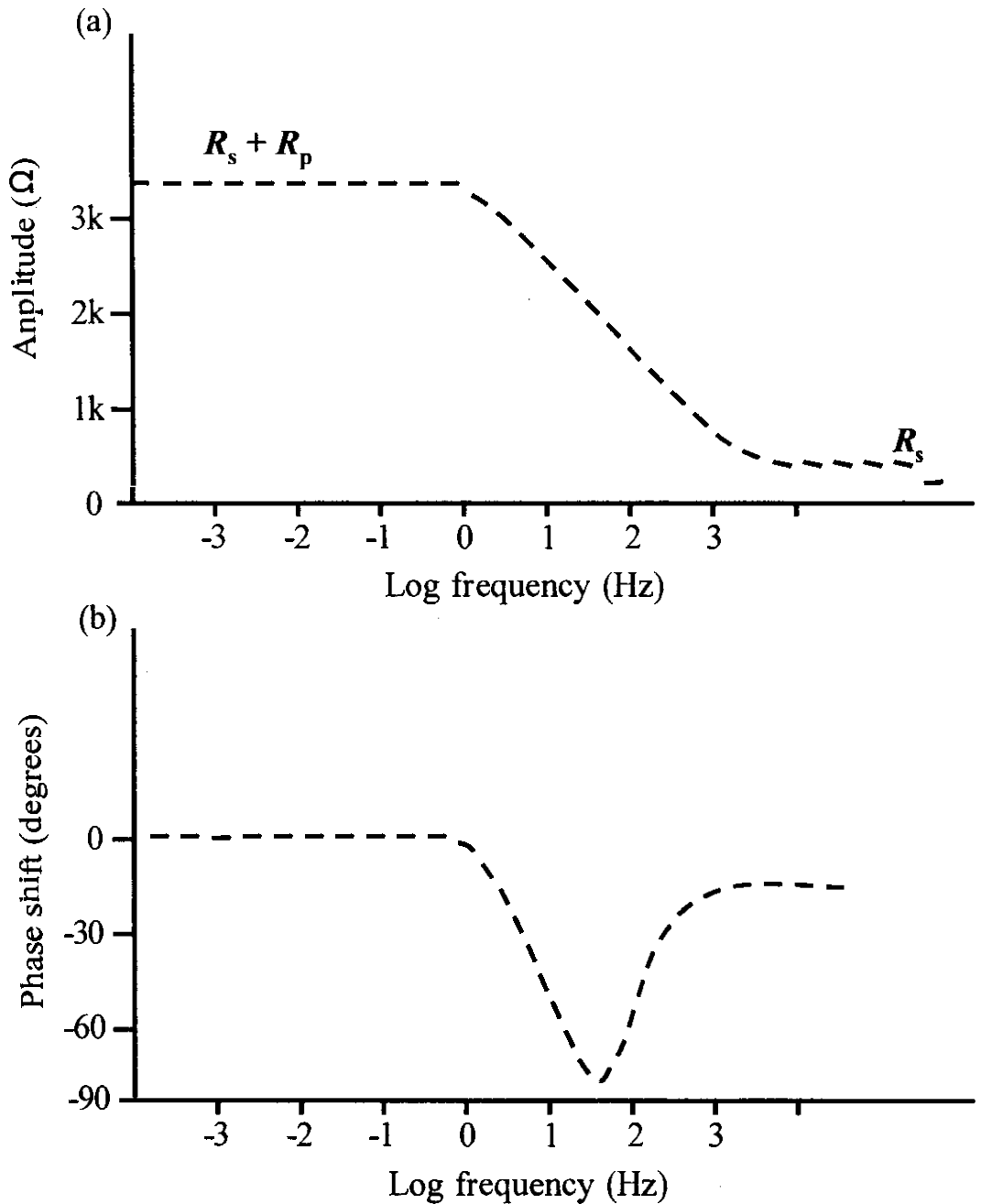
Figure 1.8 Bode plots, log of amplitudes (absolutes) of the impedance (a) or phase angles are plotted against the log of frequency (b).

1.5.3 Potentiostatic measurements

In this technique the capacitance is obtained from the current response measured at the electrode/solution interface in a potentiostatically controlled system by applying an electrical perturbation signal to the electrode. The potentiostatic control is accomplished with a three electrode system and a combination of operational amplifiers and feedback loops (Figure 1.9). The reference electrode is placed as close as possible to the working electrode and constructed to the instrument through a high resistance circuit that draws no current from it. Because the flow cannot occur through the reference electrode, a current-carrying auxillary electrode is placed in the solution to complete the current path. Hence, the current flows through the solution between the working and auxiliary electrode (Wang, 2006).

An electrode immersed in an electrolyte solution can generally be described as resembling a capacitor in its ability to store charge. For a given potential the electrode will possess a charge q_m and the solution another charge q_s, where q_m will be equal to $-q_s$. Charged species and dipoles will be oriented at the electrode/solution interface, hence making up the electrical double-layer (Figure 1.10) (Bard and Faulkner, 2001). Closest to the electrode surface, solvent and specifically adsorbed species constitute the compact Helmholtz plane or the Stern layer and solvated ions can only approach the electrode surface to a distance of a monolayer of oriented solvent molecules. When constructing a capacitive biosensor the electrode surface is usually covered with an insulating layer and the biorecognition element is immobilized on top of this layer. In this case solvated ions and water molecules are pushed further out from the electrode surface thereby giving rise to a change in capacitance. Most of the described capacitive biosensors in the literature are based on this approach (Beggren et al, 2001; Jiang et al., 2003; Limbut et al., 2006).
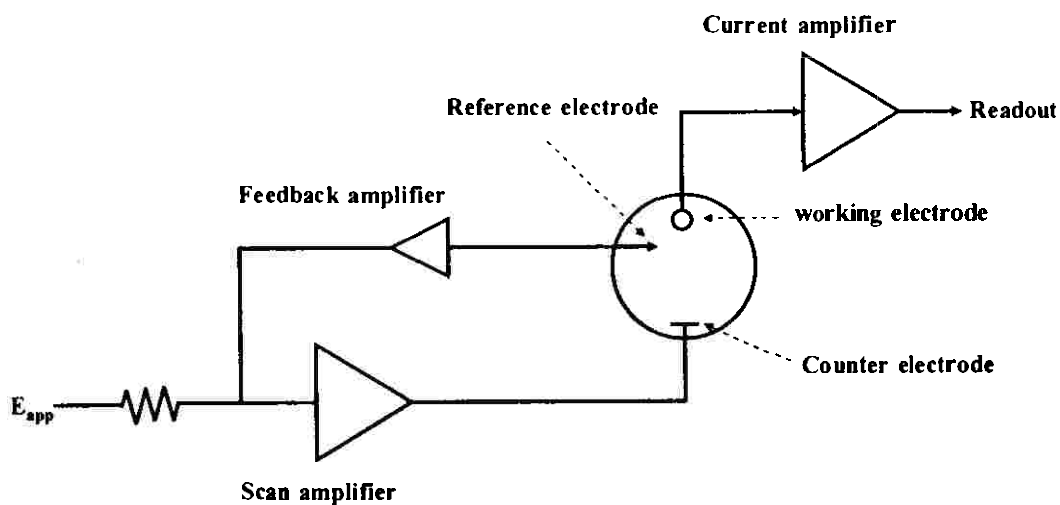
Figure 1.9 Schematic diagram of a three-electrode potentiostat (Redrawn from Wang, 2006).
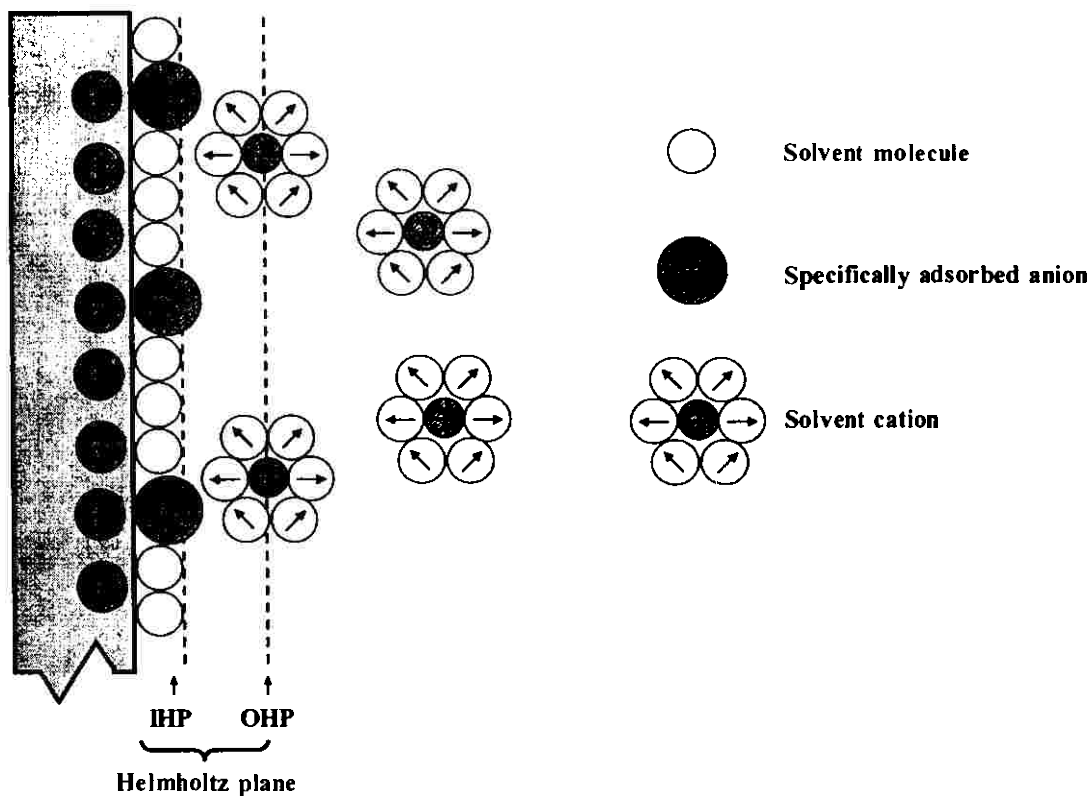
Figure 1.10 Schematic representation of a model of the double-layer region (IHP is the inner Helmholtz plane; OHP is outer Hemholtz plane).

ฝ่ายกองสมุด
คณ ะวิทยาลัย ดร จฬ ารณวุ่นทพ

The capacitance at an electrode/solution interface can be described to be built-up of several capacitors in series (Figure 1.11). The first capacitor constitutes the insulating layer on the surface, C_{ins}. The second capacitor, C_{rec}, includes the anchoring groups, the bound recognition element and any contribution from the Stern layer, which consists of hydrophobically bound water molecules between the recognition and the diffuse layers (Janek *et al.*, 1997). The third capacitor is described by the concentration dependent diffuse layer, C_{GC}, extending out into the bulk of the solution. Binding of analyte will give a change in the capacitance of the recognition layer C_{rec}. The total capacitance C_{tot} can then be described by Equation 1.4 (Berggren *et al.*, 1998: 2001).

$$\frac{1}{C_{total}} = \frac{1}{C_{ins}} + \frac{1}{C_{rec}} + \frac{1}{C_{GC}} \tag{1.4}$$
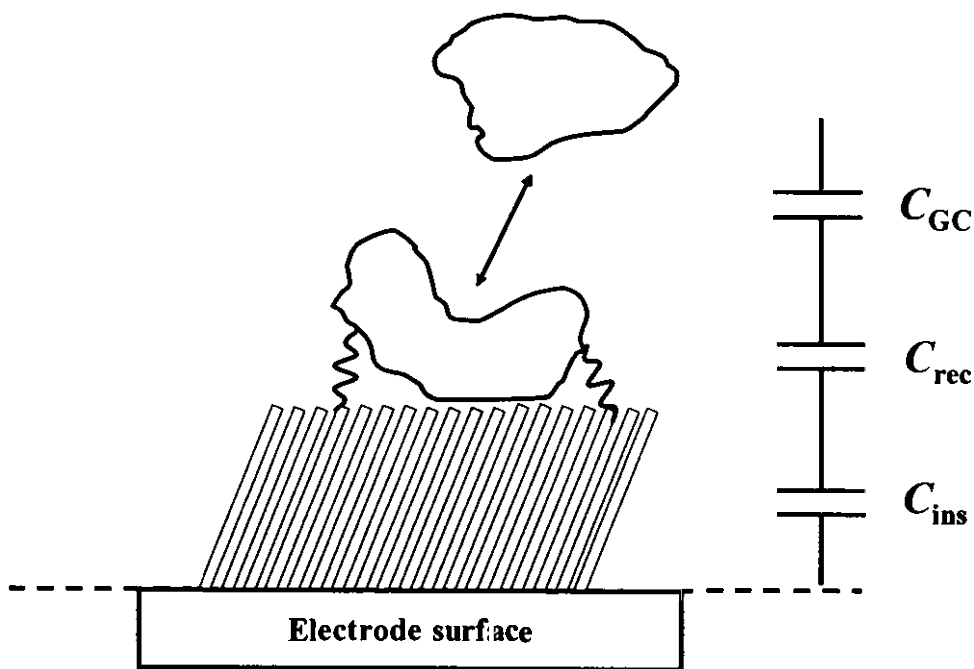
Figure 1.11 Schematic representation of a capacitive biosensor, where the total capacitance is described by several capacitors in series. The first capacitor, C_{ins}, closest to the metal surface describes the insulating layer, the second capacitor, C_{rec}, constitutes the grafting molecules, the bound recognition element, binding of analyte and any contribution from the Stern layer, the third capacitor, C_{GC}, describes the concentration dependent diffuse layer (Janek *et al.*, 1997).

The use of the potentiostatic-step method was based on an assumption that the system could be described as a simple *RC* model as shown in Figure 1.12 (a) (Berggren and Johansson, 1997; Jiang *et al.*, 2003). For the capacitive immunosensor, the electrode is coated by an insulating layer, therefore an accurate description should be *R (RC)* as in Figure 1.12 (b). Because the electrode is insulated, so, R_f (ohmic resistance of insulating layer such as SAM) is much more than R_s. This made R_f acting like an open circuit and the system could thus be simplified as an *RC* equivalent circuit.

(a)

R$_s$ C

(b)

R$_s$ C   R$_f$ ⇒   R$_s$ C
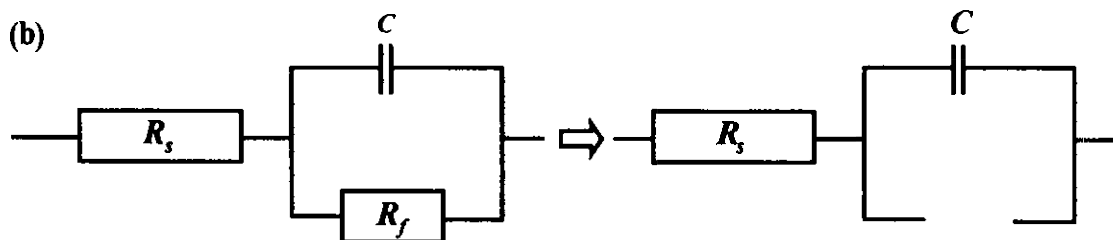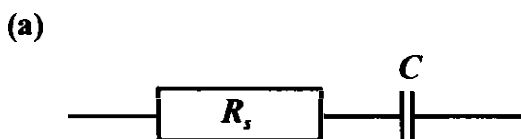
Figure 1.12(a) Simple *RC* equivalent circuit, R_s is the resistance of the element serially connected to the sensor and *C* was the capacitance. (b) *R (RC)* equivalent circuit, where R_f is the ohmic resistance of insulating layer (such as SAM) that is much higher than R_s making its act like an open circuit.

When a small voltage, such as 50 mV, is applied on the electrode (Figure 1.13 (a)) the current-time response is obtained (Figure 1.13 (b)) and this can be described by equation 1.5

$$i(t) = \frac{u}{R_s} \exp\left(\frac{-t}{R_s C_{total}}\right) \tag{1.5}$$

Where $i(t)$ is the current in the circuit as a function of time, u is the potential step, R_s is the dynamic resistance of the recognition layer, t is the time elaped after potential step was applied, and C_{total} is the capacitance measured at the working electrode/solution interface. Taking the logarithm of the current value vs. time (Figure 1.13 (b) inset)

$$\ln i(t) = \ln \frac{u}{R_s} - \frac{-t}{R_s C_{total}} \qquad (1.6)$$

results initially in an almost linear curve and R_s, C_{total} could be calculated from the intercept and slope of the curve (Berggren *et al.*, 1998, 2001; Jiang *et al.*, 2003; Limbut *et al.*, 2006).

Compared with the other electrochemical transducers, capacitive measurement has several advantages. It can be used for some special purpose i.e. investigation of formation process, thickness measurement. This technique works very well for studying insulating material, such as the interaction between antibody-antigen (Hedström *et al.*, 2005; Limbut *et al.*, 2006). Moreover the method is quick, can be used to follow bio-recognition events at the electrode surfaces or directly detect the interaction between an analyte and a biorecognition element on the surface of a biosensor system (Berggren *et al.*, 1998; Jiang *et al.*, 2003).
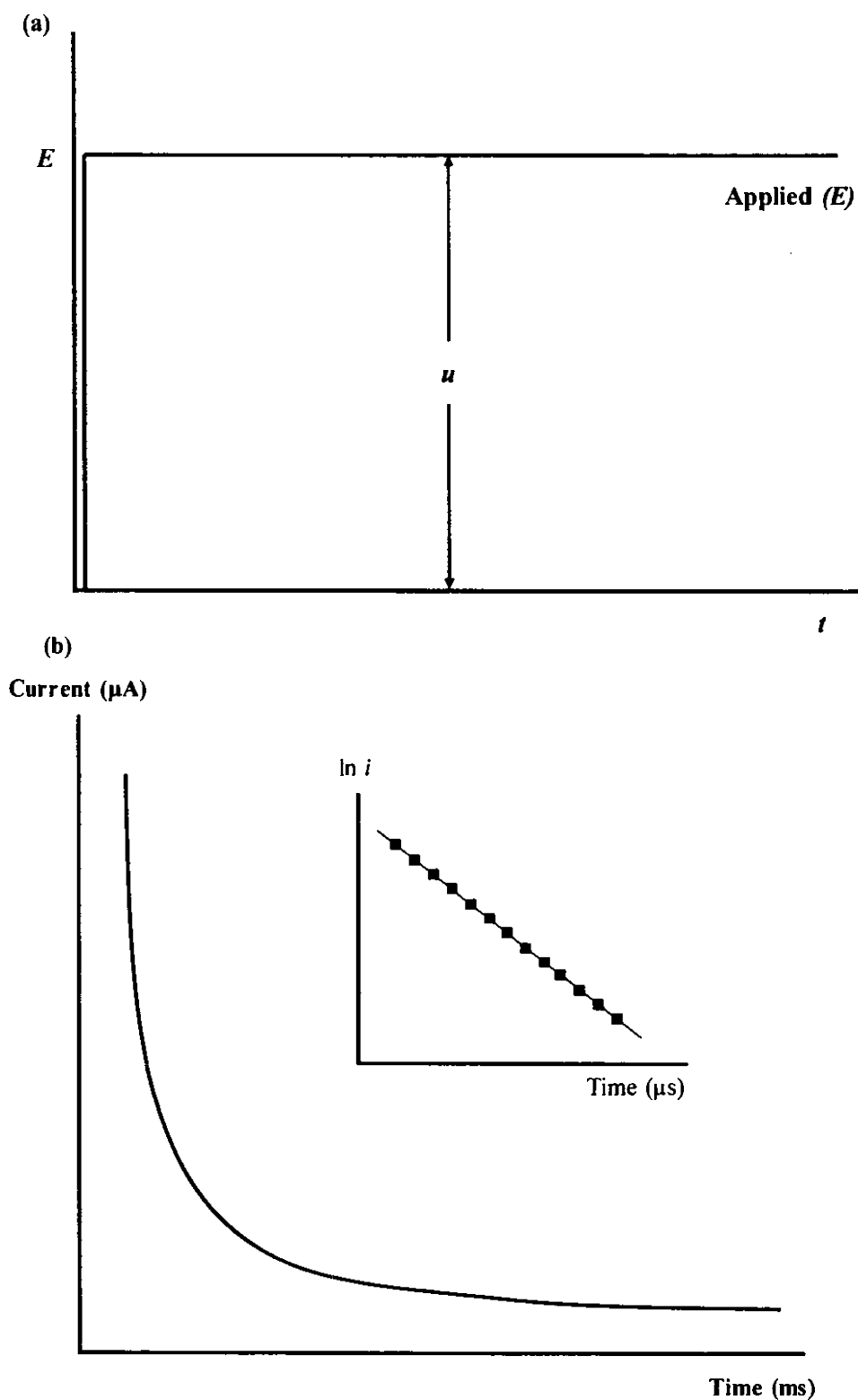
Figure 1.13 (a) applying a potentiostatic step (*u*) (b) the corresponding current vs. time response (inset: logarithm of current vs. time *(i-t)* response) (Modified from Bard and Faulkner, 2001).

1.6 Immobilization

In order to make a viable biosensor, the biological component has to be properly attached to the transducer. This process is known as immobilization (Sharma *et al.*, 2003). Several methods are available for the immobilization of biomolecules. Physical adsorbtions, entrapment, intermolecular cross-linking and covalent binding are the most commonly used. For potentiostatic step capacitive measurement it is based on the principle that for the electrolytic capacitor the capacitance depends on the thickness and dielectric behavior of a dielectric layer on the surface of a electrode (Gebbert *et al.*, 1992), therefore it is necessary to construct electrically insulated electrode surface with immobilized biomolecules.

Self-assembled monolayer (SAM) of alkanethiol on the electrode surface can generally fulfill this requirement (Berggren *et al.*, 1998; Berggren and Johansson, 1997; Hedström *et al.*, 2005; Limbut *et al.*, 2006). Thiol based SAM is one possible method that have been used to immobilized antibodies in several report (Hedström *et al.*, 2005; Rickert *et al.*, 1996; Wrobel, 2001). The strong affinity of thiols towards gold surface produces a fast initial adsorption followed by a slower process of recognization of S/SH molecules on the gold surface (Yang *et al.*, 1996). This strong affinity and self-assembly facilitates the preparation of structured oriented layers containing functional groups well ordered at the monolayer-air (or liquid) interface (Bain and Whitesides, 1988). SAM technique is a simple way to produce a reproducible, ultra thin and well-ordered layer suitable for further modification with antibodies, which have potential in improving detection sensitivity, speed and reproducibility (Fu *et al.*, 2005). However the completed adsorption of alkanethiol need several hours (Lu *et al.*, 2005; Hedström *et al.*, 2006; Limbut *et al.*, 2006).

Another strategy to obtain an insulated layer such as electropolymerization of non-conducting polymer is also of interested. *Ortho*-phenylenediamines (*o*-PD) is a non-conducting polymer which has been widely used (Garjonyte *et al.*, 2000; Yin *et al.*, 2002). Biomolecules e.g. enzymes, can be immobilized on the electrode surface using the electropolymerization of *o*-PD by a one step or a two step process. The one-step immobilization procedure was widely used for the direct electrochemical co-deposition of biomolecules and *o*-PD monomer (Malitesta *et al.*, 1990). Although this technique is easy, rapid and can successfully

performed in one step but it has limitation since some biomolecules will lost their activity during the electropolymerization (Liu *et al.*, 1995). Since the electropolymerization of *o*-PD will form a 1,4 substituted benzonoid-quinoid with free amino group expose on the backbone of the poly *o*-PD (Figure 1.14) (Yano and Nagaoka, 1996), a two-step immobilization has been proposed. This was done by cross-linking these free amino groups and the biomolecules with a bifunctional reagent such as glutaraldehyde (Curulli *et al.*, 1998; Myler *et al.*, 1997; Karalemas *et al.*, 2000). This method provides a biosensor with more stable performance and possible to apply for the immobilization of antibodies.
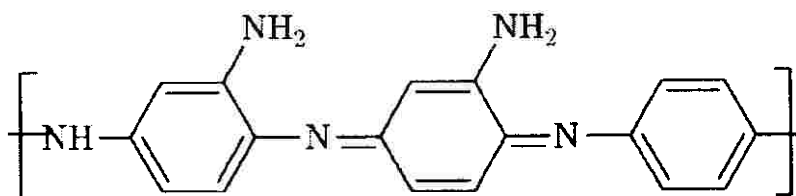
Figure 1.14 The polymer structure (1,4 substituted benzonoid-quinoid with free amino group expose on the backbone of the poly *o*-PD) obtained from electropolymerizaton of *o*-PD.

In this work, both SAM and electropolymerization of *o*-PD were tested for the immobilization of antibodies on sputtered and thermally evaporated gold electrodes, respectively.

1.7 Studied immunosensors

To evaluate the performance of the electrodes using capacitive immunosensor system, two antibody-antigen pairs, anti-host cell protein (anti-HCP) – host cell protein (HCP) and anti-human serum albumin (anti-HSA) – human serum albumin (HSA) were used as models.

1.7.1 Host cell protein (HCP)

Analyses of crude samples from biotechnology processes are often required in order to demonstrate that residual host cell impurities are reduced or eliminated during purification (Rathore *et al.,* 2003). Over the past several years, development of new recombinant proteins has increased greatly (Rathore *et al.,* 2003; Zhu *et al.,* 2005). Recombinant expression in *E. coli* is relatively simple and cost effective method for the production of certain proteins. Many of these products are intended for use as therapeutic agents in human and animals, and as such, must be highly purified. The manufacturing and purification process of these products leaves the potential for contamination by host cell protein (HCP) from *E. coli*. Such contamination can reduce the efficacy of the therapeutic agent and result in adverse toxic or immunological reactions and thus it is desirable to reduce HCP contamination to lowest level practical (O'Keefe *et al.,* 1993; (Rathore *et al.,* 2003); Wan *et al.,* 2002). Typically the acceptable concentration of HCP is in the level of ng/mg.

Although standardized quantitative methods are available for monitoring both DNA and endotoxin contamination (Ji *et al.,* 2002; Rathore *et al.,* 2003; Zhang *et al.,* 1994), but there is no generally applicable method available for detecting HCP in purified recombinant preparations. This is because each host system gives rise to a particular array of HCP and a quantitative assay must use HCP generated from a "null" production clone, i.e. a clone that lack the gene of interest but is carried through fermentation (and for a process-specific assay, through one or several purification steps) using the same conditions as the target protein (Wan *et al.,* 2002; Zhu *et al.,* 2005). An accurate quantitative HCP contaminant determination is critical for establishing product release specifications, and can be useful in developing or modifying manufacturing processes, and for use in purification process validation (Berthold and Walter, 1994; Anicetti and Hancock, 1994; Jones and O'Connor, 1985).

Immunological methods using antibodies to HCP such as Western Blot and ELISA are widely accepted due to their specificity and sensitivity (Eaton, 1995; Ghobrial *et al.,* 1997; Wan *et al.,* 2002). While Western blot is a powerful method aiding in the identity of HCP, it suffers from a number of limitations. Western blot is a complex techniques, it usually requires some solubilizing or denaturing technique before the electrophoresis step. That typically consists of treatment with a strong

detergent, reducing agent, heat, and it can destroy some antigenic determination. Moreover, this method has a low sensitivity for detecting small amounts of multiple HCPs even if the total HCP level is high. Therefore, this is not an appropriate means of quantifying residual protein in recombinant protein samples (Zhu *et al.*, 2005).

Immunoassays for detecting HCP were extensively reviewed by Eaton (1995). The microtiter plate immunoenzymetric assay (ELISA) method employed in this Kit overcomes the limitations of Western Blots providing on the order of 100 fold better sensitivity. Antibodies raised against host cell-derived proteins can be used in ELISA technique to provide quantitative determination of HCP impurity levels in recombinant products. This type of immunological detection method is possible using polyclonal antibodies prepared against strain-specific host cell proteins produced from the product purification processes. This technique is simple to use, highly sensitive, and semi-quantitative ELISA is a powerful method to aid in optimal purification process development, process control, and in routine quality control and product release testing. This kit is "generic" in the sense that it is intended to react with essentially all of the HCP that could contaminate the product independent of the purification process (Wan *et al.*, 2002). However, ELISA technique has many drawbacks, since it needs signal-generating labels, therefore this technique is expensive, time-consuminig and real time measurement impossible. Base on the basic of immunoassay, the use of antibody and antigen to form a stable complex is attractive for the development of label-free immunosensor with electrochemical detection such as capacitive measurement is vital of interest.

In this work, the purification of enzyme Lactate dehydrogenase (LDH) from *E. coli* was studied as a model system by using immobilized metal affinity chromatography (IMAC) technique

Immobilized metal affinity chromatography (IMAC) is the most widely used technique for single-step purification of recombinant proteins. The use of immobilized metal affinity chromatography (IMAC) has revolutionised protein biochemistry by allowing the production of a pure protein sample through a single purification step (Bolanos-Garcia *et al.*, 2006). The expression of a recombinant protein containing a histidine-tag (usually six consecutive histidine residues) allows it to be specifically bound by chelated divalent metal ions, and then eluted through

competition by the addition of imidazole, or through the protonation of histidine residues by a reduction in pH. This often has dramatic results in the purification of target proteins to near homogeneity from bacterial cell lysate (Hochuli *et al.*, 1987; Smith et al., 1988). Further advantages of IMAC include ligand stability, high protein loading capacity, mild or denaturing elution conditions, column regeneration, low cost and scalability (Mohanty *et al.*, 2001; Gaberc-Porekar and Menart, 2001). The most commonly used of metal-chelator system for IMAC are the tridentate ligand IDA as shown in Figure 1.15.
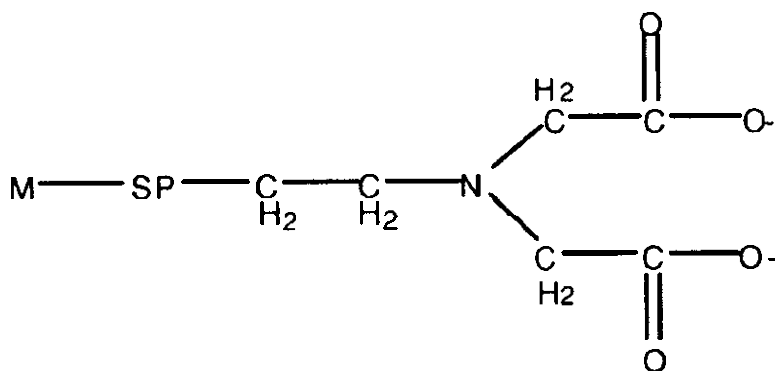
Figure 1.15 Structure of IDA chealating ligand

1.7.2 Human serum albumin (HSA)

Human serum albumin (HSA) is a single-chain, unglycosylated molecule of 585 amino acids, which comprises about 50 % of the total protein in serum, where it has a normal concentration of 35-45 g/L (Peters, 1996). Albumin plays an important role in the human body. One of its main functions is to regulate plasma osmotic pressure between the blood and tissues. This function is attributable to its high plasma concentration and relatively low molecular weight. One very important role of albumin is that it also functions as a transport molecule. This role is based on albumin's unique ability to bind a variety of exo-and endogeneous compound (Doumas *et al.*, 1997). Thus, albumin can serve as a circulating depot of metabolites and as extracellular antioxidant (Halliwell *et al.*, 1988). Variation in human albumin concentration provides valuable information related to metabolic diseases and has various diagnostic applications.

Hypoalbuminemia, a low concentration of serum albumin has been found in patients with certain hepatic desieses, elevated catabolism due to tissue damage or inflammation, extensive burns and malnutrition (Hoye *et al.*, 1998; Peters, 1996). In severe cases of hypoalbuminemia, the maximum albumin concentration of plasma is 25 g/L. Due to the low osmotic pressure of the plasma, water permeates through blood capillaries into tissue (edema). The determination of albumin allows monitoring of a controlled patient dietary supplementation and serves also as as excellent test of liver function.

Hyperalbuminemia, a high concentration serum albumin is usually seen in dehydrated patients. Urine albumin is also has been used as an indicator of renal diseases including nephritic syndrome and uremia (Ward, 1995).

The albumin concentration can be measured using electrophoretic, dye-binding and immunological method (Choi *et al.*, 2004). The widely used assays are dye-binding methods using bromocresol green (BCG) and bromocresol purple (BCP) (Carfray *et al.*, 2000). Eventhough, these techniques lack specificity (Gustafsson, 1976), but they still have been widely used because they are simple, sensitive and inexpensive (Doumas and Peters, 1997). Taking an account to specificity, the immunological method is perhaps a good choice among the analytical assays. Immuno-turbidimetric (ITM) (Carfray *et al.*, 2000), fluorescence immunoassay (Choi *et al.*, 2004) and enzyme-linked immunosorbent assay (ELISA) are such three examples. However, these methods use signal-generating labels, therefore it has the disadvantages such as expensive, time-consuminig and real time measurement impossible. Base on the basic of immunoassay, the use of antibody and antigen to form a stable complex is attractive for the development of immunosensor.

Immunosensor has been successfully used for the determination of HSA. Anti-HSA was immobilized on the transducer surface and the binding interaction between anti-HSA and HSA was determined by different methods such as surface plasmon resonance (SPR) (Sasaki *et al.*, 1998; Toyama *et al.*, 1998; Ying *et al.*, 2006), quartz crystal microbalance (QCM) (Lin *et al.*, 2000; Sakti *et al.*, 2001) and capacitive measurement (Hedström *et al.*, 2005; Shen *et al.*, 2005).

1.8 Objective

The main focus of this thesis is to develop electrodes using sputtering and thermal evaporation techniques to be used as working electrode for capacitive measurement in label free immunosensor systems, using the detection of host cell protein and human serum albumin as models.

1.9 Benefits

It is expected that gold electrodes obtained from sputtering and thermal evaporation technique can be used as disposable electrode without pretreatment step in capacitive immunosensors.

1.10 Outline of the research

1. Fabricate electrodes by using sputtering and thermal evaporation techniques.

2. Apply sputtered gold electrode in capacitive immunosensor system to detect host cell protein.

3. Apply thermally evaporated gold electrode in capacitive immunosensor system to detect human serum albumin.

CHAPTER2

MATERIALS AND METHODS

In this work, capacitive immunosensor was studied using two different antibody (Ab)-antigen (Ag) pairs, i.e. anti host cell protein (anti-HCP)-host cell protein (HCP) and anti human serum albumin (anti-HSA)-human serum albumin (HSA). Thin gold film electrodes fabricated by sputtering and thermal evaporation were used as a working electrode.

2.1 Materials

- Antibody to host cell protein (anti-HCP) raise against *E. coli* protenome (Pfizer, St. Louis, USA)

- Host cell protein (HCP) from *E. coli* (Novozyme Biopharma, Lund, Sweden)

- Anti human serum albumin (Anti-HSA, IgG; Dako, Denmark)

- Human Serum Albumin (HSA, Dako, Denmark)

- Bovine Serum Albumin (BSA, Sigma, USA)

- Microscope slide (25.4 × 76.2 × 2.0 mm) (Sailbrand 23, China)

- Gold (99.99 % purity)

- Hydrogen peroxide (H_2O_2; Merck, Germany)

- Sulfuric acid (H_2SO_4; AR Gade: LAB-SCAN, Thailand)

- Thioctic acid ($C_8H_{14}O_2S_2$; Sigma, USA)

- 1-dodecanethiol 98+% ($CH_3(CH_2)_{11}SH$; ALDRICH, USA)

- Sodium dihydrogenphostphate dehydrate (Na_2HPO_4-$2H_2O$; AR Grade: Merck, Germany.)

- Disodium hydrogenphosphate dehydrate (NaH_2PO_4-$2H_2O$; AR Grade: Merck, Germany.)

- Glycine (H_2NCH_2COOH; AR grade: Merck, Germany.)

- Glutaraldehyde 25% ; Fluka.

- Sodium hydroxide (NaOH; AR Grade: Merck, Germany.)

- Sodium chloride (NaCl; AR Grade : BDH, England.)

- Potasium Chloride (KCl; UNINAR, Australia.)

- Hydrochloric acid 36.5-38 % (HCl; Ar Grade:BDH, England)

- Ethanol (C_2H_5OH; Merck, Germany)

- Methanol (CH_3OH; Merck, Germany.)

- Potassium ferricyanide ($K_3Fe(CN)_6$; Sigma, USA)

- *Ortho*-phenylenediamine (*o*-PD ; BDH laboratory reagent, Poole, England)

2.2 Apparatus

- Peristaltic pump (Minipulse3, Gilson, France.)

- Microautolab type III, Eco Chemie B.V., Netherlands

- Potentiostat (Model EA161, EDAQ, Australia)

- Thermal evaporator (Edwards Auto 306, UK)

- Single target D.C. Sputtering (NECTEC pilot plan), Thailand.

- Sample injector (VIGO 6 port W valves, Valco, USA.)

- Syringe (NIPRO disposable syringe, Thailand.)

- Computer (LASER, Thailand)

- Vacuum (EDWARDS, England)

- Albet$^{®}$ nylon membrane filter (Albet, Spain) pore size 0.20µm

- Shaker (Model SK-101; HL, Thailand)

- Microliter pipette 100 µl, 1,000 µl and 5,000 µl (Eppendorf., Geramany)

- Microtubes1.5 ml and 2.0 ml (Axygen, USA)

- Microcentrifuge (Spectrafuge 16 M, Labnet, USA)

- Atomic Force Microscopy (AFM), (Seiko instrument, Japan).

2.3 Capacitive immunosensor for host cell protein (HCP)

2.3.1 Fabrication of sputtered gold electrodes

Microscope slides were cut in to strips (5.0 × 25.4 mm.), cleaned with Piranha solution through sonication for 5 min and rinsed with deionized water several times. They were dried in an oven at 100 °C for 1 h. Chromium was first coated on the microscope slide surface by single target D.C. sputtering (NECTEC pilot plan, Thailand). This was done by applying a current of 200 mA for 3 min at a pressure of 4.3 × 10^{-5} mB, argon flow rate 4.0 sccm (standard cubic centimetre per minute) and argon pressure of 2.8 × 10^{-3} mB. In this step chromium was deposited on glass surface. Then gold was coated on the chromium layer by applying a current of 200 mA for 7 min at a pressure of 6.6 × 10^{-5} mB, argon flow rate 4.0 sccm and argon pressure of 2.8 × 10^{-3} mB.

2.3.2 Immobilization of anti-HCP

The immobilization of anti-HCP was modified from the work of Hedström *et al.* (2005) and Limbut *et al.* (2006). Sputtered gold electrodes were placed in a plasma cleaning device (Mod. PDC-3XG, Harrich, NY) for 20 min. The plasma-cleaned electrodes were immediately put in thioctic solution (2% (w/w) in absolute ethanol) for 24 h. In this step a self assembled monolayer (SAM) was formed on gold surface (Figure 2.1 (1)). Electrodes were thoroughly rinsed with absoluted ethanol to remove unbound thioctic acid and dry under vacuum. Thereafter, the gold electrodes were put in EDC solution (1% w/w in dry acetronitrile) for 5 h where a terminal OH group of the thiol was activated to form *O*-acyllisourea (Figure 2.1 (2)). Electrodes were then rinsed with 100 mM sodium phosphate buffer, pH 7.0 and dry with chemically pure nitrogen gas. The electrodes were then immersed in anti-HCP (35µg/ml) (raised against *E. coli*) in 100 mM sodium phosphate buffer, pH 7.0 overnight at 4 °C. The terminal amine group of antibody displaces the *O*-acyllisourea and thus binds covalently to the monolayer (Figure 2.1 (3)). As a last step in the preparation, the electrodes were placed in 10 mM 1-dodecanethiol ethanolic solution for 20 min in order to cover bare parts of the gold surface (Figure 2.1 (4)).

$$\text{(CH}_2)_4\text{-C-OH}$$

2%w/w
thioctic acid

Gold electrode

(1)

S–S

TA-modified
gold electrode

EDC

(2)

$CH_3CH_2\text{-NH-C=N-(CH}_2)_3\text{-N-CH}_3$

O

$(CH_2)_4$-C-NH$_2$

H$_2$N

Anti-HCP

(3)

S–S

Anti-HCP TA
-modified gold electrode

O

$(CH_2)_4$-C-O-

S–S

O-acylisourea
active intermediate

CH_3

H Cl⁻

O

$(CH_2)_4$-C-NH$_2$

S S–S

Anti-HCP TA
-modified gold electrode

1-dodecanethiol

HS-(CH$_2$)$_{11}$CH$_3$

(4)
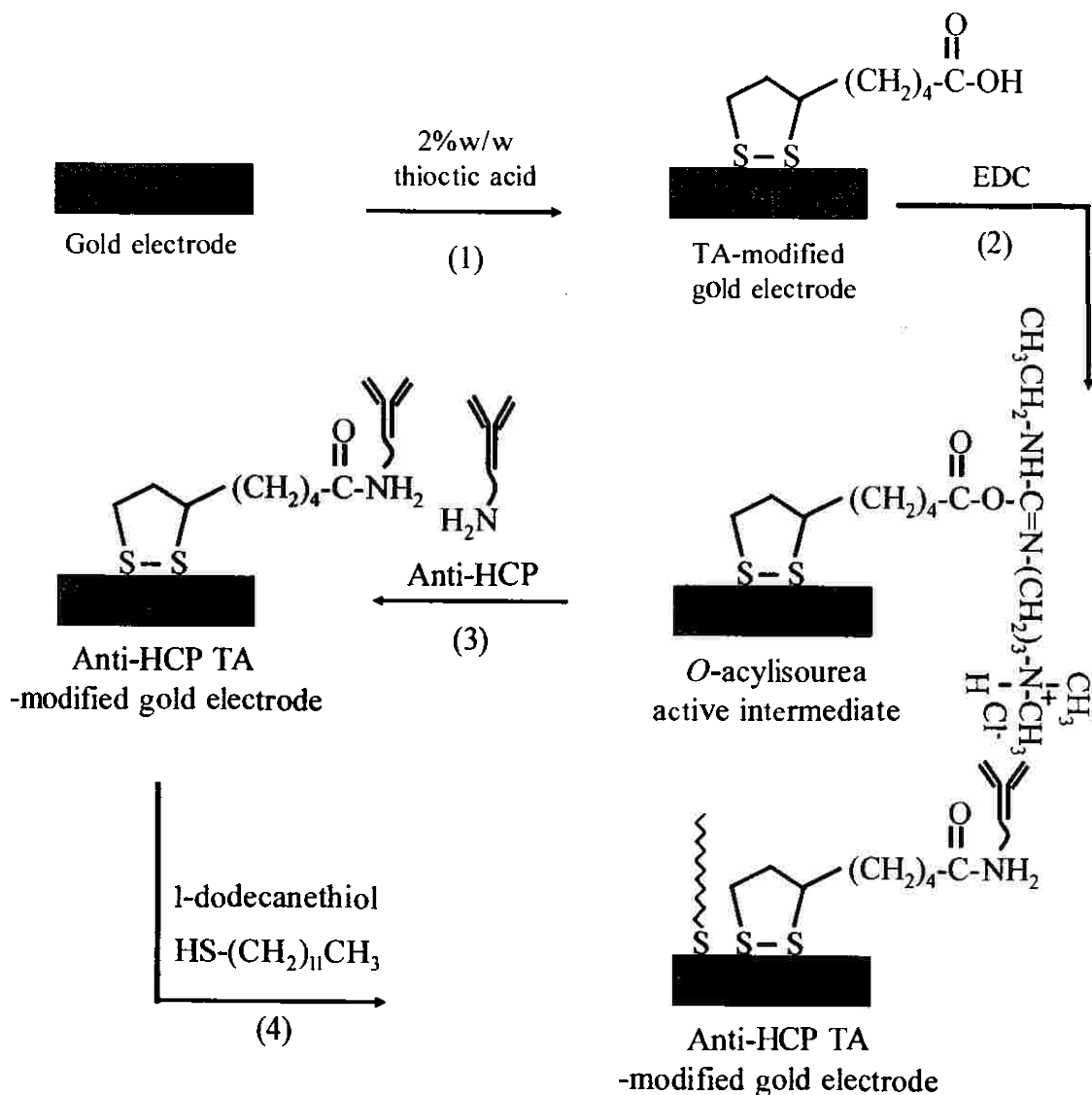
Figure 2.1 Reaction mechanism for the immobilization of anti-HCP on thioctic
modified electrode (1) self-assembly monolayer of thioctic acid was form
on gold surface (2) activation of terminal OH group of thiol to form *O*-
acyllisourea (3) covalent binding of terminal amine group of antibody to
self-assembly monolayer and (4) blocking of pinholes or bare spots on
electrode surface by 1-dodecanethiol.

2.3.3 The flow injection system

Figure 2.2 shows the basic experiment set-up of the flow injection capacitive immunosensor system which consists of;

a) A peristaltic pump, where a steady flow rate of the solution was controlled.

b) An injection valve where a specific volume of the sample was injected into the analysis system through the sample carrier buffer.

c) A detection unit consisted of a reaction flow cell and part of a potentiostatic three electrode system with an extra reference electrode. A keithley 575 measurement and control system (Keithley Instrument, Cleaveland, OH, USA) was connected between potentiostat and computer. The flow cell with a dead volume of 10 μL (Figure 2.3) consisted of a platinum wire (Ø 0.5 mm) reference electrode at the top, sputtered gold working electrode at the bottom and a disc shaped piece of platinum foil with a hole in the center as auxillary electrode. A commercial Ag/AgCl reference electrode was concomitananlty used with the platinum wire reference. The extra reference electrode was utilized to correct for any potential drift connected to the platinum wire electrode (Berggren and Johansson, 1997; Berggren *et al.*, 1998; Bontidean *et al.*, 2003).

Immunosensor for the detection of HCP was then investigated. When HCP was injected into the flow system it bound to anti-HCP modified on gold electrode, causing the surface layer thickness of the electrode to increase and the response was detected as the decrease of capacitance. (See Figure 1.9).
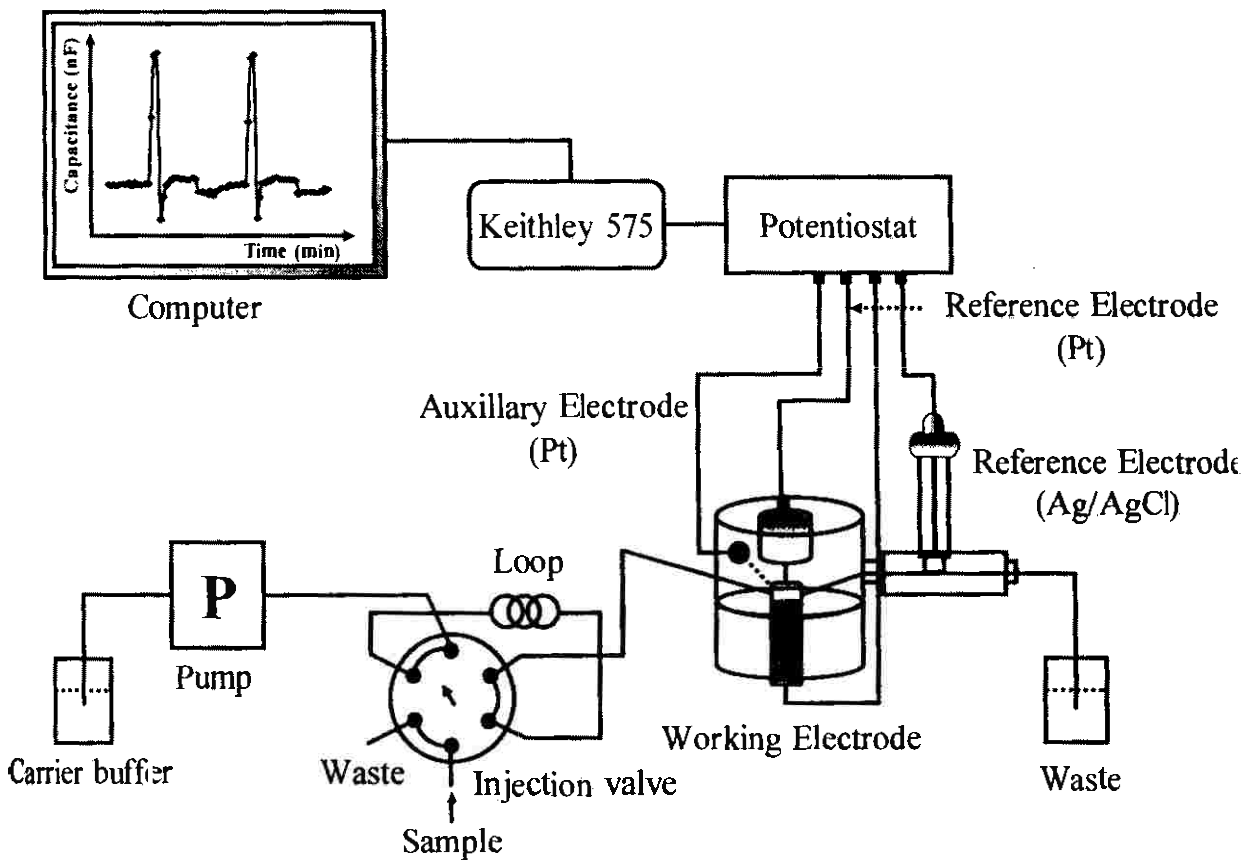
Figure 2.2 Schematic diagram showing the flow injection capacitive immunosensor system. The peristaltic pump carries the carrier buffer to the flow cell and to the waste. Samples were injected to the system through injection valve and carried by carrier buffer through the flow cell. The response due to the interaction of HCP to anti-HCP modified on sputtered gold electrode during the potentiostatic step are processed using a Keithley 575 measurement and control system powered by a computer.
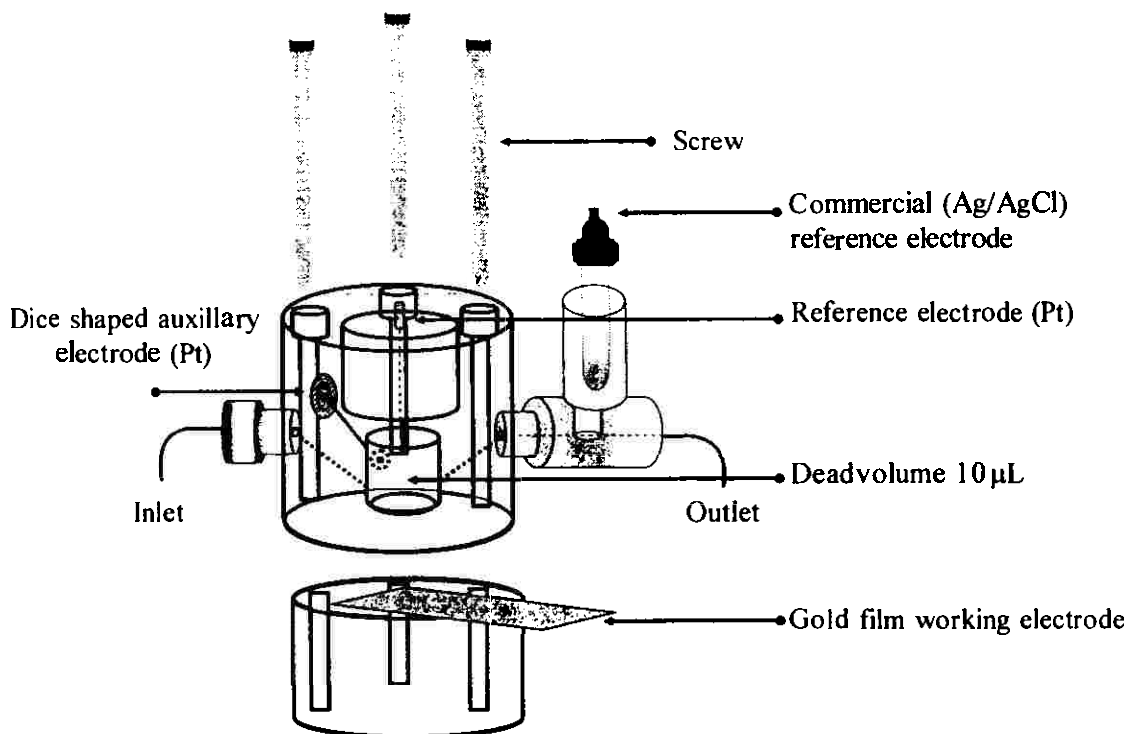
Figure 2.3 Schematic diagram showing the reaction flow cell. Sputtered gold working electode with immobilized anti-HCP was placed between the upper and lower parts of the flow cell and tighten by three screws. Reference electrode (Pt) was placed on the top and auxiliary electrode (Pt) on the side. Extra reference electrode (Ag/AgCl) was placed close to the flow cell in the out let stream.

2.3.4 Capacitive measurement

The capacitive measurement was performed by potentiostatic-step method. Potential pulses of 50 mV are applied every minute to the gold electrode yielding current response signal as described in chapter 1 (see section 1.6.3). In this set up a platinum wire was used as reference electrode, since it has no defined potential, an extra Ag/AgCl reference electrode was used to correct its potential (Bonal and Morel, 1996). The potential of the platinum wire and the Ag/AgCl reference electrode are measured just before a potentiostatic step (50 mV) is applied. The computer calculates which potential has to be applied to the platinum reference to make the platinum wire behaves as a virtual Ag/AgCl electrode. The purpose of

replacing the Ag/AgCl electrode by a platinum wire was to improve the speed of the potentiostatic control ((Bonal and Morel, 1996). Consequently, the decrease of capacitance was calculated after binding interaction between anti-HCP and HCP shown on the monitor and recorded as a function of time as illustrated in Figure 2.4. The interaction between anti-HCP and HCP were regenerated using 25 mM glycine-HCl pH 2.5.
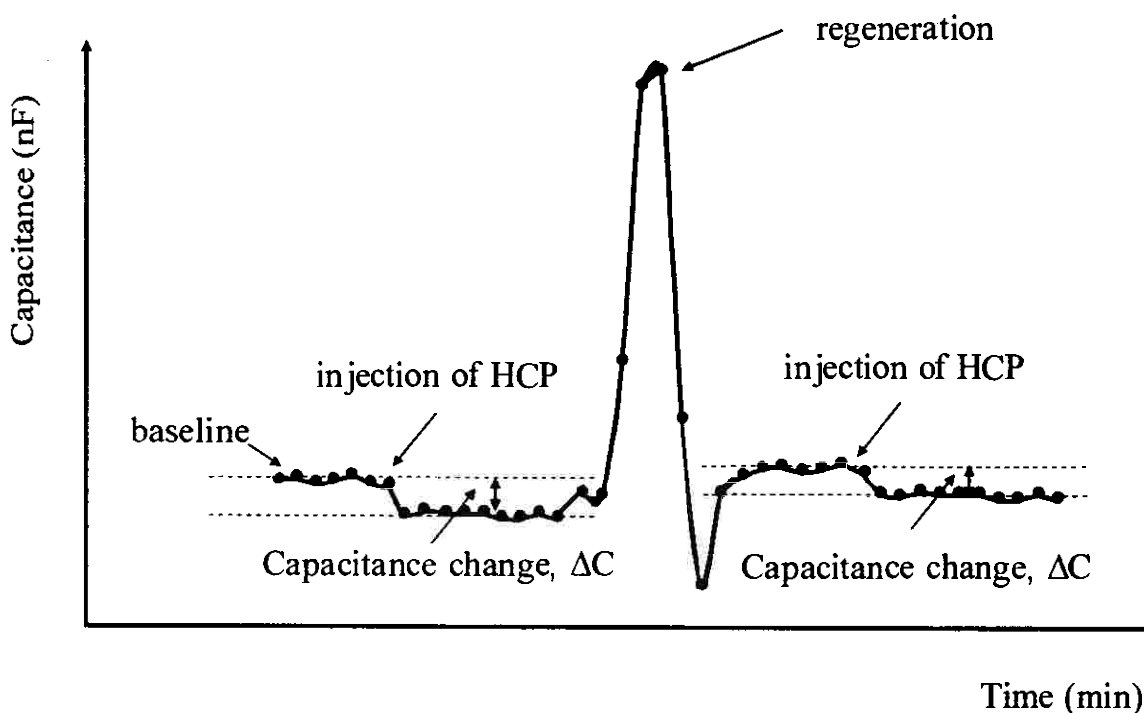
Figure 2.4 Schematic diagram showing the change in capacitance (ΔC) as a function of time caused by the binding between HCP and its antibody with subsequent signal increase due to dissociation under regeneration solution.

2.3.5 Operating conditions

The operating conditions for the study of capacitive immunosensor system were reviewed and used for the analysis of HCP as shown in Table 2.1 (Limbut et al., 2006, 2007; Wu et al., 2005; Yin et al., 2007).

Table 2.1 Operating conditions for capacitive immunosensor system

Conditions	Operating values	References
1. Regeneration solution		
Type	glycine-HCl	Wu *et al.*, 2005
Concentration (mM)	25	Limbut *et al.*, 2007
pH	2.5	Wu *et al.*, 2005
2. Sample volume (μL)	250	Limbut *et al.*, 2006
3. Flow rate (mL min^{-1})	0.1	Limbut *et al.*, 2006
4. Buffer solution	10 mM Sodium phosphate buffer pH 7.0	Yin *et al.*, 2007

2.3.6 Reproducibility

In this work, 25 mM glycine-HCl pH 2.5 was used as regeneration solution to break the affinity binding between HCP and anti-HCP. HCP was detected by regenerating the electrode intermittently over 2 days (15 times/day). The reproducibility performance of anti-HCP modified electrodes was evaluated by monitoring the change of capacitance signal at the same concentration of standard HCP 1.0×10^{-15} M.

2.3.7 Selectivity

The effect of other substances that might interfere with the response of the HCP in the capacitive immunosensor system was studied. The molecular weight of HCP was estimated as 50 kDa. The selectivity was studied by using albumin which might be a minor impurity in the purification process of LDH from *E. coli* (see 2.3.9) The selectivity was investigated by using human serum albumin (HSA) (68 kDa) and bovine serum albumin (BSA) (68 kDa).

2.3.8 Linear range, sensitivity and limit of detection

The calibration for capacitive immunosensor was performed by plotting the response vs. the analyte concentration or response change vs. logarithm of analyte concentration (Thévenot et al., 1999; 2001; Limbut et al., 2006). The linear range is the interval between upper and lower levels of the analyte concentration that have been demonstrated to be determined with linearity. Sensitivity, the slope of the calibration curve (Thévenot et al., 2001), is determined within the linear concentration range of immunosensor calibration curve.

The limit of detection (LOD) is defined as the lowest concentration of analyte in a sample that can be detected, though not necessarily quantitated (Swartz and Krull, 1997). There are several methods to evaluate LOD (Long and Wineforder, 1982; Miller and Miller, 1993; Taverniers et al., 2004). Because of the characteristic of the response, the LOD presented in this thesis follow the IUPAC Recommendation 1994 (Buck and Linder, 1994). It is defined as the concentration of the analyte at which the extraporated linear portion of the calibration curve intercepts the baseline-a horizontal line corresponding to zero change in response over several decade of concentration change (Figure 2.5)
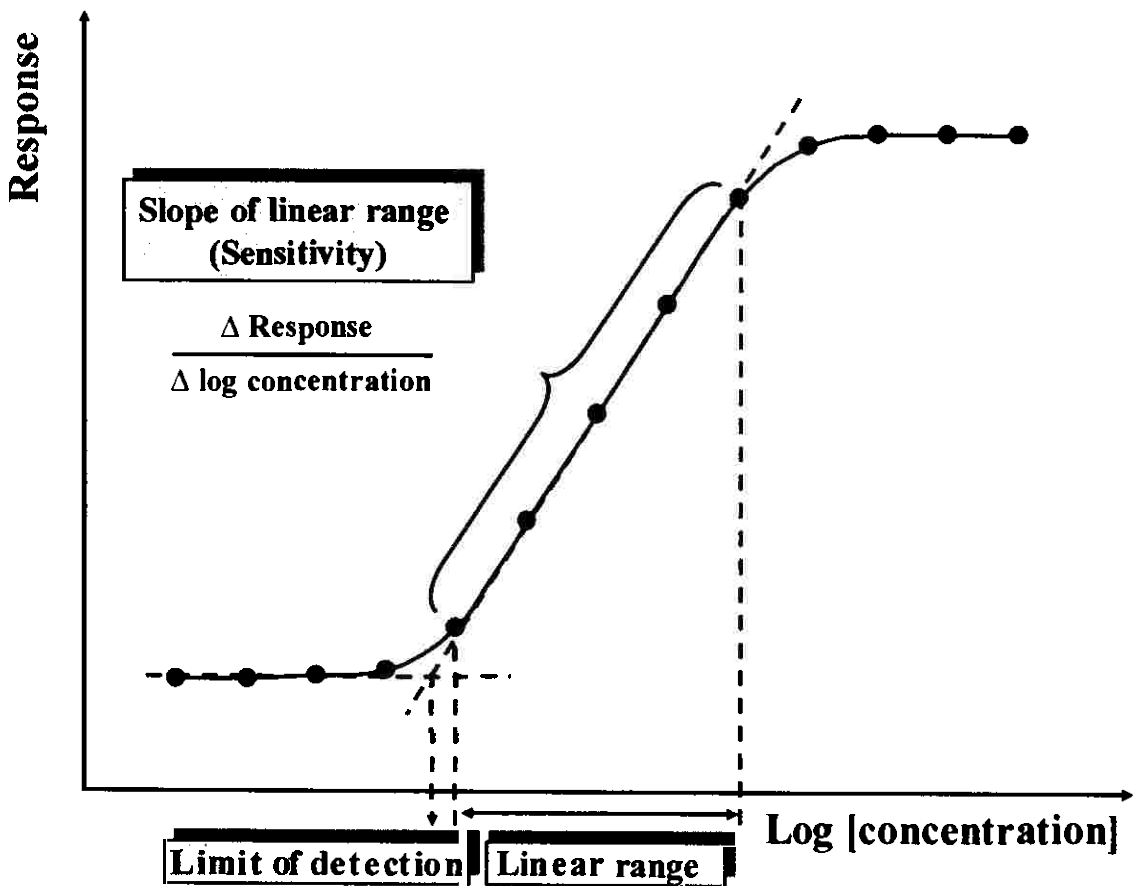
Figure 2.5 Calibration curve showing relation ship for determining linear range, sensitivity and limit of detection (Modified from Buck and Lindner, 1994).

2.3.9 Purification of enzyme Lactate Dehydrogenase (LDH)

In this study the purification of LDH was investigate as a model system. *Escherichia coli (E. coli)* was used as a host for the production of LDH. The residual HCP impurities during purification processes and in final purified protein will be investigated.

E. Coli was fermentated in two flasks (500 mL). Each flask contained 100 mL of an autoclaved 20 g/L Lulia-Bertani (LB) Broth (Difo^{TM}, Lennox). The culture was shaked for 24 h at 180 rpm, 30 °C. In this step, the cell will grow and can be seen by the increase turbidity of the medium (Figure 2.6 (1)). Cells were then centrifuged at 3,600 rpm (2,550 × g) for 30 min. One milliliter of supernatant was collected and labeled as S$_1$ (Figure 2.6 (2)), the rest was discarded. The cell pellet was

added with 20 mL of 0.1 M phosphate buffer, pH 7.0 and then mixed using a Vortex. Cell disruption to release LDH was accomplished by sonication technique using a sonication probe at an amplitude of 60 for 1 minute. One milliliter of sample was collected in 30 second and this was S_2. Sonication and sample collection were repeated for another 4 cycles where purification samples S_3-S_6 were obtained (Figure 2.6 (3)). Disrupted cell was then centrifuged at 3,600 rpm (2,550 × g) for another 30 min and 1 mL of the supernatant was collected for S_7(Figure 2.6 (4)).

The rest of the supernatant, after sampling for S_7, was used for further purification with immobilized metal affinity chromatography (IMAC) technique. Samples (S_1-S_7) were kept for the analysis of LDH activity and the present of HCP.
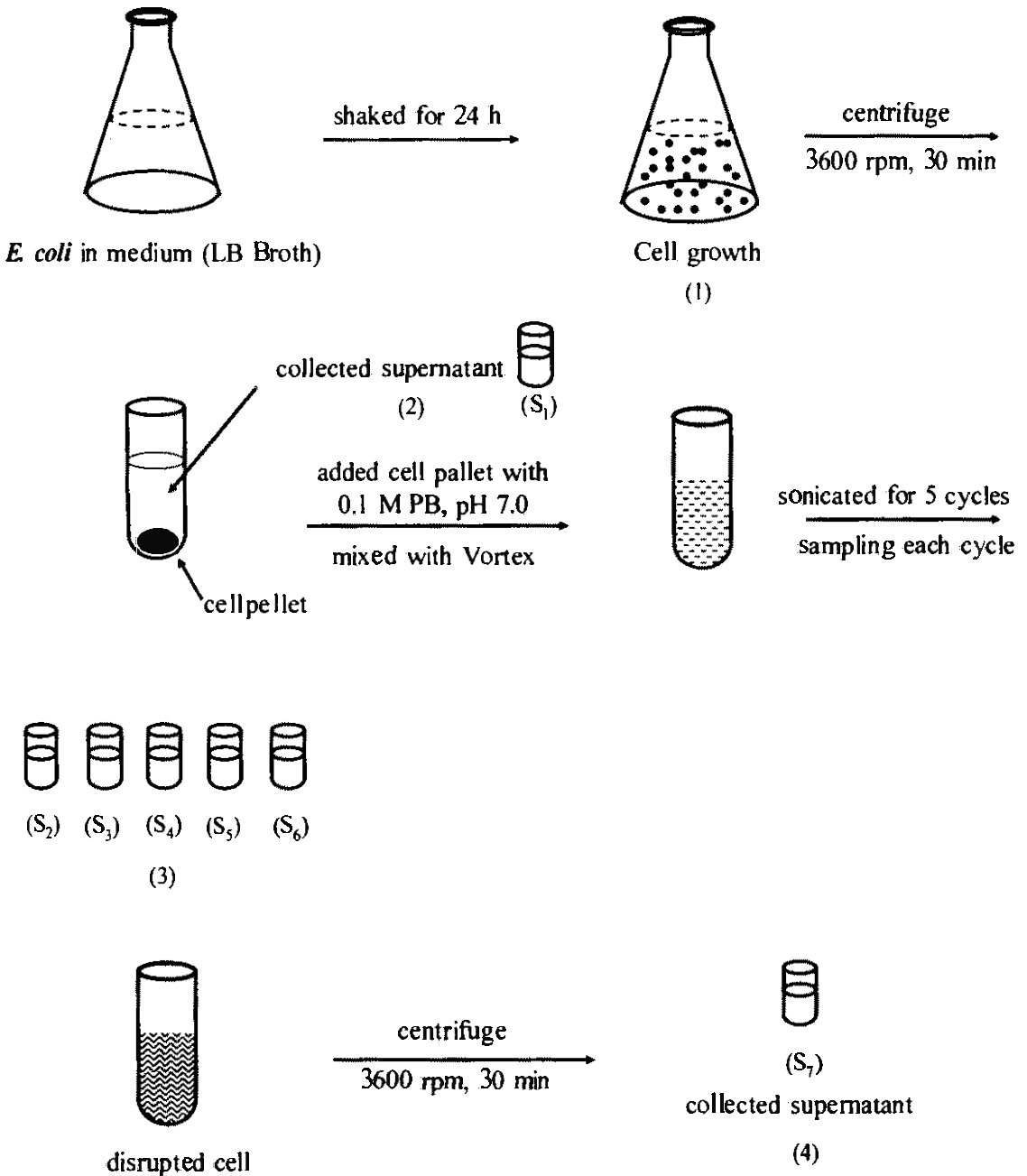
Figure 2.6 Schematic diagram showing the preparation of *E.coli* for the purification of LDH (1) fermentation of cell in LB broth medium, (2) collection of supernatant S_1, (3) collection of samples in each sonication cycle ($S_2 - S_6$) and (4) collecting supernatant of the disrupted cell after sonication step (S_7).

2.3.10 Immobilized Metal Affinity Chromatography (IMAC)

Figure 2.7 shows the experimental set up of IMAC system. The system consists of;

a) A 20 mL column where a transition metal (Cu^{2+}) was immobilized to the resin.

b) Peristaltic pump, where a steady flow rate of the solution was controlled at 0.6 mL min^{-1}.

c) Sample collector, where the sample were collected into the tubes.

Firstly, 5 mg mL^{-1} of Copper ($CuSO_4$) was immobilized to the Imino-DiAcetic acid (IDA) resin packed in the column by passing this solution into the column for 30 min. The column was then equilibrated with 20 mL of 100 mM EDTA to remove unbound Cu^{2+}. After that the column was passed with 60 mL of milli-Q water to remove excess EDTA. The supernatant (6 mL) was introduced. The column was then washed with 20 mM Tris-HCl buffer, pH 7.0. The fractions of washing step were collected into the test tubes for 10 min to obtain 6 mL at above flow rate by sample collector. In this step, the unbound protein will first be washed out through the column. The absorbance at 280 nm was measured until the value was close to zero, i.e. no more unbound protein in the column. His$_6$-tag protein of LDH which bound to the Cu-IDA with high affinity was then eluted with 200 mM imidazole. Fractions during the eluting step were collected in the same way as described above. They were then assayed for the activity of LDH.
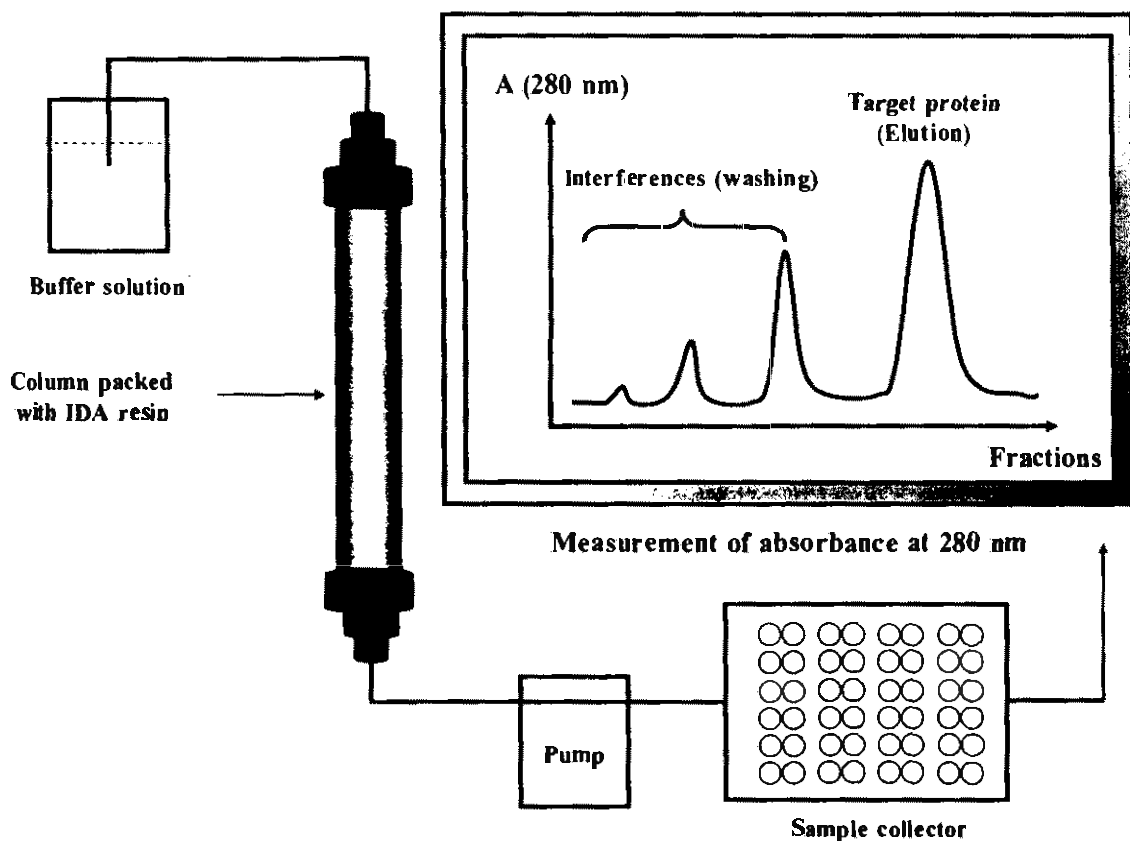
Figure 2.7 Experimental set up of immobilized metal affinity chromatography
(IMAC) for the purification of Lactate dehydrogenase (LDH). The set up
consists of a column packed with Imino-DiAcetic acid (IDA) resin.
Peristalltic pump carries solution flow through the column. During the
purificstion step, the washing and elution firactions are collected where the
absorbance was measured at 280 nm.

2.3.11 Assay for LDH activity

The assay ofi Lactate dehydrogenase (LDH) activity was investigated
through the following reaction;

$$\text{Pyruvate} + \text{NADH} \xrightarrow{\text{LDH}} \text{Lactate} + \text{NAD}$$

The reaction velocity is determined by a decrease in absorbance at 340
nm resulting from the oxidation of NADH. One unit causes the oxidation ofi one
micromole of NADH per minute at 25°C and pH 7.3, under the specific condition.

The assay was done by adding 2.8 mL of 0.2 M Tris-HCl, pH 7.3 with 0.05 mL of 6.6 mM NADH and 0.05 mL of 30 mM Sodium pyruvate. In this step no reaction occurred. The reaction was started by adding 0.05 mL of appropriated diluted standard LDH and ΔA_{340}/min was recorded and the calibration curve was plotted. All purification samples were assayed for the activity of LDH by adding 0.05 mL of appropriated dilution of each samples. The reaction rate (ΔA_{340}/min) was recorded and the concentration of LDH in the samples were evaluated by comparing the reaction rate of the samples to the standard curve prepared using standard LDH.

2.3.12 Analysis of Host Cell Protein (HCP)

In this study the purification of LDH using IMAC was used as a model study for the investigation of HCP residued in purification process. The samples obtained from first collected supernatant, S_1 and cell disruption steps, S_2-S_7 were analysed for HCP using capacitive immunosensor system. In this case we expected to see the present of HCP released from the cell during disruption. The analysis of HCP was also performed in purification process of IMAC. Fractions of washing and elution steps were tested. For capacitive measurement, standard HCP solution from 1.0×10^{-17} to 1.0×10^{-13} M were used to perform the calibration curve. Unknown samples were diluted 10 times before analyzing by the capacitive immunosensor system. The capacitance change (-nF cm^{-2}) of each unknown samples were then compared to the calibration curve to obtained the concentration of the residual HCP.

2.4 Capacitive immunosensor for human serum albumin (HSA)

2.4.1 Fabrication of thermally evaporated gold electrodes

Microscope slides were cut into strips (5.0×25.4 mm.), cleaned with Piranha solution through sonication for 5 min and rinsed with deionized water several times. They were dried in an oven at 100 °C for 1 h. Chromium was first coated on the microscope slide surface using a thermal evaporator (Edwards Auto 306, UK) by applying a current of 60 mA at 5×10^{-6} mB. In this step chromium of ca. 5 nm was deposited on glass surface. Then gold was coated on the chromium layer by applying a current of 40 mA at the same pressure until a thickness of ca. 200 nm was obtained.

The fabricated electrodes were then characterized with regard to their surface properties using Atomic Force Microscopy (AFM), (Seiko instrument, Japan). The scans were obtained by the computer controlled device SPI4000 by contacting mode using cantilever of the type CSG10 (Molecular Device and Tools for Technology (NT-MDT)).

2.4.2 Immobilization of anti-HSA

Since the strategies of immobilization using SAM is time consuming (Hedström et al., 2005; Limbut et al., 2006; Thavarungkul et al., 2007) due to the completed adsorption of thiol compound need several hours (Hedström et al., 2005; Limbut et al., 2006; Thavarungkul et al., 2007). Therefore, electropolymerization of non-conducting polymer was studied for the immobilization of antibody.

In this work the electropolymerization of *ortho* phenylenediamine (*o*-PD) was used to generate a thin film of polymer on the electrode for the immobilization of anti-HSA. The method of immobilization was modified from the work of Karalemus *et al* (2000), Cheng *et al* (2001) and Limbut *et al* (2006). Electropolymerization of *o*-PD was performed by cyclic voltammetry (Figure 2.8) in the potential range of 0-0.8 V (vs. Ag/AgCl) at a scan rate of 50 mVs^{-1} from a 5 mM solution of *o*-PD in 10 mM acetate buffer pH 5.18. In this step, polymer was coated on the electrode surface where amino groups are provided at the backbone of the polymer chain as shown in Figure 2.9 (1) (Yano and Nagoaka, 1996)

Gold electrodes with modified polymer were rinsed with distilled water to remove undeposited polymer before being dipped in 5.0% (v/v) glutaraldehyde in 10 mM sodium phosphate buffer pH 7.0 at room temperature for 20 min. The electrodes were throughly rinsed with 10 mM sodium phosphate buffer pH 7.0. In this step the amine group of the polymer will be modified to expose free aldehyde group (Figure 2.9 (2)). The modified electrodes were then dried with nitrogen gas and finally, 20 μL of anti-HSA (0.5 g/L) was placed on the surface of gold electrode and coupling reaction took place overnight at 4 °C (Figure 2.9-3). The electrodes were then wash with 10 mM phosphate buffer for several times to remove unbound anti-HSA and they were then immersed in 0.1 M ethanolamine pH 8.0 for 20

min to occupy all aldehyde groups that did not couple to anti-HSA. When not in use electrodes were kept at 4 °C in Petri dish saturated with nitrogen gas.

The number of cycles for the electropolymerization of o-PD was studied at 5, 10, 15 and 20 cycles. Then the sensitivities of the electrode to standard HSA 1.0×10^{-14} to 1.0×10^{-10} M obtained from four different number of cycles were measured and compared.

Electrochemical characteristics of the modified electrode were investigated after each modification step. The degree of insulation was examined with a permeable redox couple ($K_3[Fe(CN)_6]$) through electron transfer kinetics of $[Fe(CN)_6]^{4-}/[Fe(CN)_6]^{3-}$ redox reactions using cyclic voltammetry in the electrolyte solution. The experiment set up of cyclic voltammetry measurement was shown in Figure 2.10.
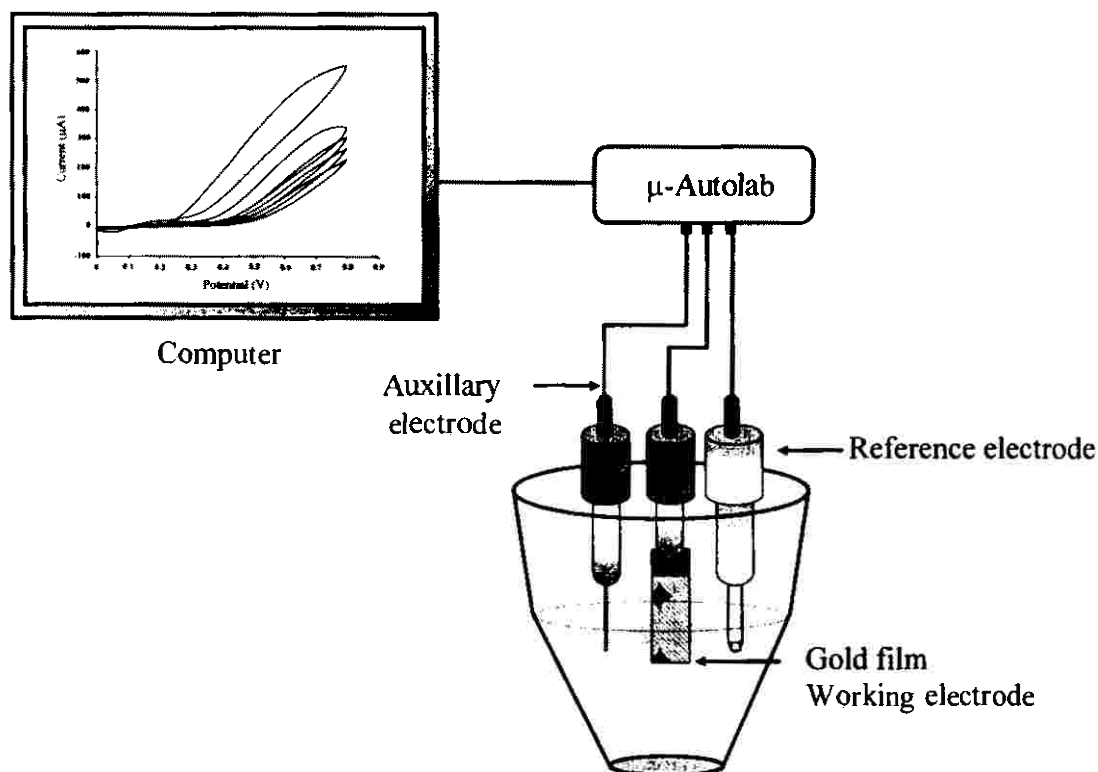
Figure 2.8 Schematic diagram showing the cyclic voltammetry system for electropymerization of *ortho*- phenylenediamine (*o*-PD).
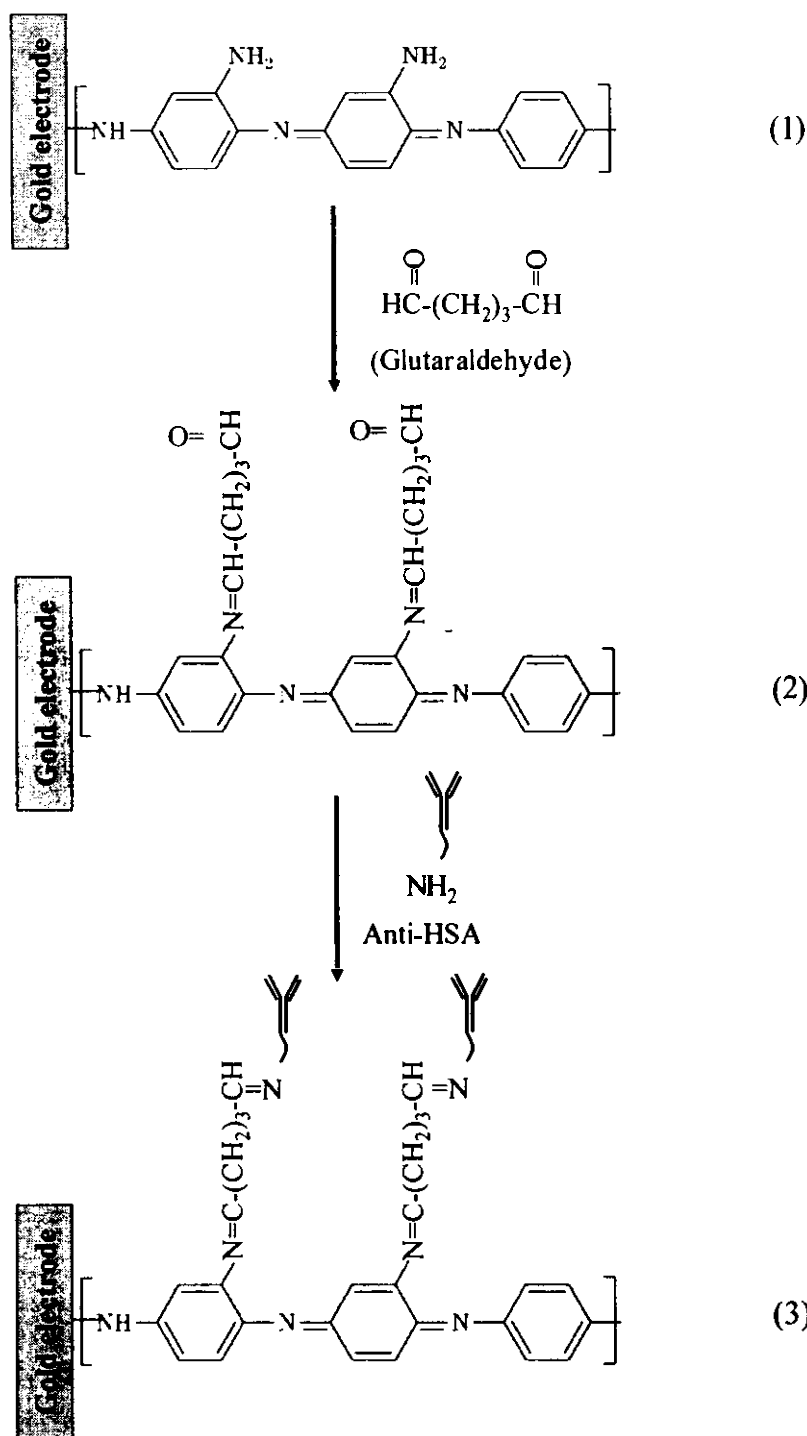
Figure 2.9 Reaction mechanisms for the immobilization of anti-HSA (1) modified
electrode with free amino group of *o*-PD by electropolymerization, (2)
treated with glutaraldehyde to modify amine group of polymer to expose
free aldehyde group and (3) immobilization of anti-HSA through covalent
coupling reaction.
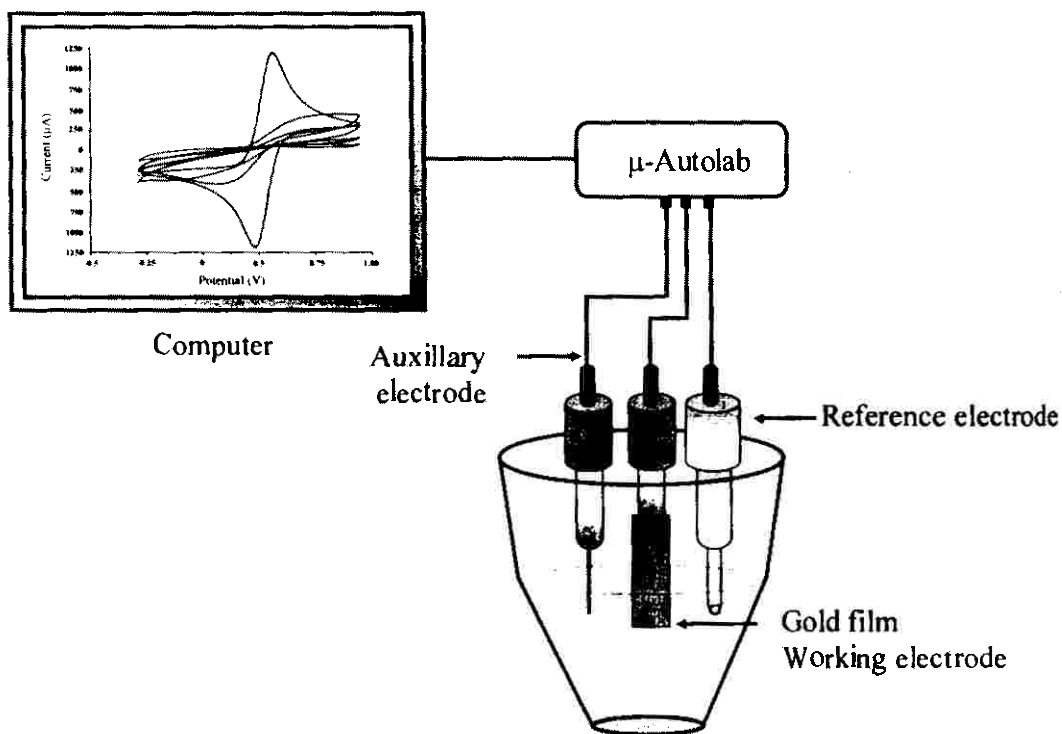
Figure 2.10 Schematic diagram showing the cyclic voltammetry system for the study
of electrochemical characteristic of modified electrode (Modified from
Limbut, 2006).

2.4.3 The flow injection system

Figure 2.11 shows the basic experiment set-up of the flow injection
capacitive immunosensor system. This set up is similar to the one described in section
2.3.3 except the part of the detection unit.

The detection unit consisted of a reaction flow cell and an
electrochemical detection system, Potentiostat (EA161, Australia) and e-corder 401
hardware unit (ED401, Australia). The eDAQ scope^{TM} 4.0.2 software was used to
monitor the current response signal. The flow cell (Figure 2.11) with a dead volume
of 10 μL consisted of three electrodes, a Ag/AgCl reference electrode at the top, gold
working electrode at the bottom and stainless steel tube (i.d. 0.4 mm, o.d. 1.1 mm,
length 20 mm) acting as an auxilliary electrode and solution outlet. The potentiostatic
step (50 mV) can be applied to the working electrode compared to the potential of
Ag/AgCl.

A capacitive immunosensor for the detection of HSA was investigated. When HSA was injected into the flow system it bound to anti-HSA modified on gold electrode, causing the decrease of capacitance (see Figure 2.4).
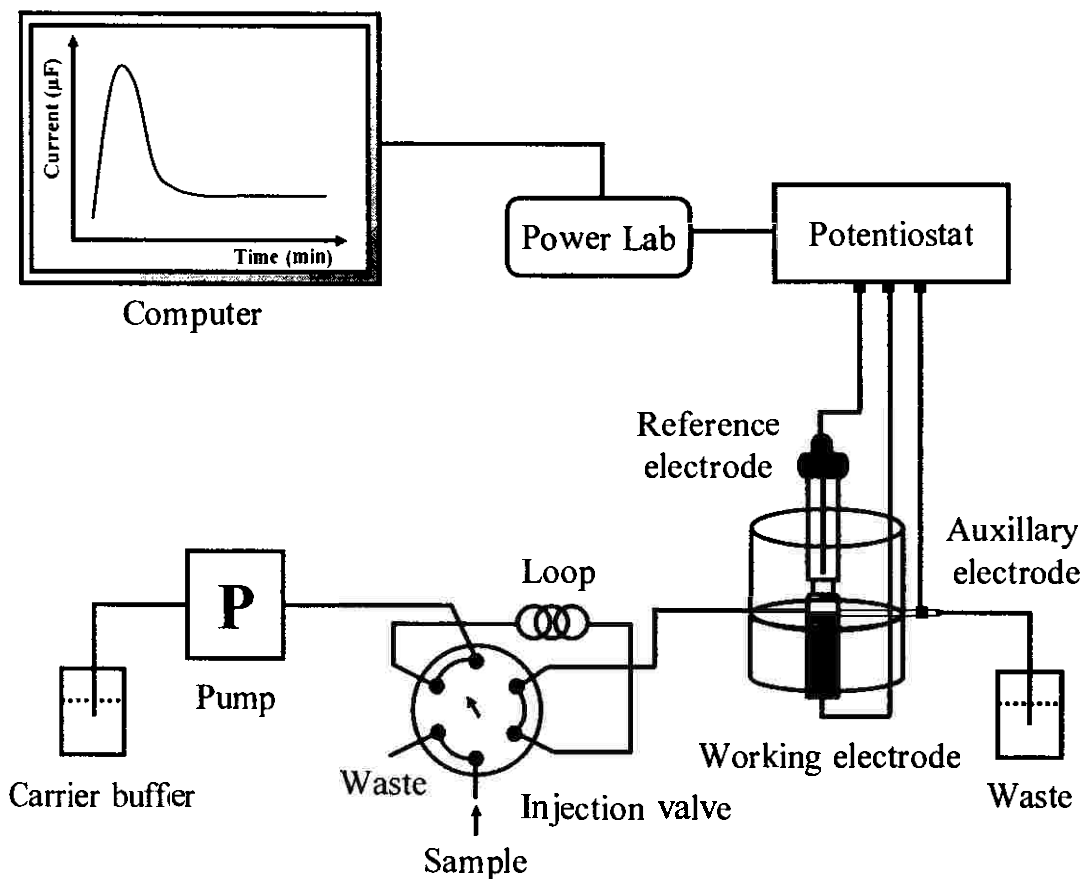
Figure 2.11 Schematic diagram showing the flow injection capacitive immunosensor system. The peristaltic pump carries the carrier buffer to the flow cell and passes to the outlet. Samples were injected to the system through injection valve and carried by carrier buffer through the flow cell. The results retrieved during the potentiostatic step due to the interaction of HSA to anti-HSA modified electrode are processed using a potentiostat (EA161) measurement and control system powered by a computer.
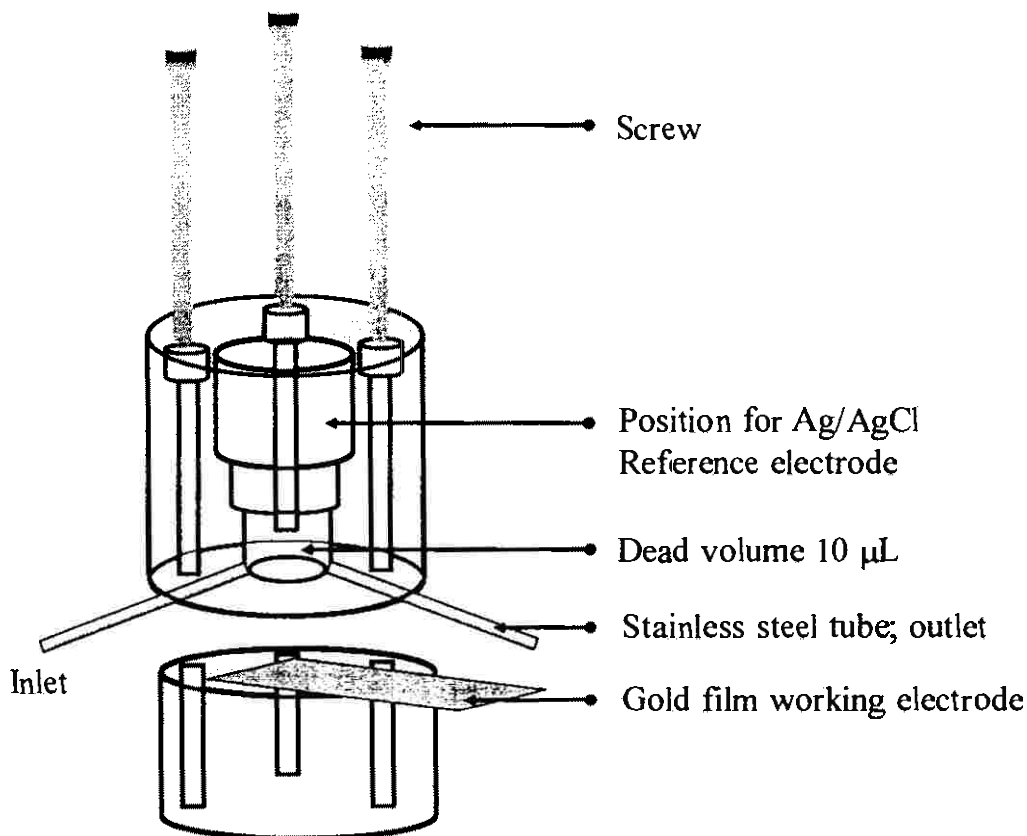
Figure 2.12 Schematic diagram showing the reaction flow cell. Thermally evaporated gold electrode was placed between the two parts of flow cell.

2.4.4 Capacitive measurement

The capacitive measurement was measured through a potentiostatic-step as described in section 2.3.4. When the solution containing HSA was injected to the system, HSA bound to the immobilized anti-HSA on the electrode. This will increase the thickness on the surface of electrode causing the capacitance to decrease until it reaches a stable value. In this measurement the current-time response signal was obtained and shown on the computer (see Figure 1.13) and its behavior can be described as equation 1.5 Taking logarithm of equation 1.5, equation 1.6 was obtained and then capacitance could be calculated from the intercept of the curve.

The change in capacitance due to the binding was obtained by subtracting capacitance after the binding from the capacitance before the binding. The surface of the electrode was then regenerated with HCl pH 2.5 to remove HSA from the immobilized anti-HSA on the electrode.

2.4.5 Optimization

The operating conditions were optimized for the type and pH of regeneration solution, sample volume, flow rate, type, concentration and pH of carrier buffer. The operating conditions were considered by balancing between high capacitance signal and the time needed for one analysis. All optimizations were carried out using standard HSA 1.0×10^{-14} M except the part for the type of carrier buffer, standard HSA in the range from 1.0×10^{-4} to 1.0×10^{-10} M were investigated.

2.4.5.1 Regeneration solution

To ensure reproducible measurements, a complete regeneration of the surface between sample injections must be obtained without affecting the characteristics of ligand. Ideally the regeneration solution should remove all compounds that bind non-covalently to surface, the binding capacity of the surface should not be affected by the regeneration and the baseline should remain at constant level. The binding interaction between anti-HSA and HSA is based on hydrogen bonding with can be regenerated by using low pH solution (Wu *et al.*, 2006). Glycine-HCl and HCl were used for the optimization. 50 mM glycine-HCl was initially tested at pH 2.2 and 2.8 since this value are the lowest and highest pH of the studied range and then HCl at pH 2.2, 2.4, 2.5, 2.6 and 2.8 were tested.

2.4.5.2 Flow rate and sample volume

In the flow injection capacitive immunosensor system, the flow rate and volume of the sample passing through the capacitive flow cell are two main factors affecting the yield of interaction between HSA and anti-HSA immobilized on the electrode. Therefore, these two parameters were optimized at the same time. The sample volume was investigated at 150, 200, 250, 300 and 350 μL. For each sample volume flow rate was studied at 0.025, 0.05, 0.1, 0.15 to 0.2 mL min⁻¹.

2.4.5.3 Concentration and pH of buffer solution

The concentration and pH of Tris-HCl buffer was optimized at the same time. The concentration was first tested at 5 mM and the pH was varied from 7.0, 7.2, 7.4, 7.6 and 7.8. Higher concentrations were then tested at 10, 15 and 20 mM with the pH varied from 7.0 to 7.8. The optimization of concentration and pH of phosphate buffer solution were done in the same way. The concentration and pH that provided highest capacitance change response ($-nF\ cm^{-2}$) will be selected and used as optimum condition for concentration and pH of buffer solution.

2.4.5.4 Type of buffer solution

Two types of buffer at their optimum condition, 10 mM tris-HCl pH 7.0 and 10 mM sodium phosphate buffer pH 7.0 (optimum condition from 2.3.5.3) were studied for the optimization of type of buffer. The capacitance change ($-nF/cm^{-2}$) to standard HSA from 1.0×10^{-14} M to 1.0×10^{-10} M was studied and the sensitivity (slope of the calibration curve) obtained by the two buffers were compared. The buffer that provides higher sensitivity will be selected as an optimum type of buffer solution.

The tested values for all optimization of the operating parameters are summarized in Table 2.2.

2.4.6 Reproducibility

In this work, HCl pH 2.5 was used as regeneration solution (the optimum from 2.3.5.1) to break the affinity binding between HSA and anti-HSA. HSA was detected by regenerating the electrode intermittently over 3 days (12 times/day). The reproducibility performance of anti-HSA modified electrodes was evaluated by monitoring the change of capacitance signal at the same concentration of standard HSA (1.0×10^{-14} M) at optimum conditions.

Table 2.2 Tested values for operating conditions.

Conditions	Tested value
1. Regeneration solution	
- Glycine-HCl (pH)	2.2, 2.8
- HCl (pH)	2.2, 2.4, 2.5, 2.6, 2.8
2. Sample volume (µL)	150, 200, 250, 300, 350
3. Flow rate (mL min^{-1})	0.025, 0.05, 0.10, 0.15, 0.20
4. Buffer solution	
Type	Tris-HCl, sodium phosphate buffer
pH	7.0, 7.2, 7.4, 7.6, 7.8
concentration (mM)	5, 10, 15, 20

2.4.7 Selectivity

Selectivity is the ability to discriminate between difference substrates and concerns the range of chemical species which can interact with the sensor. The effect of substances that might interfere with the response of the HSA in the capacitive immunosensor system was studied. Bovine serum albumin (BSA) with molecular weight of 68 kD closed to the molecular weight of HSA (68 kD) was used to test the selectivity of the system.

2.4.8 Linear range, sensitivity and limit of detection

The criteria for the evaluation of linear range, sensitivity and limit of detection for the study of capacitive immunosensors system for the detection of HSA was the same as described in section 2.3.8.

2.4.9 Determination of albumin in human serum samples

Human serum samples obtained from Songklanakarin hospital, Hat Yai, Thailand were analysed to demonstrate the use of the capacitive immunosensor system. All samples were analysed by the flow injection capacitive immunosensor system under optimum conditions. The samples were diluted appropriately (see section 2.4.15) and sample solutions were injected to the capacitive immunosensor system. The change in capacitance value for each sample was used to determine the concentration of albumin in the samples using standard calibration curve done prior to the test.

2.4.10 Method validation

Method validation is the process of defining an analytical requirement, and confirming that the method under consideration has performance capabilities consistent with what the application required (Eurachem Guide, 1998). In this work, the purpose of method validation is to demonstrate that the developed capacitive immunosensors system can be used for the determination of HSA. Matrices interference and recovery were studied to validate the method.

2.4.11 Matrices interference

Matrices effects play an important role in analytical measurement and have a number of effects to the analysis (Eurachem Guide, 1998). Interferences usually affect the slope of calibration curve differently than will the analyte of interest, so the slope of the calibration curve in the method of additions may effects the linearity of the curve.

Fortified samples with known amount of HSA were used to determine the matrices interference. HSA standard, 3.0×10^{-D}, 5.0×10^{-D}, 7.0×10^{-10} and 1.0×10^{-9} M were used to construct the standard curve. Human serum samples were added

with different concentration of standard HSA. Sample with different dilution factors were injected to the system. The dilution factor provided signal in the range of calibration will be used for the investigation matrices effect. The responses were plotted against the known concentration of added HSA standard. The slope of the standard curve and matrices-based curve were compared to evaluate the effect of matrices interference using two-way analysis of variance (two-way ANOVA) with R program. The study of matrices interference was also performed in the lower range. The standard curve was studied from 3.0×10^{-11}, 5.0×10^{-11}, 7.0×10^{-11} and 1.0×10^{-10} M. In this case, the evaluation of matrices interferences was done in the same way as describe previously.

2.4.12 Recovery

The study of recovery was done by addition method. The standard curve and the fortified sample curve (matrices-based curve in 2.4.15) from the study of matrices interference were used to evaluate the recovery. Percentage recoveries were calculated by equation 2.1

$$\text{Recovery}(\%) = \frac{C_1 - C_2}{C_3} \times 100 \qquad (2.1)$$

Where C_1 is the concentration determined in fortified sample, C_2 is concentration determined in unfortified sample and C_3 is concentration of fortification (Eurachem Guide, 1998).

2.4.13 Method comparison

Concentrations of albumin in human serum samples determined by the developed capacitive immunosensors system were compared with Albumin BCG method (the result obtained from Songklanakarin hospital).

CHAPTER3

RESULTS AND DISCUSSION

In this work, electrodes were fabricated by sputtering and thermal evaporation techniques. They were tested in capacitive immunosensor system with two different antibody (Ab)-antigen (Ag) pairs. Sputtered gold electrodes were tested with anti host cell protein (anti-HCP)-host cell protein (HCP) pair and thermally evaporated gold electrodes were tested with anti human serum albumin (anti-HSA)-human serum albumin (HSA).

3.1 Capacitive immunosensor for host cell protein (HCP)

3.1.1   Fabrication of sputtered gold electrode

Thin gold film electrodes fabricated by coating of gold on microscope slides with Cr as an adhesion layer using sputtering technique are shown in Figure 3.1. These electrodes were immobilized with anti-HCP using self assembled monolayer (SAM) of thioctic acid and were used as working electrodes in a capacitive immunosensor system.

3.1.2   Capacitive measurement

Capacitive measurement was performed by potentiostatic method. For preliminary study, the flow injection detection of HCP by the immobilized anti-HCP electrode, under the operating conditions of Table 2.1, was tested. The decrease in capacitance due to the binding interaction between anti-HCP immobilized on sputtered gold electrode and various concentrations of HCP is shown in Figure 3.2.
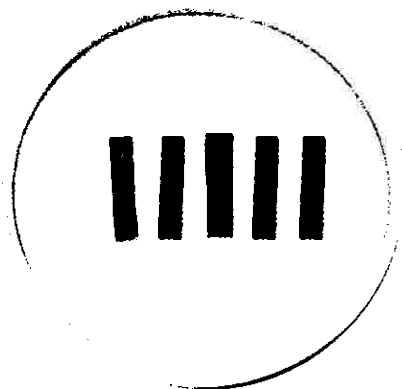
Figure 3.1 Thin film gold electrodes fabricating by sputtering technique.

$$y = (1.9 \pm 0.3) \, Log \, (x) + (81 \pm 6)$$

$$R = 0.9950$$
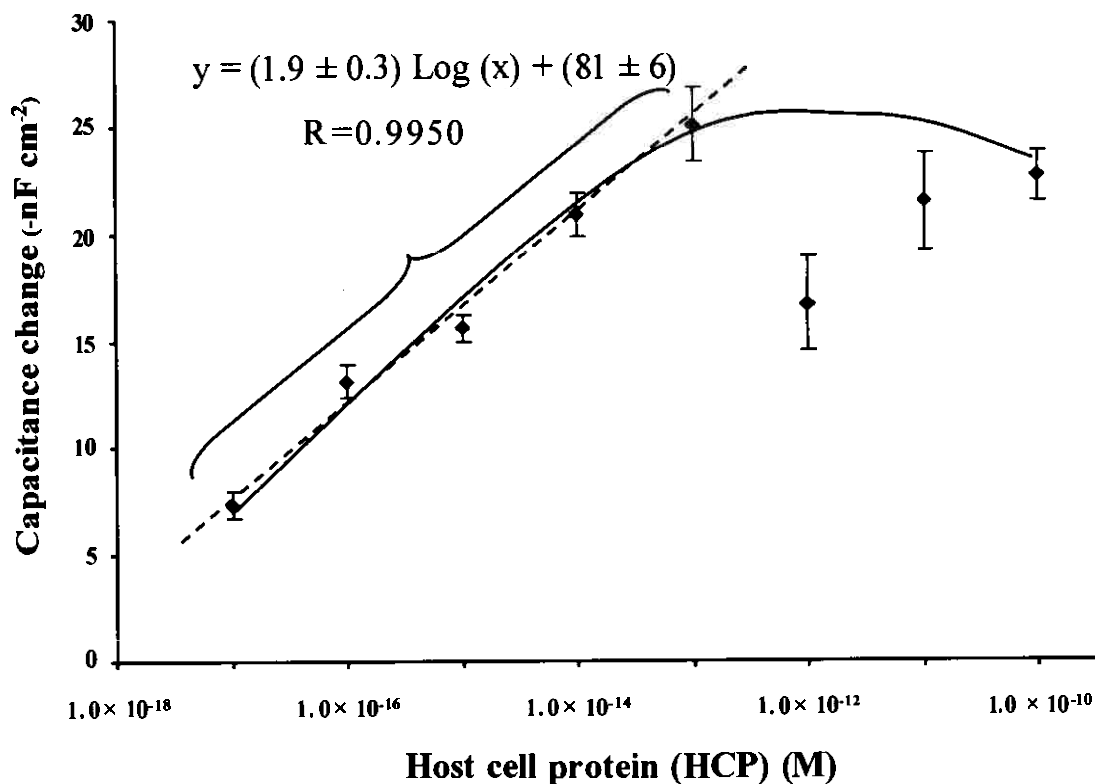
Figure 3.2 Response of a flow injection capacitive immunosensor system for the preliminary test of the binding between HCP and anti-HCP (n=3).

From this preliminary study, the binding interaction between HCP and anti-HCP modified electreode provides a linear relationship between capacitance change (-nF cm^{-2}) and logarithm of HCP concentration in the range of 1.0×10^{-17} to

1.0×10^{-13}M. A detection range of 1-100 ppm ($2.0 \times 10^{-8} - 2.0 \times 10^{-6}$ M) of residual HCP has been quoted as a regulatory (and analytical) benchmark for therapeutic proteins (Eaton, 1995; Liu, 1983) and 1-10 ppm ($2.0 \times 10^{-8} - 2.0 \times 10^{-7}$ M) for biopharmaceutical requirement (Garnick *et al.*, 1998). This suggests that the detection range of the capacitive immunosensor system is low enough for the analysis of HCP in biotechnology purification process. Therefore optimization of the flow injection of capacitive immunosensor system was omitted.

3.1.3 Reproducibility

The reproducibility of anti-HCP modified electrode was evaluated by monitoring the capacitance change ($-nF$ cm^{-2}) at the same concentration of standard HCP (1.0×10^{-15}M), 14 times per day for 2 days. After each analysis, 250 µL of 25 mM glycine-HCl pH 2.5 was injected to break the binding between anti-HCP and HCP. The percentage of residual activity of anti-HCP electrode versus the number of injections is shown in Figure 3.3. During the first 25 cycles the binding activity of anti-HCP electrode retained about 98 ± 5 % of the original capacitance change. This suggests that anti-HCP electrode can be reused with good reproducibility up to 25 times with a relative standard deviation (RSD) of 5 %. After 25 times of regeneration the binding activity of anti-HCP electrode decreased rapidly. The reduction of the activity may cause by the lost of anti-HCP activity after prolong used, removal of the antibody from the surface, or the lost of SAM layer. However, it was reported that the immobilization using SAM is very strong and was not lost after several regeneration (Thavarungkul, 2007). Therefore, the decrease of residual activity was most likely due to the lost of antibody and/or its activity.
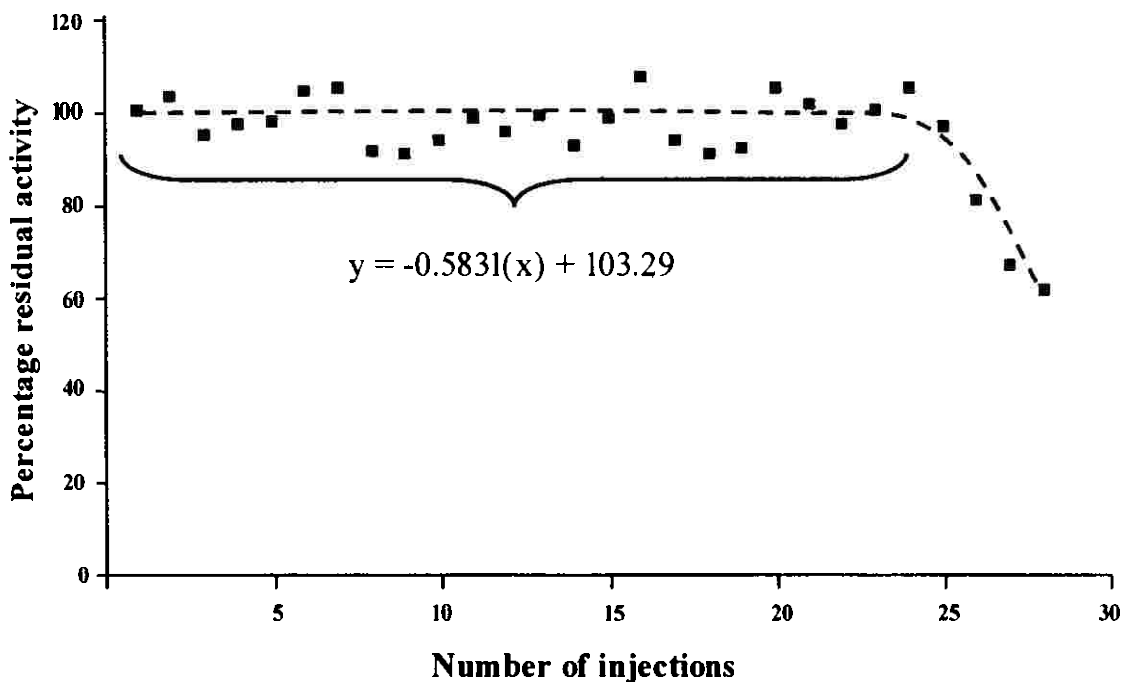
Figure 3.3 Reproducibility of the response from an anti-HCP modified electrode to injection of 250 μL of a standard solution of anti-HCP (1.0×10^{-15} M) with regeneration and reconditioning steps between each individual assay.

3.1.4 Selectivity

Human serum albumin (HSA) and bovine serum albumin (BSA), the proteins that might be a minor impurity in the purification process of LDH from *E. coli*, were used to investigated the selectivity of the system. Figure 3.4 shows the response of HCP, HSA, and BSA at the same concentration ranging from 1.0×10^{-15} to 1.0×10^{-13}M. The capacitance change ($-nF$ cm^{-2}) obtained from HCP was higher than the two obtained from HSA and BSA. The decrease of the capacitance change of HCP corresponded to the concentration. In contrast, the capacitance changes of HSA and BSA at every concentration were almost the same. The results show that the anti-HCP modified electrode was selective to HCP. However at 1.0×10^{-15} M. The responses obtained from HSA and BSA are closed to HCP and these are higher than response form the injection of blank (4.3 ± 0.2 $-nF$ cm^{-2}). Therefore, the present of HSA and/or BSA might effect the analysis of HCP in real samples.
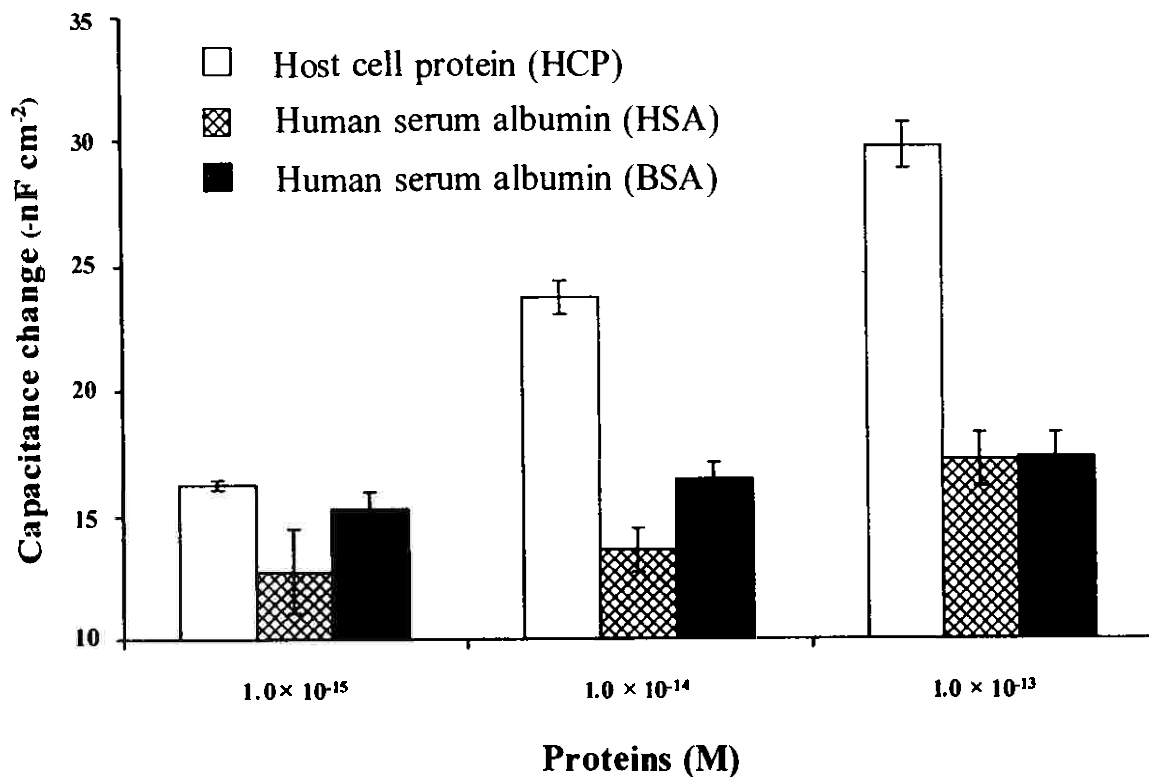
Figure 3.4 Effect of anti-HCP to host cell protein (HCP), human serum albumin (HSA) and bovine serum albumin (BSA) (n=3).

3.1.5 Linear range, sensitivity and limit of detection

Standard solution of HCP in the range of 1.0×10^{-20} to 1.0×10^{-11} M were injected to the capacitive immunosensor system to investigated the lineality, sensitivity and limit of detection. The plot of this investigation was done between the capacitance change (-nF cm^{-2}) and logarithm of HCP concentration (M) (Figure 3.5). A linear relationship were obtained between 1.0×10^{-17} to 1.0×10^{-13} M. The detection limit was 8.0×10^{-17} M, based on IUPAC recommendation 1994 (Buck and Linder, 1994). The LOD was very much lower than the one reported by Zhu *et al.* (2005) i.e. 1.2×10^{-10} M who mentioned that their LOD is lower than ELISA technique. Therefore, the capacitive immunosensor is suitable for quanitative analysis of the residual HCP in biotechnology process.
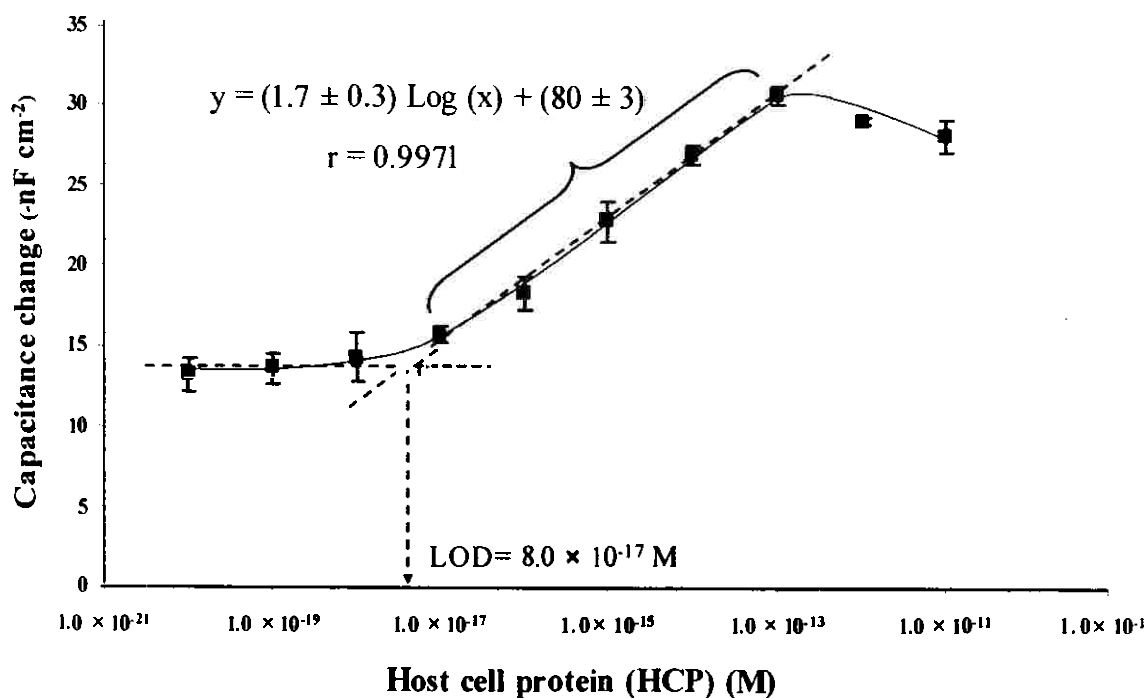
Figure 3.5 Capacitance change (-nF cm^{-2}) vs. logarithm of host cell protein (HCP) concentration (response from blank is 5.2 ± 0.3 –nF cm^{-2}) (n = 3).

3.1.6 Purification of enzyme Lactase Dehydrogenase (LDH).

Escherichia coli (E. coli) was used as a host for the production of LDH. The purification of LDH was used as a model in order to investigate the residual HCP impurities during purification processes and in final purified protein. The strategies for the purification of LDH have been discussed in section 2.3.9. The samples during purification process, i.e. supernatant after cell cultivation (S_1), cell disruption ((S_2-S_6), supernatant after cell disruption (S_7) and sample during purification with immobilized metal affinity chromatography (IMAC) (W_2-W_5, W = washing step and E_{23}-E_{30}, E = eluting step) were tested for the activity of LDH, total protein and residual HCP impurities.

3.1.7 Immbilized metal affinity chromatography (IMAC)

The supernatant after cell disruption (S_7) obtained from section 2.3.9 was used for the purification of LDH using IMAC technique. A volume of 6 mL of S_7 was introduced to Cu^{2+} immobilized IMAC column packed with Imino DiAcetic acid (IDA) resin. The column was then washed with 20 mM Tris-HCl, pH 7.0 and 6 mL of

fractions in this step were collected. The measurement of the absorbance at 280 nm for the investigation of proteins during the washing step is shown in Figure 3.6. Proteins without his_6-tag that do not bind to the Cu-IDA will be washed out and can be observed as the increase of the absorbance at 280 nm. Most of these unbound proteins are found in fraction 2 (A = 1.96) and were gradually decrease in further fractions. After 20 fractions of the washing step, the absorbance at 280 nm is closed to 0. This indicates that all of unbound proteins have been washed out and only the target proteins are retained in the column. His_6-tag protein bound to the Cu-IDA with high affinity was then eluted with 200 mM imidazole. As shown in Figure 3.6, fraction 24 (A = 0.65) and 25 (A = 0.96) provide high absorbance at 280 nm. Lactase Dehydrogenase (LDH) is expected to be presented in these two fractions and they were then assayed for the activity of LDH.
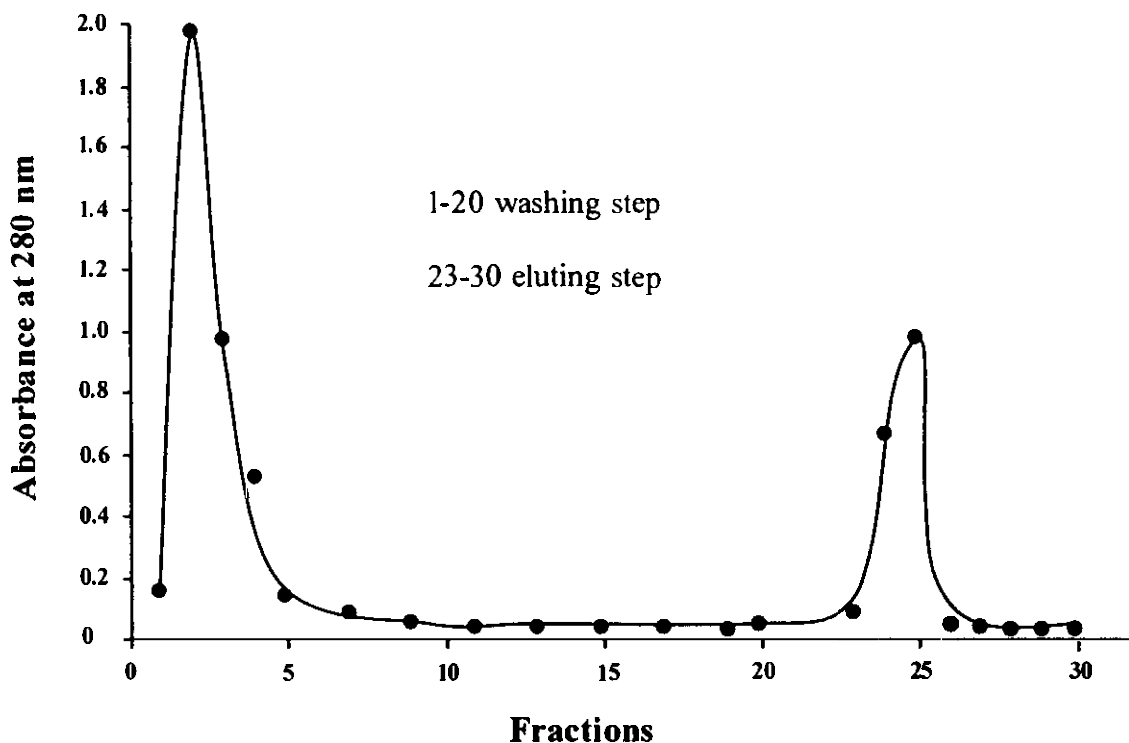
Figure 3.6 Absorbance of the fractions obtained from washing and eluting step in the purification of LDH from *E. coli* using immobilized affinity chromatography (IMAC) technique, (1-20 and 23-30 are fractions from the washing and eluting steps, respectively).

3.1.8 Assay for LDH activity

Fractions obtained from the washing and eluting steps (section 3.1.9) in purification processes of LDH using IMAC technique were assayed for LDH activity. Other samples were also tested, i.e. supernatant after cell cultivation (S_1), cell disruption ((S_2-S_6) and supernatant after cell disruption (S_7). The calibration curve of standard LDH was first performed (Figure 3.7) by plotting between reaction velocities at 340 nm (ΔA_{340}/min) and concentration of standard LDH (0.49, 0.61 and 0.73 μg mL^{-1}). Since the standard deviation of calibration curve (n = 3) are in the range of 0.0009-0.001 which is relatively small, therefore the assay for LDH activity for purification samples are performed in duplicates. The concentrations of LDH in unknown samples were determined by comparing their reaction velocities to the standard curve prepared using standard LDH.
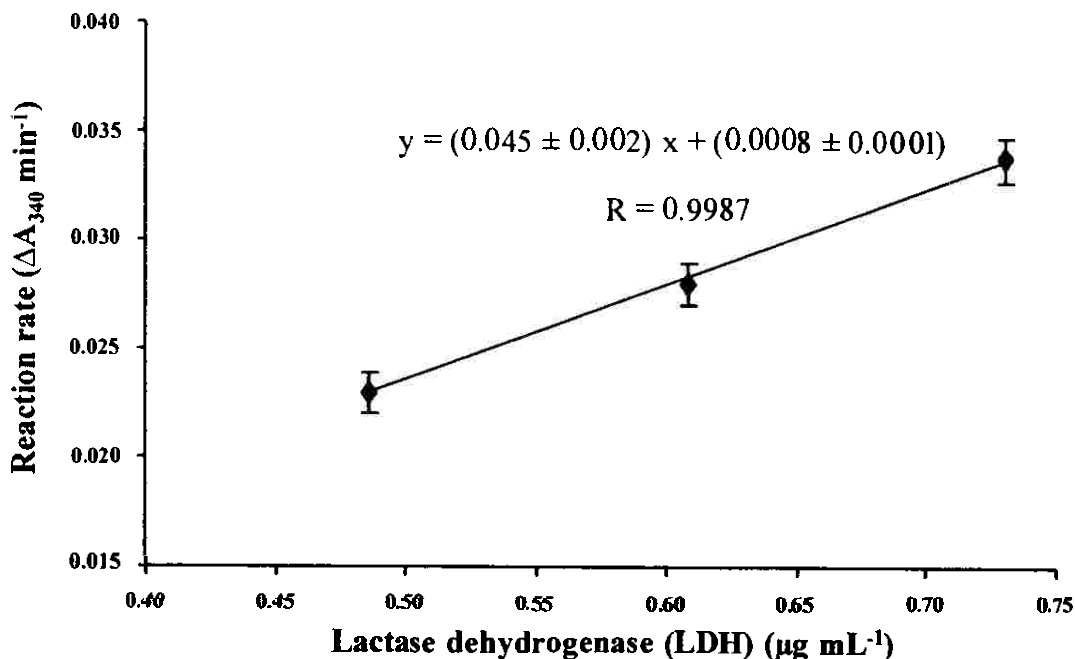
Figure 3.7 Calibration curve plot between reaction velocities (ΔA_{340}/min) and concentration of standard Lactase Dehydrogensase (LDH) (n = 3).

The LDH concentration of samples obtained from purification process are shown in Figure 3.8. No LDH was found in sample S_1 which is the supernatant of the cultivation cell since LDH is still inside the cell. In the cell disruption process (S_2-

S_6), the cells were lysed and released LDH into the solution. The LDH concentration increased from 1.87 to 2.56 μg mL^{-1} with the cycles of cell disruption from S_2-S_4. LDH concentrations of cycles S_5-S_6 slightly decreased (2.49 μg mL^{-1}). This might cause by the heat generated from the sonication probe during cell disruption. For S_7, the mixture of S_2-S_6, the LDH concentration is 2.23 μg mL^{-1}. In the purification of LDH using IMAC technique, there no LDH was found in the washing fraction (W_2-W_5). This indicates that LDH did not come out from the column during washing steps. LDH was only found in the eluting fraction E_{25} with a concentration of 0.47 μg mL^{-1}. From Figure 3.6 LDH should be also found in fraction E_{24} since it showed the absorbance at 280 nm. However since 6 mL was collected for each fraction LDH concentration might be diluted with the eluting solvent and this made the concentration of LDH lower than the working range of the calibration curve.
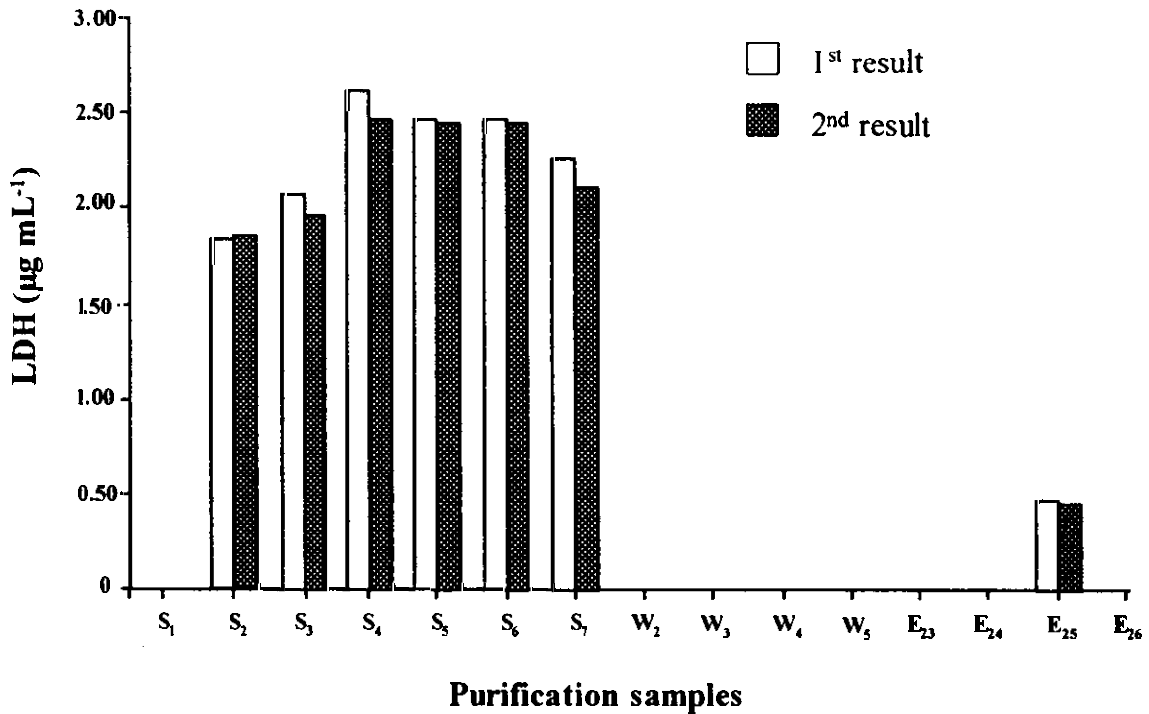
Figure 3.8 Concentrations of Lactase Dehydrogenase (LDH) obtained from purification samples which are supernatant after cell cultivation (S_1), cell disruption (S_2-S_6), supernatant after cell disruption (S_7) and sample during purification with immobilized metal affinity chromatography (IMAC), washing (W_2-W_5) and eluting (E_{23}-E_{30}) steps (n = 2).

3.1.9 Analysis of host cell protein (HCP)

In this study, the purification of LDH using IMAC was used as a model study for the investigation of residual HCP impurity in the purification process. The analysis was performed by using capacitive immunosensor system. A calibration curve between capacitance change ($-nF$ cm^{-2}) and concentration of HCP ranging from 1.0×10^{-17} to 1.0×10^{-13} M was plotted as shown in Figure 3.9. The calibration curve was performed in triplicates for three concentrations. Purification samples were analyzed for single measurement since the analysis needs to be performed within the same electrode due to electrode's life time.

Figure inset equations:

$$y = (1.6 \pm 0.6) \, Log \, (x) + (78.6 \pm 9)$$
$$R = 0.9995$$
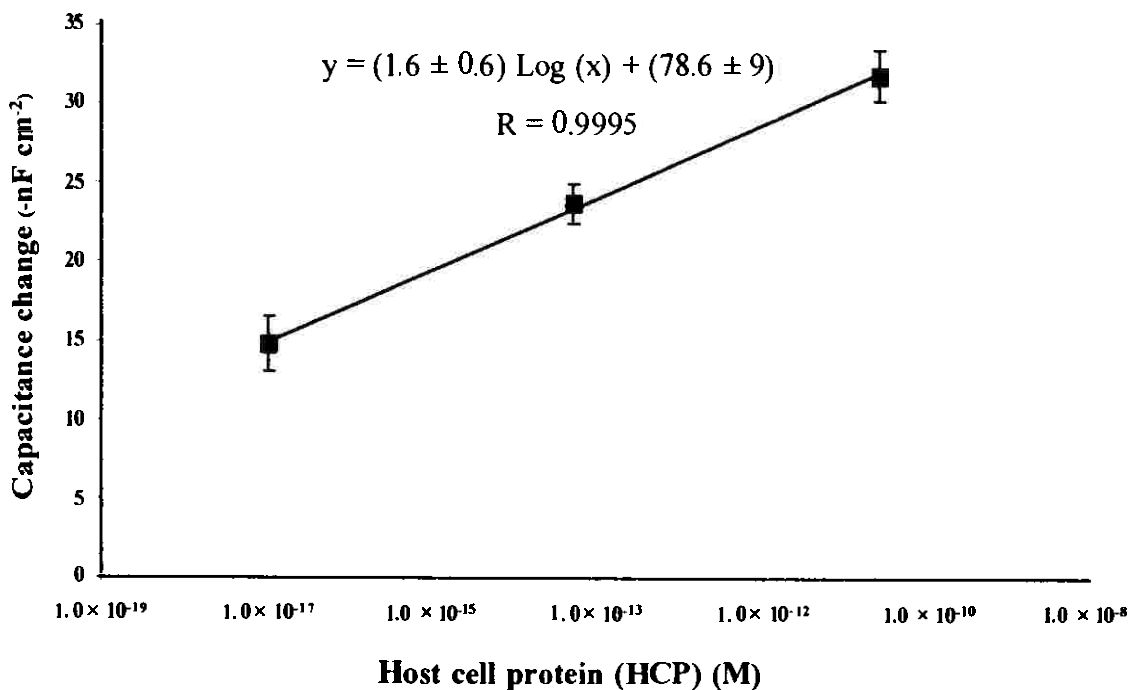
Figure 3.9 Calibration curve plotted between capacitance change ($-nF$ cm^{-2}) and concentration of HCP (M) for the analysis of HCP in the purification process of Lactase Dehydrogenase (LDH) from *E. coli* (n = 3).

The samples from the first collected supernatant, S1 and cell disruption step, S2-S7, were diluted for 10 and 100 times, respectively, and injected to the capacitive immunosensor system. The capacitance change ($-nF$ cm^{-2}) signal were compared to calibration curve and the concentration of HCP in each sample were obtained (Figure 3.10).

Host cell protein (HCP) (M)

9.0×10^{-12}
8.0×10^{-12}
7.0×10^{-12}
6.0×10^{-12}
5.0×10^{-12}
4.0×10^{-12}
3.0×10^{-12}
2.0×10^{-12}
1.0×10^{-12}
0

8.3×10^{-12}

4.4×10^{-12}

2.4×10^{-12}

2.5×10^{-12}

1.4×10^{-12}

1.2×10^{-12}

5.3×10^{-14}

N.D.

N.D.

S_1 S_2 S_3 S_4 S_5 S_6 S_7 W_3 E_{25}

Purification samples
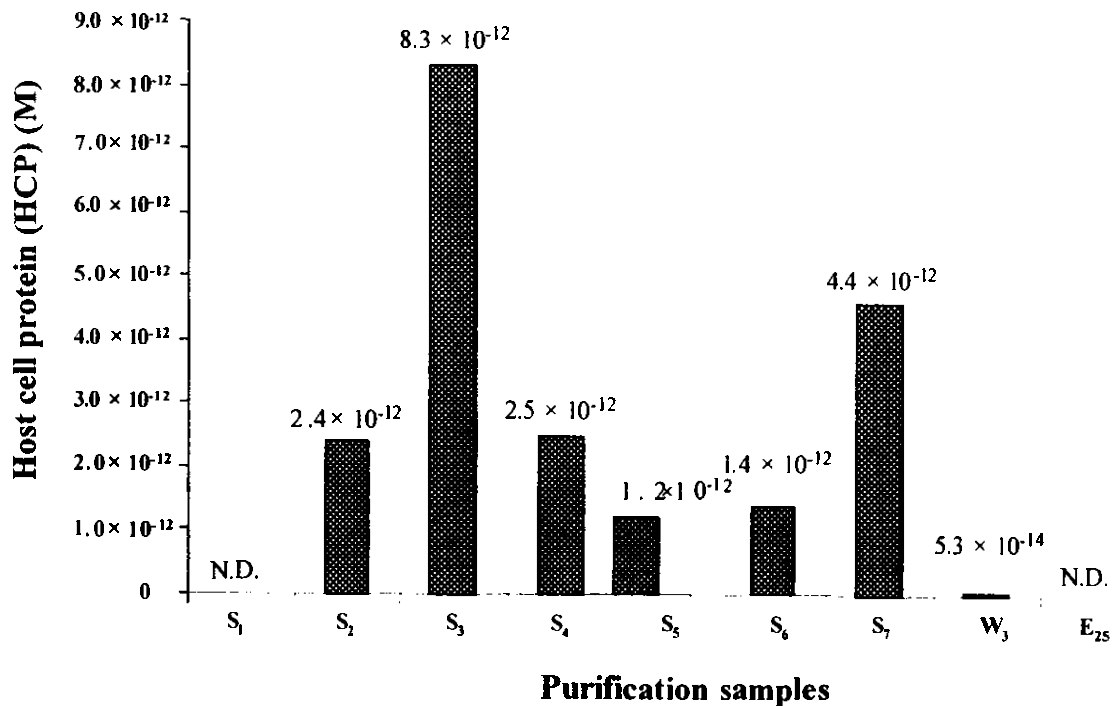
Figure 3.10 Concentration of host cell protein (HCP) in samples obtained from the purification process of Lactase Dehydrogenase (LDH) from *E. coli*. The samples are first collected supernatant (S_1), cycles of cell disruption (S_2-S_6), supernatant after cell disruption (S7) sample during purification with immobilized metal affinity chromatography (IMAC), washing (W_2) and eluting (E_{25}) step, (N.D. = not detectable).

The concentration of HCP is not detecable for the sample S_1 since HCP was still inside the cells. For the first disrupted cycle (S_2), the cells were broken and HCP was released. The concentration of HCP in sample S_2 was 2.4×10^{-12} M which is much higher than S_1. Further disruption will release more HCP as can be seen for sample S_3 (8.3×10^{-12} M). However, some of HCP might denature during cell disruption due to the heat generated by sonication probe. The concentration of HCP was decreased for the third cycle ($S_4 = 2.5 \times 10^{-12}$ M) and fourth cycle ($S_2 = 1.2 \times 10^{-12}$ M). After the fifth (S_6) cycle the concentration of HCP was 1.4×10^{-12} M. When samples S2-S6 were mixed together and then centrifuged at 3,600 rpm (2,550 × g) (S_7), the concentration of HCP was 4.4×10^{-12} M. The concentration of HCP in this sample was higher than the average value of S_2-S_6 (3.2×10^{-12} M). The higher

concentration may cause from nonspecific due to other protein i.e. albumin. From this study, we can investigate the present of HCP released from the cell during disruption step.

The analysis of HCP using capacitive immunosensor was also performed in the purification process of IMAC. The fraction from washing (W3) step was investigated. The concentration of HCP found in this sample was 5.3×10^{-14}M. The eluting fraction E_{25} was also investigated for HCP concentration. This sample is the final product for the purification of LDH using IMAC technique. The concentration of residual HCP impurity was not detectable since the response ($-nF$ cm^{-2}) was lower than detection limit.

This study shows that sputtered gold electrodes can be used for the immobilization of anti-HCP and used as working electrode for the construction of capacitive immunosensor system with anti-HCP-HCP as a model study. The capacitive immunosensor was an effective method for the determination of HCP in purification of Lactase dehydrogenase (LDH) from *E.coli* using immobilized metal affinity chromatography (IMAC). However, the concentrations HCP found in the purification process need to be analyzed further for their precision since the analysis of HCP in samples were only performed once. Moreover, anti-HCP can also bind to the other proteins (Eaton, 1995) which will give positive results, however, the concentrations of HCP in the samples are informative in order to investigate the trends for HCP releasing during purification process. Since, the idea of this work is to introduce the use of disposable thin film sputtered gold electrodes is shown here that it can be used as working electrode for the construction of capacitive immunosensor system and this could be possible to apply to many classes of biomolecules.

3.2 Capacitive immunosensor for human serum albumin (HSA)

3.2.1　Fabrication of thermally evaporated gold electrode

Thin gold film electrodes fabricated by coating of gold on microscope slides with Cr as an adhesion layer using thermal evaporation technique are shown in Figure 3.11. Its surface characteristics was investigated using Atomic Force Microscopy (AFM). Figure. 3.12 (a) shows a two-dimensional AFM perspective view

of nanoscopic images of gold surface thermally evaporated on glass slide. The gold grain and grain boundaries are clearly visible. The three-dimensional AFM image is also shown in Figure 3.12 (b). The gold electrode surface exhibits granular domain structures with a diameter of 20-28 nm. The surface of the gold electrode was obtained with the average roughness of 2.3 nm and the root-mean-square roughness of 2.9 nm.

Figure 3.11 Thin film gold electrodes fabricating by thermal evaporation technique.

3.2.2 Immobilization of anti-HSA

Immobilization of antibody was modified from the work of Karalemus *et al.* (2000) Cheng *et al.* (2001) and Limbut *et al.* (2006). Electropolymerization of *o*-PD was performed by cyclic voltammetry in the potential range of 0-0.8 V (vs. Ag/AgCl) at scan rate 50 mVs^{-1} from a 5 mM solution of *o*-PD in 10 mM acetate buffer pH 5.18. Cyclic voltammograms of gold electrode during electropolymerization are shown in Figure 3.13. Along with the increase in the number of potential cycles, the anodic current decreased significantly. This decrease in oxidation current was due to the loss of activity of the electrode surface when covered with newly formed polymer film (Dai *et al.*, 1998).

In the capacitive immunosensor system the insulating property of polymeric layer on the surface of electrode is of vital importance (Wu *et al.*, 2005). In this study the concentration of *o*-PD was fixed at 5 mM. Therefore, the number of cycles of *o*-PD electropolymerization is the main parameter affecting the insulating property.
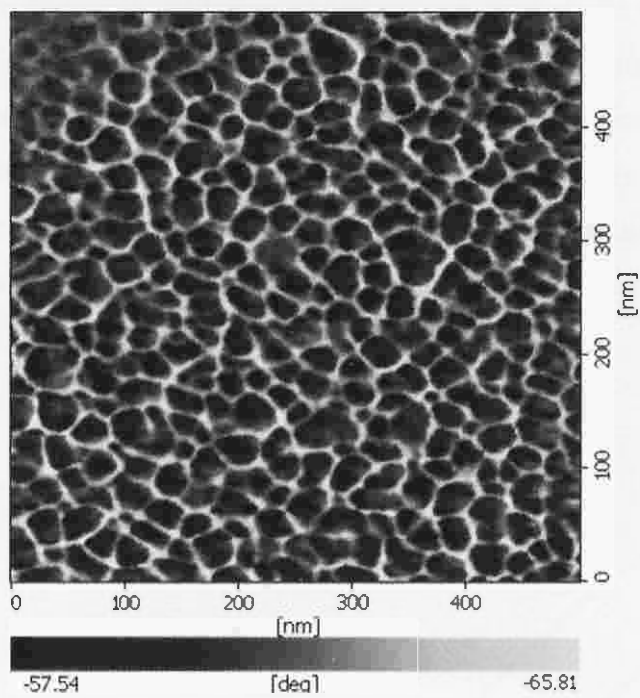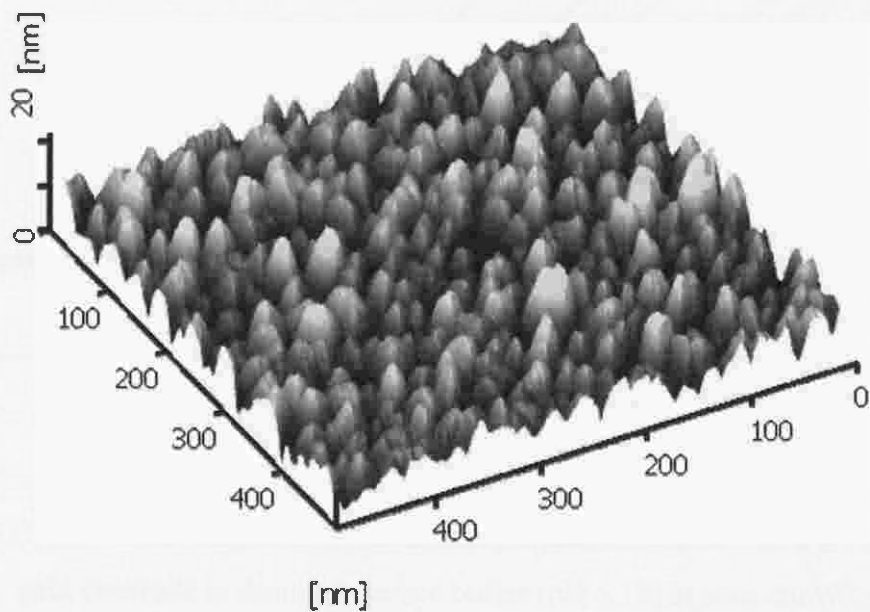
Figure 3.12 (a) 2-dimensional and (b) 3-dimensional AFM images of bare gold surface fabricated by thermal evaporation technique.

The degree of insulation was examined using cyclic voltammetry with $K_3[Fe(CN)_6]$ in electrolyte solution. The degree of insulation increased with increasing number of cycles. However, when these electrodes, coated with different electropolymerization cycles of o-PD, were activated with 5.0% (v/v) glutaraldehyde, immobilized with anti-HSA and then treated with 0.1 M ethanolamine at pH 8.0, all electrodes were completely insulated. Therefore, the responses of these electrodes to standard HSA (1.0×10^{-14} to 1.0×10^{-12} M) were investigated.
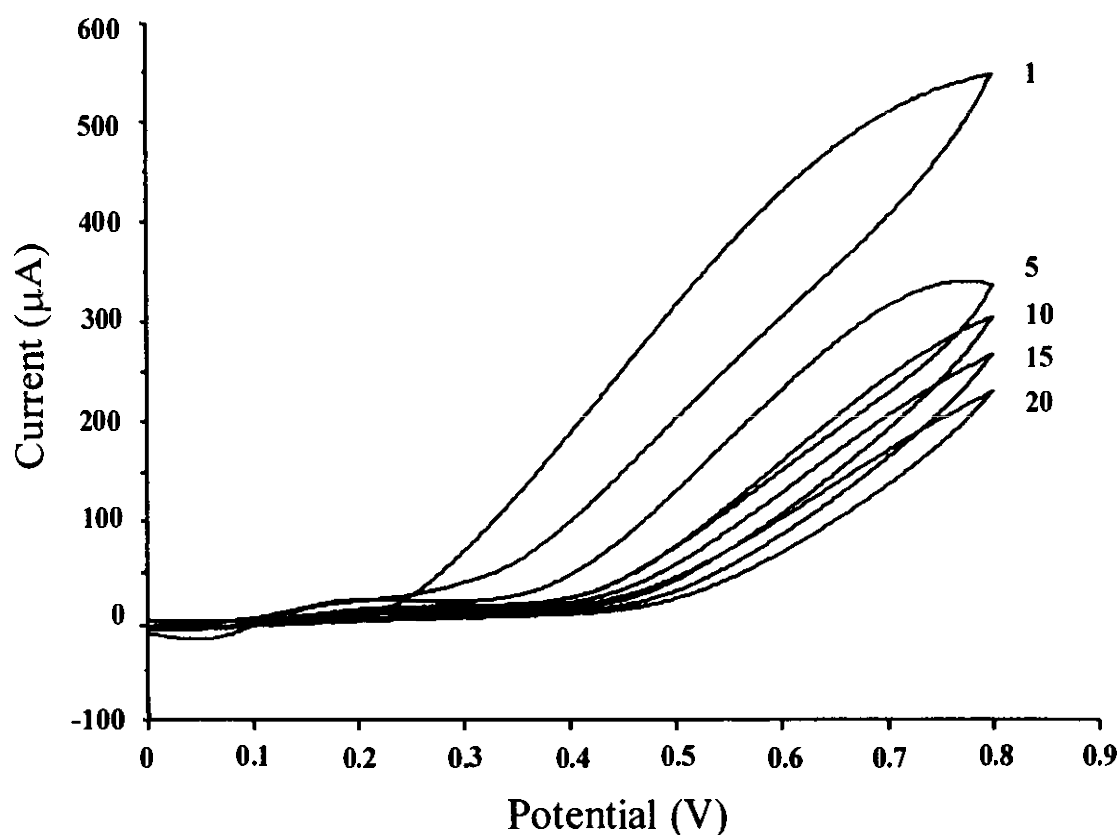
Figure 3.13 Cyclic voltammograms for the electropolymerization of 5 mM o-PD at a gold electrode in dearated acetate buffer (pH 5.18) at scan rate 50 mV s^{-1}. The numbers show the cycles.

The results in Figure 3.14 showed that the sensitivity (slope of calibration curve) increased when the number of cycles increased from 5 to 15 cycles. This is probably due to the increase of free amino group with increase electropolymerization cycles. At 20 cycles the sensitivity (38.2 ± 0.1 –nF cm^{-2} log M^{-1}) was nearly the same

as 15 cycles (38.3 $\pm$ 3.8 $-$nF cm^{-2} log M^{-1}). It is possible that at 15 cycles the electrode was almost completely covered with the polymeric layer, therefore higher number of cycle will not increase the amount of amino group. Thus, 15 cycles was chosen as an optimum number of cycles for electropolymerization of o-PD for the coating procedure and this was used throughout the experiment.
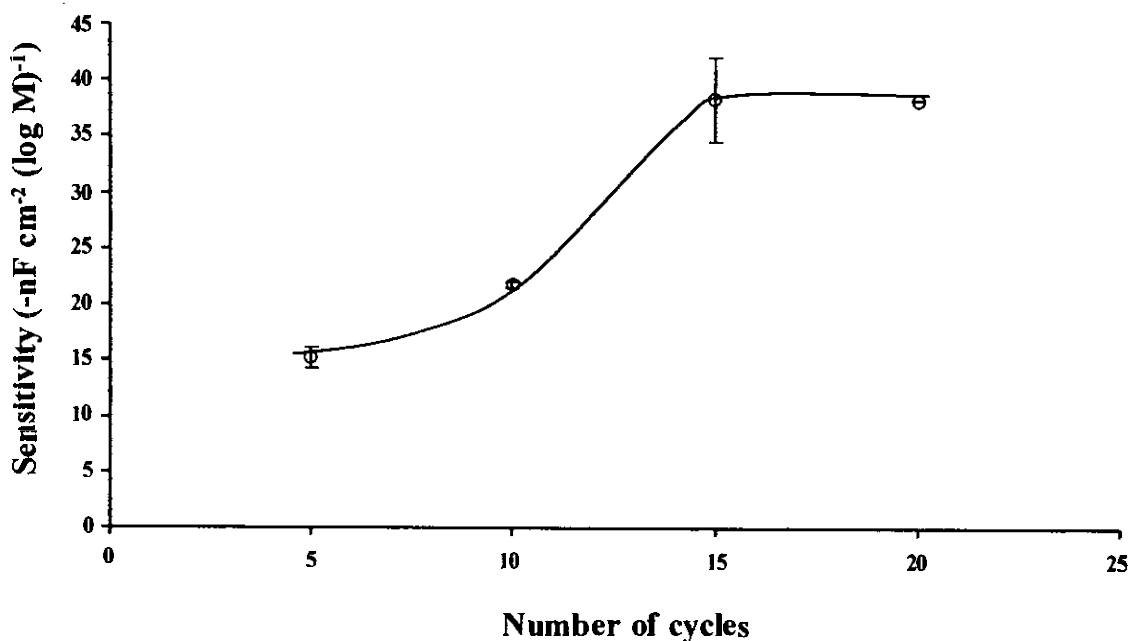
Figure 3.14 Sensitivity of electrodes obtained from diffierent number of cycles of electropolymerized o-PD (n=3).

Figure 3.15 shows the cyclic voltammograms of gold electrode during immobilzation steps using 15 cycles. The redox couple was oxidized and reduced at bare gold electrode (curve a). After o-PD was electropolymerized on the electrode surface, the redox peak decrease (curve b). This degree of insulation was further increased when aldehyde group of glutaraldehyde was reacted with the amine (curve c) and the anti-HSA was immobilized via covalently reaction with aldehyde group (curve d). Finally, the surface of gold electrode was completely insulated when this modified electrode was treated with 0.1 M ethanolamine, pH 8.0 as shown in curve e.
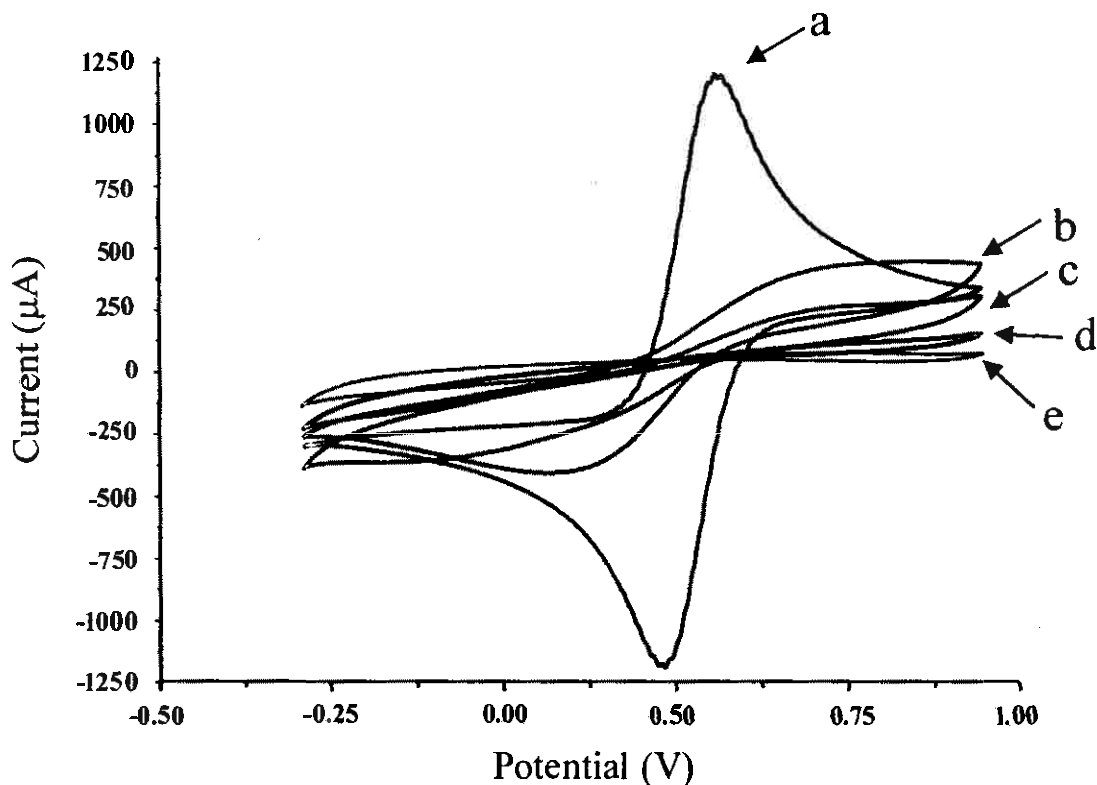
Figure 3.15 Cyclic voltmmogram responses recorded in ($K_3[Fe(CN)_6]$) solution

during the immobilization of anti-HSA (a) bare gold electrode (b)
electropolymerization of o-PD (c) glutaraldehyde (d) anti-HSA and (e)
as in (d) with 0.1 M ethanolamine, pH 8.0.

3.2.3 Optimization

Primary test for the detection of HSA by the modified electrode with
15 cycles of electroplymerization of o-PD provides the response as shown in Figure
3.16. Since at 1.0×10^{-14} M seems to be in the middle of linear curve it was applied
for the optimization of all operating conditions.
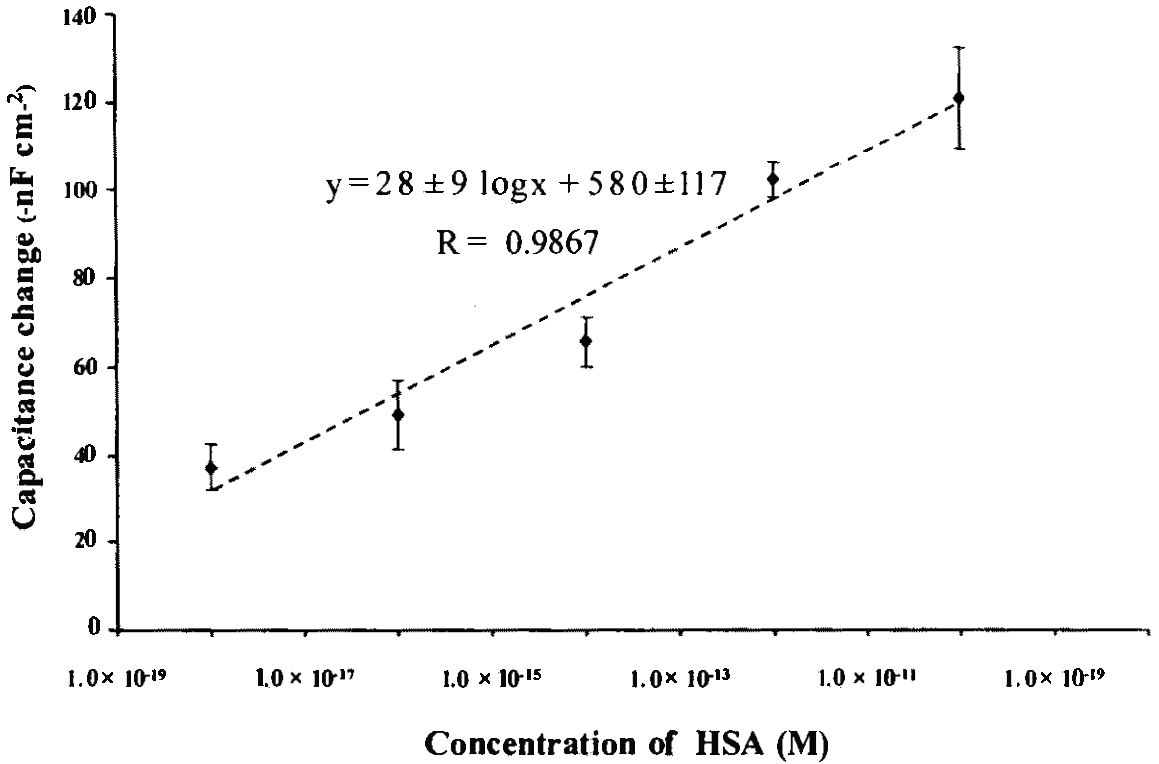
Figure 3.16 Response of a flow injection capacitive immunosensor system for the primary test between anti-HSA-HSA binding (n=3)

2.3.3.1 Regeneration solution

During each analysis HSA binds to anti-HSA on the electrode surface causing the capacitance to decrease. The analyte (HSA) needs to be removed so it can be used again for the next analysis. This was done by passing a volume of regeneration solution. Ideally, regeneration of the working electrode should remove any non-covalently bound HSA without disrupting the activity of the anti-HSA immobilized on the electrode. To evaluate the performance of the regeneration solution, the percentage residual activity was evaluated as equation (3.1) (Limbut *et al.*, 2006).

$$\text{\%residual activity} = \frac{\Delta C_2}{\Delta C_1} \times 100 \qquad\qquad 3.1$$

Where ΔC_1 and ΔC_2 are the capacitance change before and after regeneration, respectively. The criteria for regenerating the electrode surface is "if post –regeneration binding remain above 90% compared to the binding efficiency

before regeneration, the used conditions should be seen as adequate" (Andersson *et al.*, 1999; van der Merew, 2000).

Initially glycine-HCl and HCl at pH 2.2 and 2.8 were tested and both provided similar results. However for glycine-HCl the signal took very long time before returning to the baseline. Therefore, only HCl solution was further tested (Table 3.1). The influence of pH of HCl solution, ranging from 2.8 to 2.2 was studied. The highest percentage residual activity were obtained at pH 2.5 (99 ± 2%) and pH 2.4 (99 ± 5%) but at pH 2.5, the standard deviation is lower, therefore, pH 2.5 was used as regeneration solution for further experiments.

Table 3.1 Residual activity of modified electrode for preliminary and further test of regeneration solution (n=3).

Regeneration solution	% residual activity (mean± SD)	Regeneration time (min)
Preliminary test		
50 mM Glycine-HCl		
pH 2.2	113 ± 15	70
pH2.8	86 ± 19	70
HCl		
pH2.2	97±4	25
pH2.8	89±3	25
Further test		
HCl		
pH 2.2	96 ± 3	25
pH 2.4	99± 5	25
pH 2.5	99±2	25
pH 2.6	96± 2	25
pH 2.8	90±4	25

2.3.3.2 Flow rate and sample volume

In the flow injection capacitive immunosensor system, the flow rate and volume of the sample passing through the capacitive flow cell are two main factors affecting the yield of interaction between HSA and anti-HSA immobilized on the electrode. Sample volume corresponds with the amount of analyte passing through the system while flow rate corresponds with the time that the analyte will retain in the flow cell. The system with a large sample volume but high flow rate may give the same signal as the system with small volume but low flow rate. Therefore, these two parameters were optimized at the same time. The sample volume was investigated at 150, 200, 250, 300 and 350 μL. For each sample volume flow rate was studied at 25, 50, 100, 150 and 200 μL min^{-1}.

Figure 3.17 shows the optimization of flow rate at different sample volume. For every sample volume, the capacitance change resulting from the injections of standard HSA 1.0×10^{-14} M gave the highest response at flow rate 25 μL min^{-1}. However, the analysis time (the time taken from injection of HSA until the response was stable) at this flow rate is also high (30-50 min). At flow rate 50 and 100 μL min^{-1} the capacitance change was nearly the same, but the analysis time at 100 μL min^{-1} (13-28 min) was much shorter than 50 μL min^{-1} (25-45) min). So flow rate at 100 μL min^{-1} was chosen for all sample volume except at sample volume 200 μL in which flow rate 150 μL min^{-1} was selected instead. Table 3.2 shows the optimum flow rate and analysis time at each sample volume.
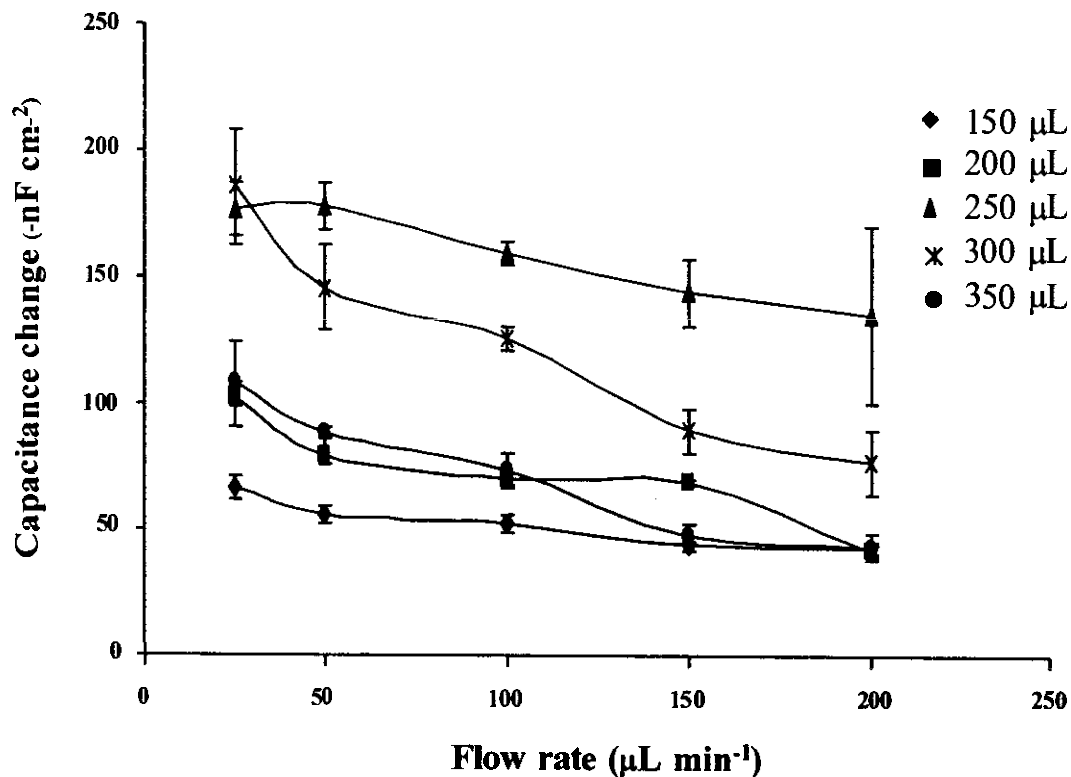
Figure 3.17 Response of the capacitive immunosensor system to the different sample volume of 1.0×10^{-14} M HSA at different flow rates ($n = 3$).

Table 3.2 Optimum flow rate and analysis time for different sample volume (n=3).

Sample volume (µL)	Optimum flow rate (µL min⁻¹)	Analysis time* (min)
150	100	13
200	150	10
250	100	15
300	100	15
350	100	20

* analysis time is the time taken from injection of HSA until the response was stable

For the optimization of sample volume and flow rate, each sample volume at its optimum flow rate was reinvestigated within the same electrode. This is shown in Figure 3.18.
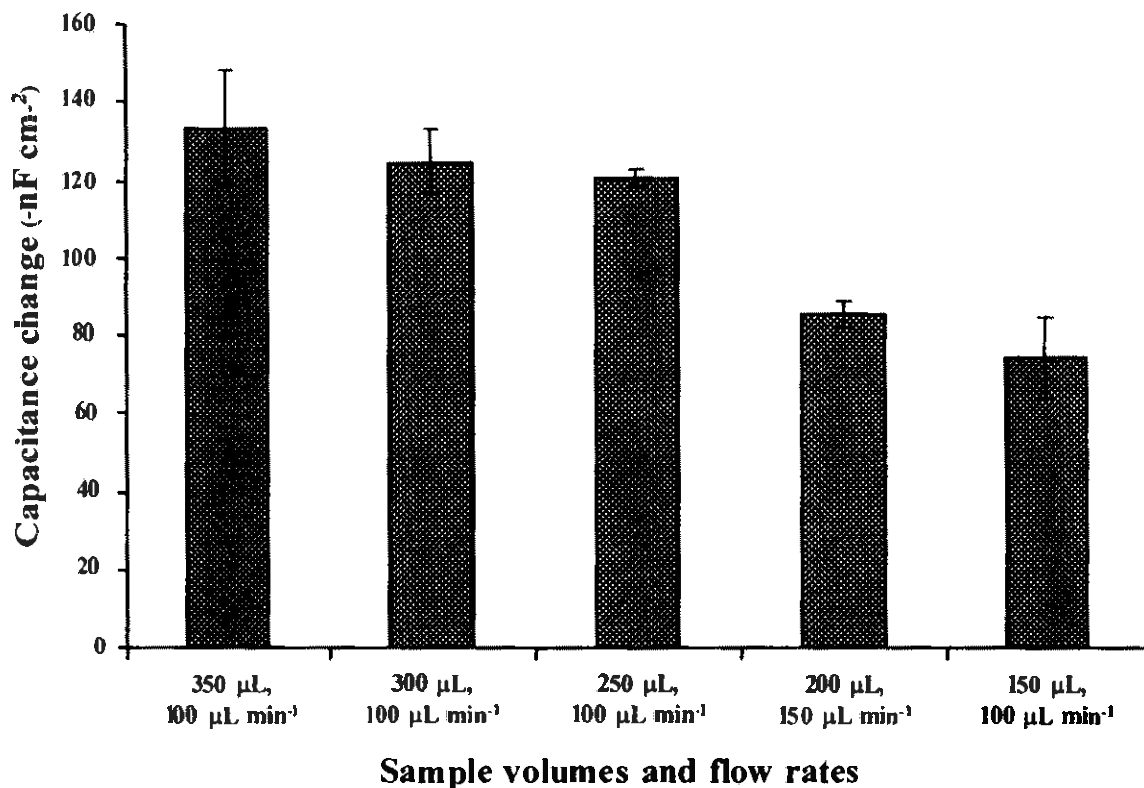
Figure 3.18 The response to each sample volume at its optimum flow rate (n = 3).

The capacitance change resulting from the injections of standard HSA 1.0×10^{-14} M at sample volume 350, 300, and 250 μL (flow rate 100 μL min^{-1}) were nearly the same but the analysis time at flow rate 250 μL (13 min) was shorter than 300 μL (15 min) and 350 μL (20 min). In order to use less amount of sample and require short analysis time, sample volume 250 μL at flow rate 100 μL min^{-1} was chosen.

It can be seen from Figure 3.18 that the response is highest at the maximum sample volume of 350 μL. However, this is not the same as in Figure 3.17 where the response obtained from sample volume 350 μL is lower than both obtained from 250 and 300 μL. This may due to the fact that, the response of each modified

electrode is not reproducible. From observation freshly prepared electrode gave better response and since the preparation of electrode (immobilization) took long time, four electrodes have been prepared together for each set and used one at a time, the rest were kept at 4°C in Petri dish saturated with nitrogen gas. Therefore, the response of the first electrode is the highest and lowest for the fourth electrode. To avoid the effect due to this irreproducible, the analysis should be performed in the same electrodes.

2.3.3.2 Concentration and pH of buffer solution

The concentration and pH of tris-HCl and sodium phosphate buffer were optimized. The concentration of buffer was fixed at 5, 10, 15 and 20 mM and the pH was varied between 7.0 and 7.8. Figure 3.19 shows the results for tris-HCl buffer, it was found that at every concentration, pH 7.0 provided the highest responses and it was chosen as the optimum pH for all concentration.

As described in 2.3.3.1, the responses of electrodes are not reproduced, thus the concentrations at optimum pH were reinvestigated using the same electrode. This is shown in Figure 3.20. At 10 mM, pH 7.0 the capacitance signal was the highest. Therefore, this condition was chosen as an optimum concentration and pH of tris-HCl buffer.

The result for the optimization of concentration and pH for sodium phosphate buffer is shown in Figure 3.21. At every concentration, pH 7.0 provided the highest responses. The concentrations at pH 7.0 of sodium phosphate buffer were reinvestigated using the same electrode. This is shown in Figure 3.22. At 10 mM, pH 7.0 the capacitance signal was the highest and this condition was chosen as the optimum concentration and pH.
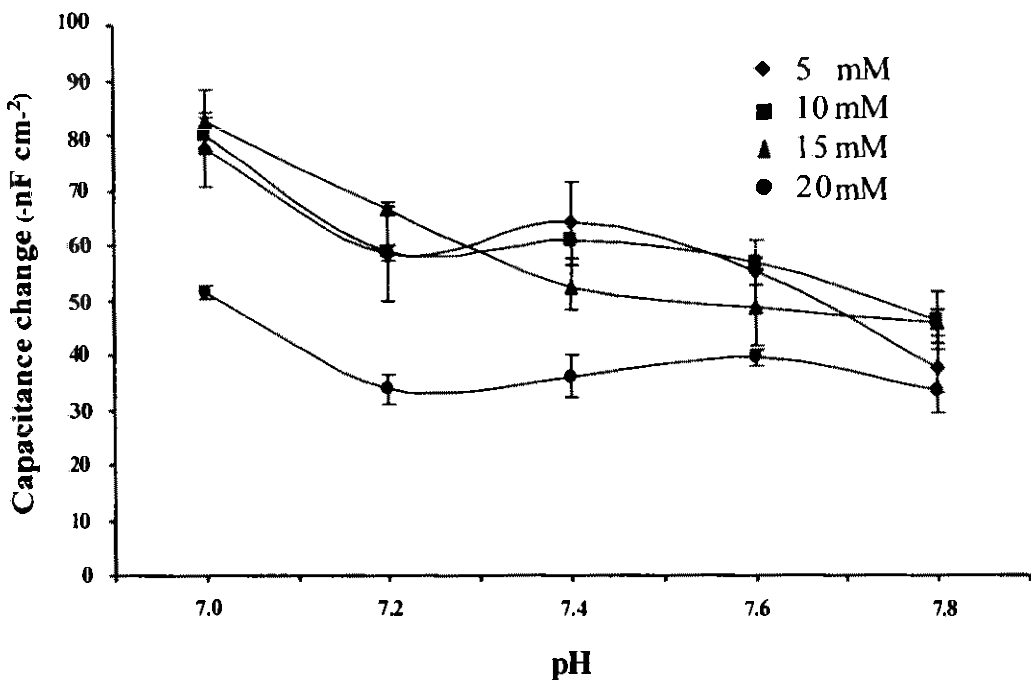
Figure 3.19 Response of the capacitive immunosensor system to the different concentration of tris-HCl buffer at different pH (n = 3).
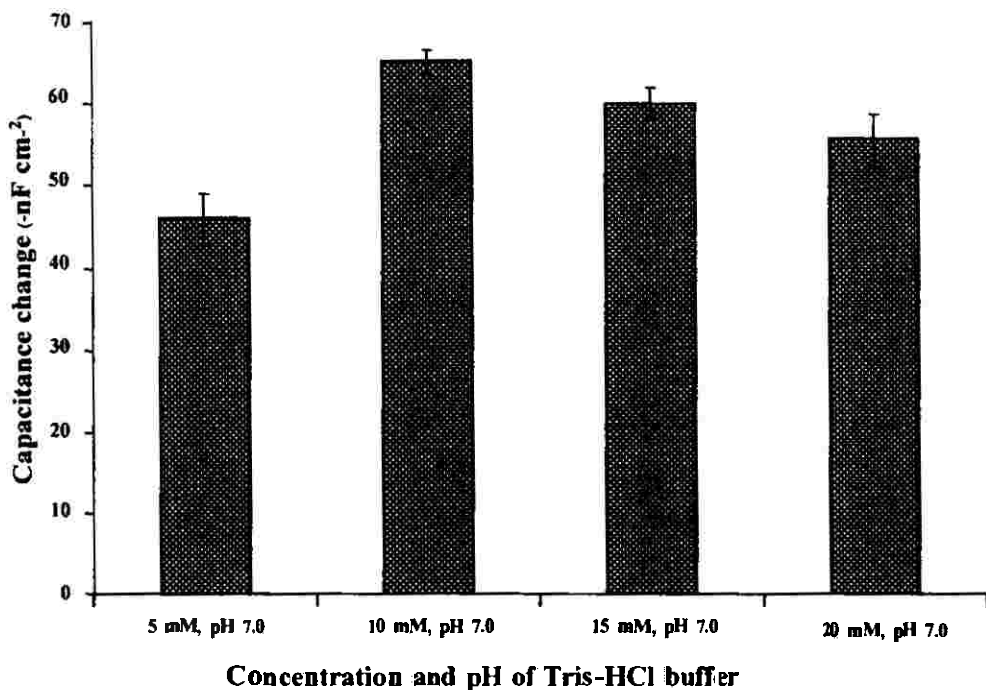
Figure 3.20 The response to each concentration at its optimum pH of tris-HCl Buffer (n = 3).
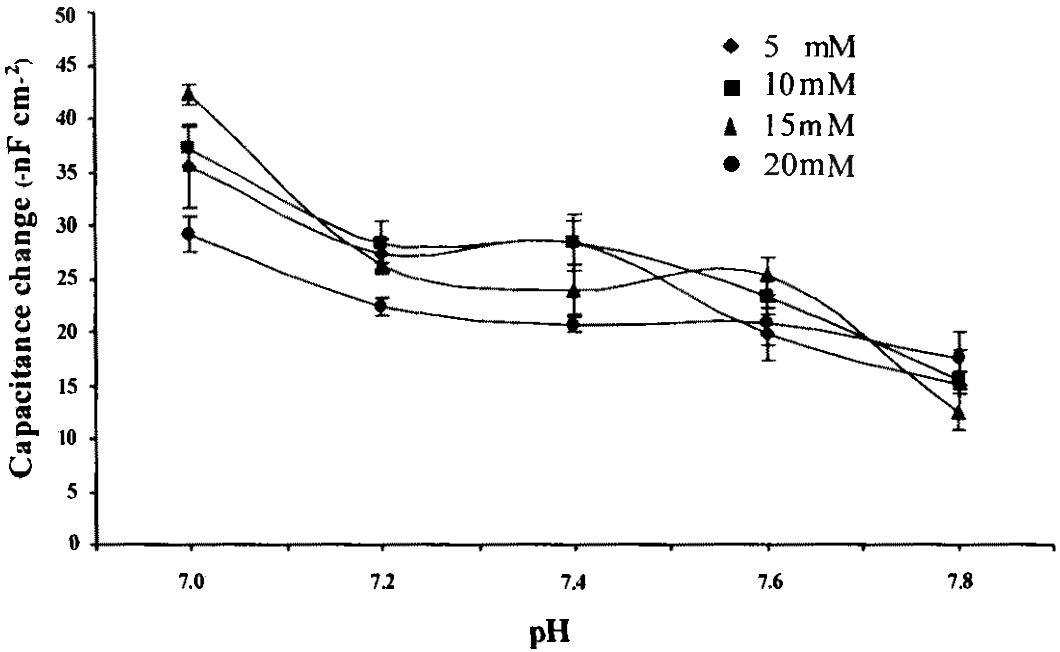
Figure 3.21 Response of the capacitive immunosensor system to the different concentration of sodium phosphate buffer at different pH (n = 3).
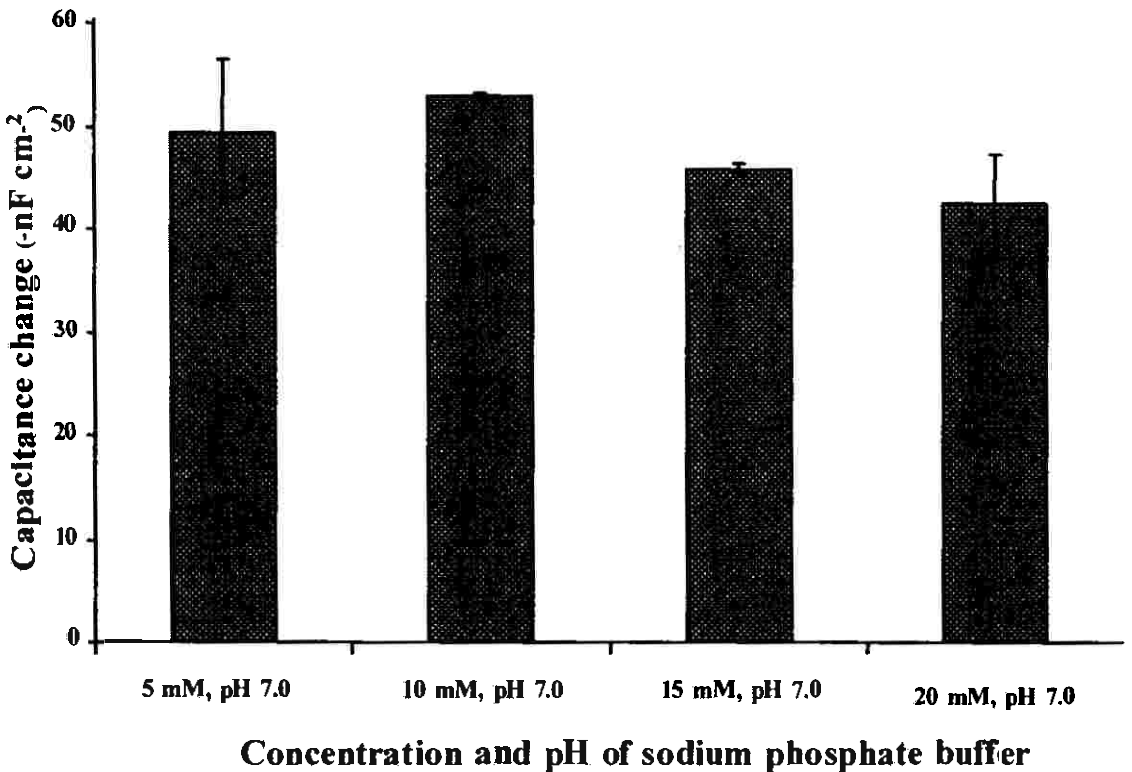
Figure 3.22 The response to each concentration at its optimum pH of sodium phosphate buffer (n = 3).

2.3.3.2 Type of buffer solution

Tris-HCl and sodium phosphate buffer at their optimum concentration and pH were compared by injected HSA between 1.0×10^{-14} to 1.0×10^{-10} M (Figure 3.23). Tris-HCl(10 mM pH 7.0) gave better sensitivity ($y = 7.9 \pm 0.4 \log x + 163 \pm 6$, $R = 0.9978$) than 10 mM sodium phosphate buffer pH 7.0 ($y = 6.98 \pm 0.04 x + 135 \pm 3$, $R = 0.9998$). Therefore, 10 mM Tris-HCl pH 7.0 was chosen as the carrier buffer.
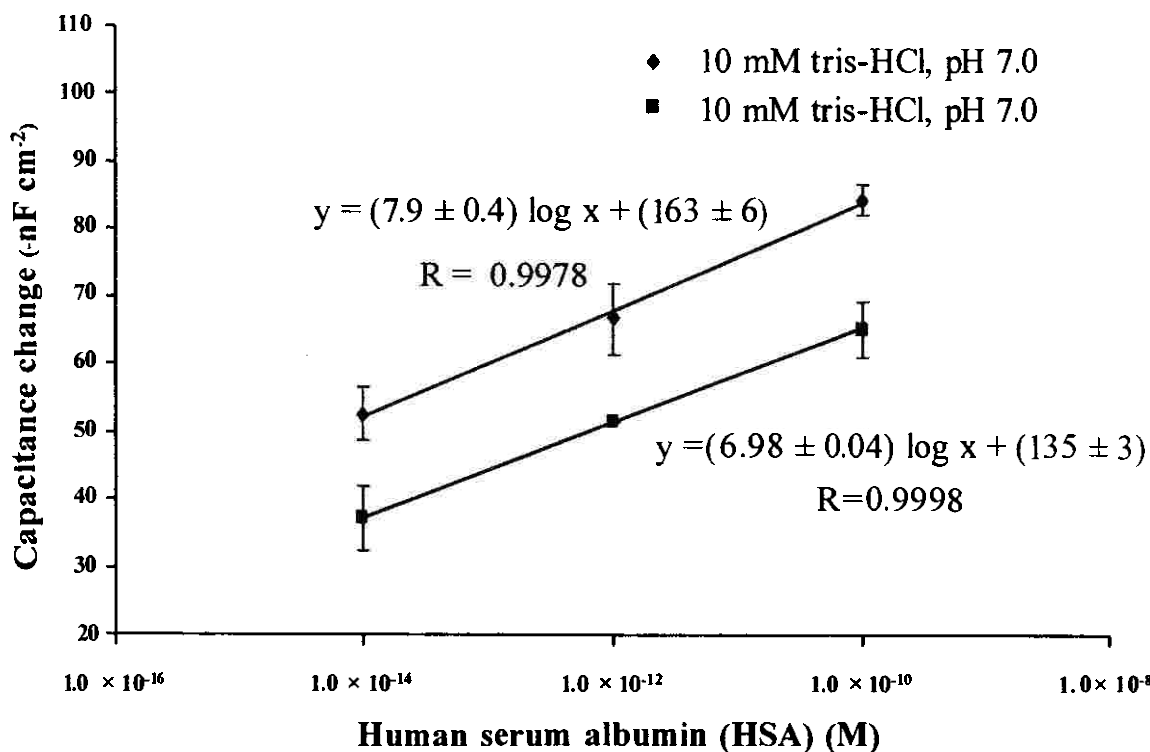
Figure 3.23 Response when using tris-HCl compared to sodium phosphate buffer at their optimum concentration and pH (sample volume 250 μL, Flow rate 100 μL min⁻¹).

Optimum and tested value of operating conditions of a flow injection capacitive immunosensor system are summarized and shown in Table 3.3.

Table 3.3 Optimum and investigated value of operating conditions (n=3).

Parameters	Investigated value	Optimum
Regeneration		
50 mM Glycine-HCl (pH)	2.2, 2.8	-
HCl (pH)	2.2, 2.4, 2.5, 2.6, 2.8	2.5
Sample volume (μL)	150, 200, 250, 300, 350	250
Flow rate (μL min^{-1})	25, 50, 100, 150, 200	100
Buffer solution		
type	tris-HCl, glycine-HCl	tris-HCl
concentration	5, 10, 15, 20	10
pH	7.0, 7.2, 7.4, 7.6, 7.8	7.0

3.2.4 Linear range, sensitivity and limit of detection

Using the optimum conditions in Table 3.3, injections of standard HSA solutions ranging from 1.0×10^{-18} to 1.0×10^{-6} M with intermediate regeneration steps using HCl solution, pH 2.5 were studied (Figure 3.24). A linear relationship between the capacitance change and the logarithm of HSA concentration was obtained in the range of 1.0×10^{-14} to 1×10^{-9} M. The linear regression equation was y (-nF cm^{-2}) = (15.2 ± 0.7) log HSA (M) + (245 ± 8). The detection limit was 8.0 × 10^{-15} M based on IUPAC recommendation 1994 (Buck and Lindner.,1994). The performance of the capacitive immunosensor system presented in this work is better than the one reported by Hedström et al. (2005) (Linear range 2.5 × 10^{-11}-2.5 × 10^{-9} M). In their work, SAM of alkanethiol was used for the immobilization of anti-HSA on gold rod electrode, indicating that electropolymerization of o-PD on thermally evaporated gold electrode can be used successfully for the construction of capacitive immunosensor system.
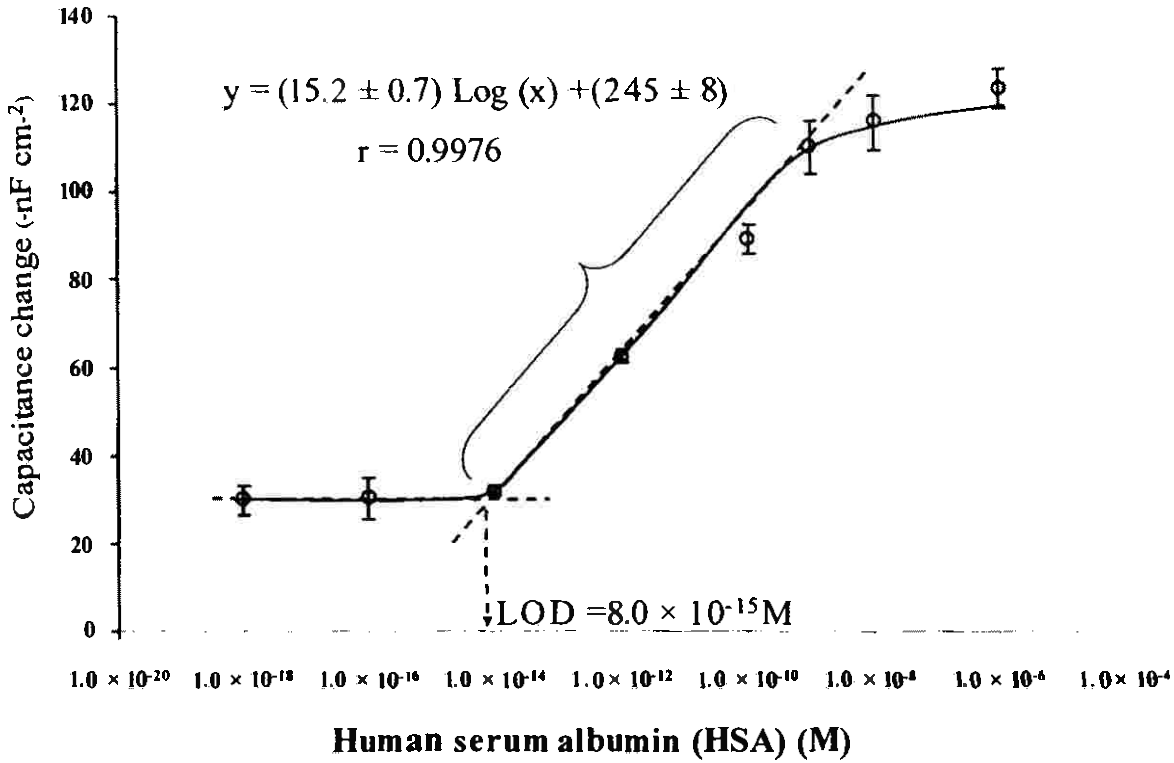
Figure 3.24 Capacitance change vs. logarithm of HSA concentration for an anti-HSA modified electrode under optimum conditions (flow rate 100 µL min^{-1}, sample volume 250 µL, 10 mM Tris-HCl buffer pH 7.0).

3.2.5 Reproducibility

To study the reproducibility of responses, standard HSA 1.0×10^{-14} M was injected to the capacitive immunosensor system with subsequent regeneration with HCl pH 2.5. The performance of the electrode was evaluated intermittently over 3 days (12 times/day) (Figure 3.25). For the first 30 cycles of regeneration the average percentage capacitance change was $92.5 \pm 3.5\%$. Then, the response decreased rapidly to about $78.3 \pm 2.2\%$. To confirm that the insulating layer of the polymer was not destroyed after long term of regeneration, cyclic voltammograms of the electrode were obtained in ($K_3[Fe(CN)_6]$) solution before and after the reproducibility study (Figure 3.26). Both cyclic voltammograms were very similar, showing no redox peaks, which indicated that the insulating layer of the polymer was not destroyed.

Therefore, the decreasing in the response after 30 times of injections may due to the lost of activity of anti-HSA after long period of analysis.
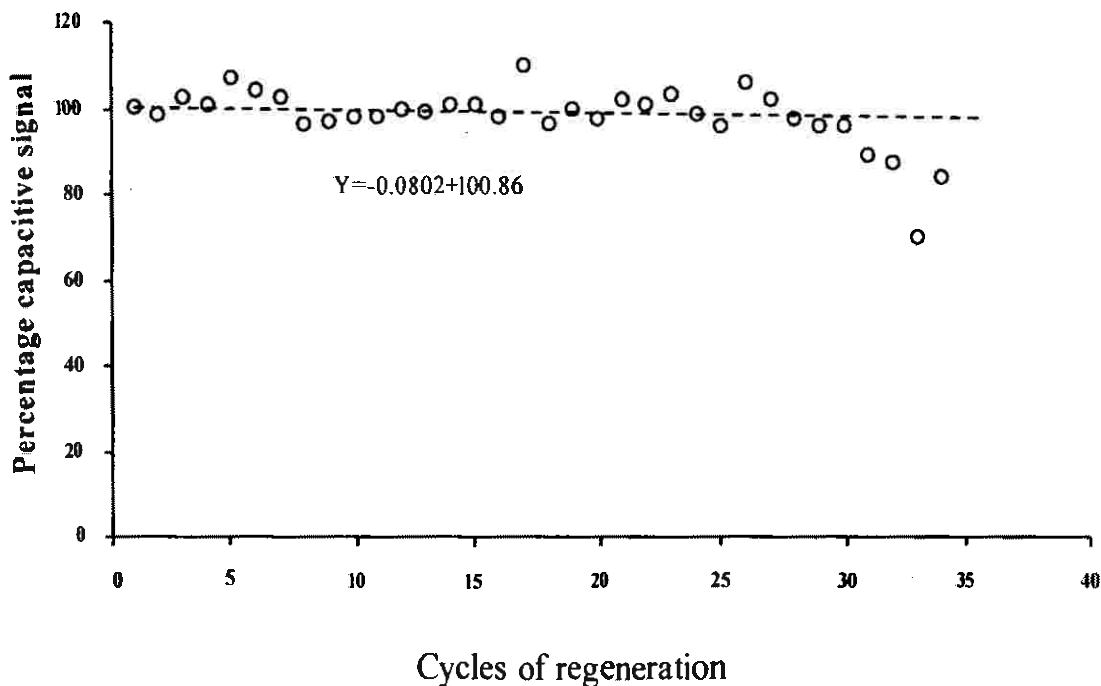
Figure 3.25 Reproducibility of the response from an anti-HSA modified electrode to injections of a 250 µL standard solution of HSA (1.0×10^{-14}M) with regeneration steps between each individual assay.
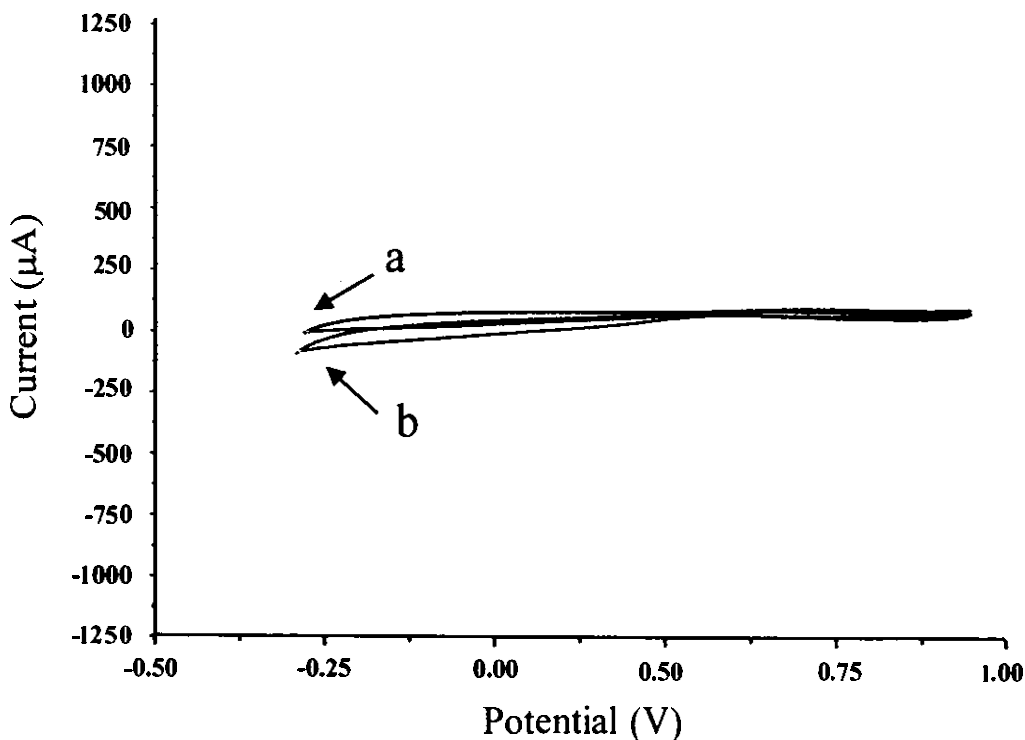
Figure 3.28 Cyclic voltammogram of the modified gold electrode obtained in 0.05 M
$(K_3[Fe(CN)_6])$ solution, (a) is the response when pinholes on electrode
surface were blocked by 1-dodecanethiol before used and (b) is the
response after reused more than 35 times.

3.2.6 Selectivity

To demonstrate that the developed capacitive immunosensor system is
specific to HSA, bovine serum albumin (BSA), the protein that has molecular weight
close to HSA was studied. The capacitance changes from the binding of BSA to the
anti-HSA modified electrode in the linear concentration range of HSA, 1.0×10^{-14} to
1.0×10^{-9} M, were studied. The results are shown in Figure 3.27. At 1.0×10^{-9} M, the
capacitance change due to BSA was -18 ± 3 nF cm^{-2}. The maximum capacitance
change obtained from the injection of BSA is -21 ± 5 nF cm^{-2} at the concentration 1.0
$\times 10^{-10}$ M which is almost 4 times lower than the response obtained by the injection of
HSA at the same concentration. This is also lower than the response of HSA at the
limit of detection LOD (-41 nF cm^{-2}). This indicates that the anti-HSA modified
electrode has high selectivity to the detection of HSA.
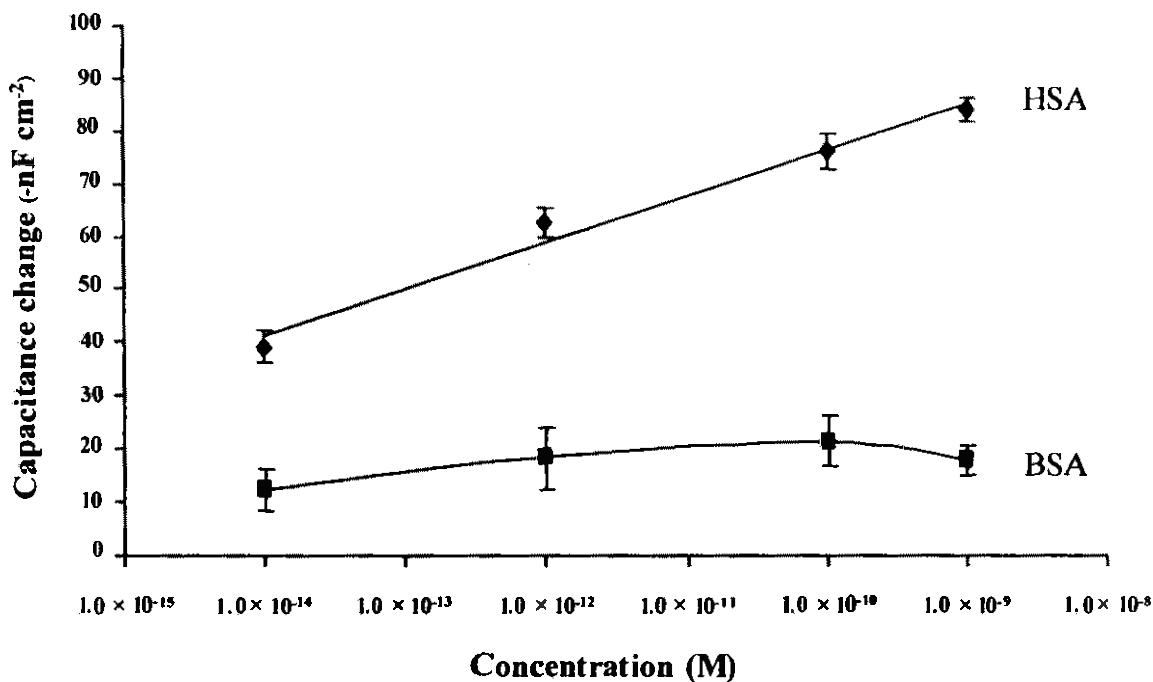
Figure 3.27 Selectivity of anti-HSA modified electrode to BSA at concentration 1.0×10^{-14} to 1.0×10^{-9} M (n = 3).

3.2.7 Method validation

Method validation is done by evaluating matrices interference and recovery of the method.

3.2.7.1 Matrices interference

Concentrations of albumin in human serum of patients are in the range of 7.3×10^{-5} to 1.0×10^{-3} M. In this work a linear relationship between the capacitance change and the logarithm of HSA concentration was obtained in the range of 1.0×10^{-14} to 1.0×10^{-9} M. Therefore, to apply this range for the analysis of albumin in human serum, the sample should be diluted starting from 10^6 times. For the study of matrices interference, the dilution factor was started at 10^6 times and the concentration range from 3.0×10^{-11} to 1.0×10^{-10} and 3.0×10^{-10} to 1.0×10^{-9} M was used for the study of matrices interference.

For the range between 3.0×10^{-10} and 1.0×10^{-9} M. The standard curve was first performed. This was the plot between response (-nF cm^{-2}) and concentration

of HSA (M) in a linear scale. The serum sample were spiked with different concentration of standard HSA and then diluted for 10^6 times. The final concentration were 3.0×10^{-10}, 5.0×10^{-10}, 7.0×10^{-10} and 1.0×10^{-9} M. Figure 3.28 shows the standard curve and spiked curve for the study of matrices interference of sample 1. The response of the spiked curve is higher than the one obtained from standard curve. This may be because of the albumin in human serum samples, therefore, for spiked samples, the concentration of albumin is higher than standard. To confirm this hypothesis, the response of the unspiked sample was used to calculate the concentration of HSA in the sample using calibration curve of the standard HSA. The concentration of HSA in the unspiked sample is closed to the concentration obtained from Songklanakarind hospital (Sample 1 Table 3.4). The process was repeated with four other samples and similar results were obtained. Therefore, the higher response of spiked curve than standard comes from HSA in the samples. The slope of regression line of the standard HSA prepared in 10 mM Tris-HCl buffer pH 7.0 for every sample was not significantly different from the slope of the diluted real samples $(P < 0.05)$ indicating that there is no effect of matrix interfered to the analysis at 10^6 times dilution (Table 3.5).

Matrices interfence was also tested at at higher dilution factor (10^7 times) for the same five samples. The standard curve was first performed for the range 3.0×10^{-11} to 1.0×10^{-10} M. The serum sample were spiked with different concentration of standard HSA and then diluted for 10^7 times. The final concentration were 3.0×10^{-11}, 5.0×10^{-11}, 7.0×10^{-11} and 1.0×10^{-10} M. Figure 3.29 shows the standard and spiked curve for the study of matrices interference of sample 1. As in Figure 3.28 the response of the spiked curve is higher than the standard curve due to the existing concentration of HSA in samples. Another four samples were tested to confirm the results (Table 3.4). For all samples, the slopes of both curves were not significantly different $(P < 0.05)$ (Table 3.5). Therefore, there is no effect of matrices interference at this dilution.

From these results, the developed capacitive immunosensor system can be diluted starting from 10^6 times.
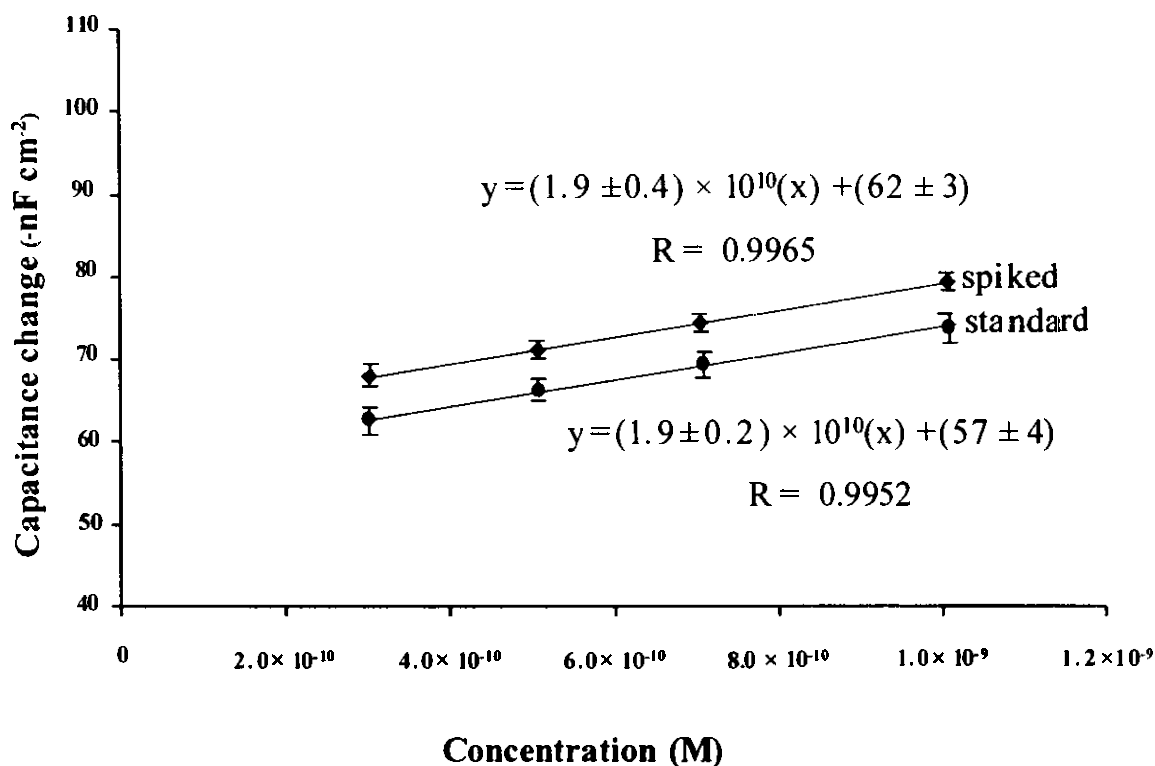
Figure 3.28 The standard curve and spiked curve for the study of matrices interference of sample 1 (dilution 10^6 times) (n = 3).

Table 3.4 The concentration of albumin in human serum compared to the values obtained from Songklanakarind Hospital (n=3).

Samples	Dilution 10^6 times		Dilution 10^7 times	
	Found ($\times 10^{-4}$ M)	Hostipal ($\times 10^{-4}$ M)	Found ($\times 10^{-4}$ M)	Hostipal ($\times 10^{-4}$ M)
Sample 1	2.84 ± 0.01	3.1	3.5 ± 0.3	3.1
Sample 2	3.1 ± 0.3	3.2	3.2 ± 0.3	3.2
Sample 3	2.85 ± 0.07	3.1	2.7 ± 0.2	3.1
Sample 4	3.5 ± 0.5	4.0	3.9 ± 0.2	4.0
Sample 5	3.6 ± 0.2	3.9	3.91 ± 0.04	3.9

Table 3.5 The study of matrices interference in five human serum samples (n=3).

Dilution/Samples	Linear equation of standard curve $y = (m \pm SD)x + (C \pm SD)$	Linear equation of spiked curve $y = (m \pm SD)x + (C \pm SD)$
10^6 times	Slope (m) × 10^{10}	Slope (m) × 10^{10}
Sample 1	$y = (1.9 \pm 0.2)x + (57 \pm 4)$ R= 0.9952	$y = (1.9 \pm 0.5)x + (62 \pm 3)$ R= 0.9965
Sample 2	$y = (3.1 \pm 0.3)x + (49 \pm 2)$ R= 0.9993	$y = (2.9 \pm 0.4)x + (58 \pm 3)$ R= 0.9986
Sample 3	$y = (3.2 \pm 0.2)x + (47 \pm 6)$ R= 0.9958	$y = (3.1 \pm 0.4)x + (55 \pm 3)$ R= 0.9987
Sample 4	$y = (3.5 \pm 0.4)x + (46 \pm 4)$ R= 0.9970	$y = (3.5 \pm 0.3)x + (57 \pm 2)$ R= 0.9995
Sample 5	$y = (3.7 \pm 0.2)x + (45 \pm 1)$ R= 0.9997	$y = (3.7 \pm 0.3)x + (57 \pm 2)$ R= 0.9967
10^7 times	Slope (m) × 10^{11}	Slope (m) × 10^{11}
Sample 1	$y = (3.7 \pm 0.6)x + (64 \pm 4)$ R=0.9984	$y = (3.5 \pm 0.3)x + (76 \pm 2)$ R= 0.9995
Sample 2	$y = (2.9 \pm 0.4)x + (38 \pm 3)$ R=0.9990	$y = (2.8 \pm 0.3)x + (46 \pm 2)$ R=0.9994
Sample 3	$y = (2.6 \pm 0.5)x + (38 \pm 3)$ R= 0.9982	$y = (2.7 \pm 0.5)x + (44 \pm 4)$ R= 0.9979
Sample 4	$y = (2.4 \pm 0.5)x + (44 \pm 3)$ R= 0.9977	$y = (2.5 \pm 0.3)x + (53 \pm 2)$ R=0.9990
Sample 5	$y = (2.2 \pm 0.4)x + (39 \pm 9)$ R= 0.9978	$y = (2.1 \pm 0.5)x + (48 \pm 3)$ R= 0.9971

No significantly different of slope for standard and spiked curve for all samples
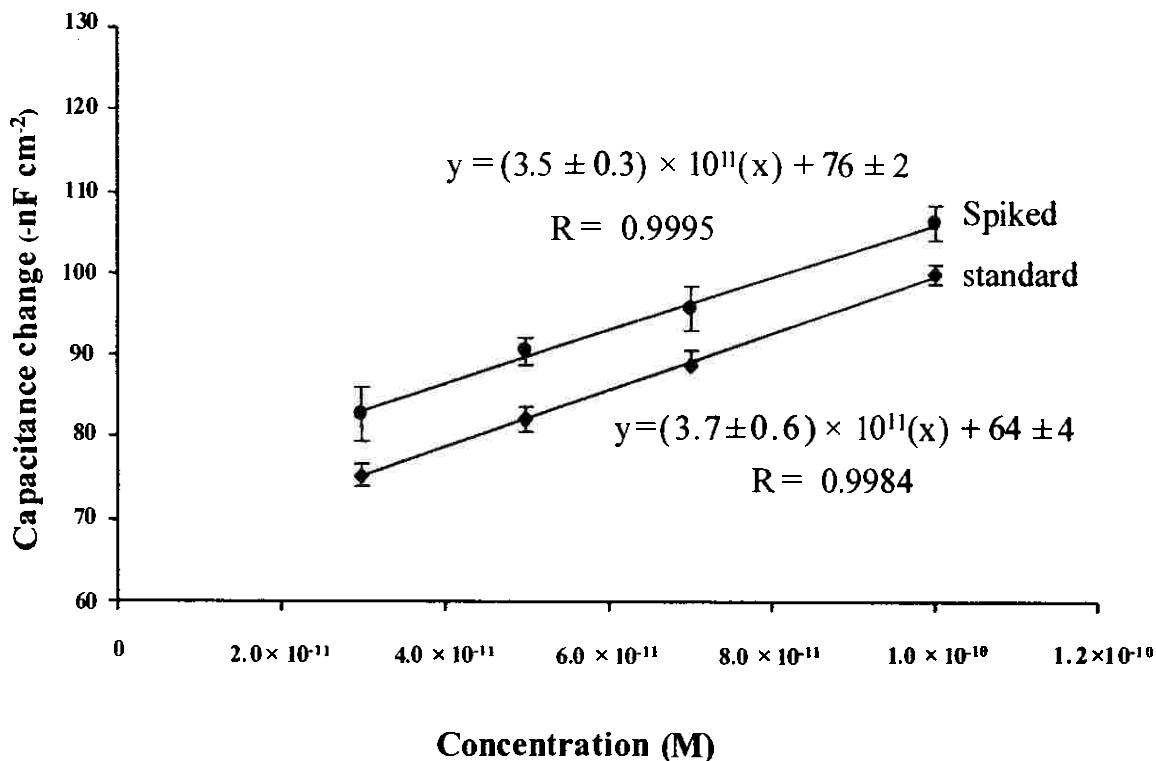
Figure 3.31 The standard curve and spiked curve for the study of matrices interference of sample 1 (dilution 10^7 times) (n=3).

3.2.7.2 Recovery

Percentage recovery was evaluated by addition method as in 3.2.7.1. Recoveries of five human serum samples were summarized in Table 3.6 Since the acceptable recovery in analytical analysis in the 1×10^{-4} M level is 90-107 % and RSD is $5.3 - 8$ % (Taverniers *et al.*, 2004). Therefore, recoveries for all samples are acceptable.

Table. 3.6 Percentage recovery of albumin in five human serum samples at concentration of fortification 3.0×10^{-4}, 5.0×10^{-4}, 7.0×10^{-4} and 10.0×10^{-4} M with dilution 10^{6} and 10^{7} times respectively (n=3).

Spiked concentration (M)	Sample 1 Detected ($\times 10^{-4}$ M)	Recovery (%)	Sample 2 Detected ($\times 10^{-4}$ M)	Recovery (%)	Sample 3 Detected ($\times 10^{-4}$ M)	Recovery (%)	Sample 4 Detected ($\times 10^{-4}$ M)	Recovery (%)	Sample 5 Detected ($\times 10^{-4}$ M)	Recovery (%)
Dilution 10^{6}										
3.0×10^{-4}	2.9±0.2	96±6	2.7±0.2	91±6	2.74±0.06	91±2	2.7±0.2	91±7	2.7±0.2	90±7
5.0×10^{-4}	4.7±0.2	94±4	4.60±0.05	92±1	4.6±0.2	92±4	4.75±0.06	95±1	4.8±0.2	96±4
7.0×10^{-4}	6.33±0.07	90±1	6.3±0.2	90±2	6.4±0.2	91±3	6.6±0.2	9±3	6.3±0.2	90±2
10.0×10^{-4}	9.8±0.3	98±3	9.6±0.43	96±4	9.6±0.3	96±3	9.7±0.4	97±4	9.8±0.3	98±3
Dilution 10^{7}										
3.0×10^{-4}	2.7±0.2	91±6	2.7±0.2	91±7	2.79±0.09	93±3	2.72±0.09	91±3	2.8±0.08	93±3
5.0×10^{-4}	4.5±0.2	91±4	4.7±0.3	93±6	4.7±0.2	94±4	4.8±0.3	97±5	5±0.1	100±3
7.0×10^{-4}	6.4±0.4	92±6	6.8±0.4	97±5	7.3±0.4	103±5	7.1±0.4	102±6	7.1±0.2	101±1
10.0×10^{-4}	9.5±0.3	95±3	9.6±0.4	96±4	10.0±0.2	100±2	9.9±0.5	99±5	9.5±0.7	95±7

3.2.8 Determination of albumin in human serum samples

For real sample analysis, in order to obtain more accurate results, the calibration curve was the plotted between capacitance change (-nF cm^{-2}) and concentration of HSA instead of the capacitance change (-nF cm^{-2}) and logarithm concentration of HSA. Concentration of HSA in the range of 1.0×10^{-11} to 1.0×10^{-9} M was investigated in a linear scale and was found to have two linear ranges, 1.0×10^{-11} to 1.0×10^{-10} M ($y = (2.5 \pm 0.2) \times 10^{-11}(x) + (31 \pm 1)$, R=0.9957) and 3.0×10^{-10} to 1.0×10^{-9} M ($y = (1.25 \pm 0.02) \times 10^{-11}(x) + (60.5 \pm 0.2)$, R = 0.9996) (Figure 3.30).
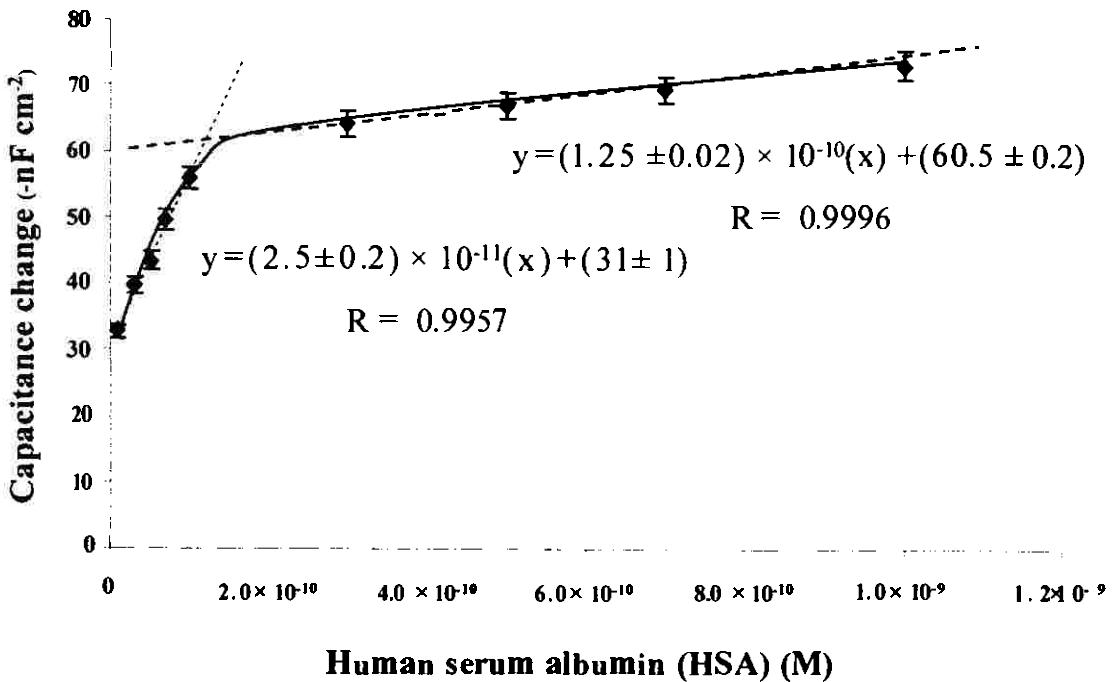
Figure 3.30 Calibration curve for relationship between capacitance change (-nF cm^{-2}) and concentration of HSA in the range of 1.0×10^{-11} to 1.0×10^{-9} M.

The determination of albumin in human serum samples were performed by calibration method using the concentration range 3.0×10^{-11} to 1.0×10^{-9} M. Human serum samples were diluted at 10^6 times for the calibration curve in the range of 3.0×10^{-10} to 1×10^{-9} and 10^7 times for 3.0×10^{-11} to 1.0×10^{-10} M. Four calibration curves were constructed, two for each range, and each calibration curve was used to analyze four human serum samples. Therefore totally sixteen

samples were analyzed. The concentration of HSA in sample was evaluated by comparing the response ($-nF \ cm^{-2}$) to the response of the standard HSA. The concentrations of albumin analyzed by capacitive immunosensor system and Albumin BCG method (results obtained from Songklanakarind Hospital) were shown in Table 3.7.

3.2.9 Method comparison

The results of 16 human serum samples obtained by a capacitive Immunosensor systemwere compared with albumin BCG method. Figure 3.31 shows the linear regression line plotted between the two method.

Concentrations of HSA determined by capacitive immunosensor system were lower than the results obtained from BCG method for all samples. Several authors have reported that BCG method can overestimate albumin concentration. This is because the lack of specificity of Bromocresal Green (BCG) since other proteins, particulary α-and β globulin in human sample, also bind to the dye (Cafray *et al.*, 2000; Stokol *et al.*, 2001).

Table 3.7 Cocentration HSA obtained by capacitive immunosensor and Albumin BCG method (results obtained from Songklanakarind Hospital).

Human serum samples	Capacitive immunosensor $(\times 10^{-4})$ (M)	Albumin BCG method $(\times 10^{-4}M)$	Difference	% Difference
Sample 1	5.5 ± 0.7	6.2	-0.7	- 11.3
Sample 2	3.9± 0.5	4.4	-0.5	- 11.4
Sample 3	3.6± 0.2	3.8	-0.2	- 5.2
Sample 4	7.17 ± 0.03	7.2	-0.03	- 0.4
Sample 5	4.8 ± 0.2	5.2	-0.4	- 7.7
Sample 6	5.5 ± 0.2)	5.7	-0.2	-3.5
Sample 7	6.2 ± 0.1	6.5	-0.3	-4.6
Sample 8	7.16± 0.06	7.4	-0.24	- 3.24
Sample 9	5.3 ± 0.3	5.6	-0.3	- 5.3
Sample 10	3.0±0.1	3.1	-0.1	- 3.2
Sample 11	3.3 ±0.1	3.4	-0.1	- 2.9
Sample 12	7.0± 0.2	7.2	-0.2	- 2.7
Sample 13	4.8± 0.2	5.7	-0.9	- 15.7
Sample 14	5.6± 0.2	6.3	-0.7	- 11
Sample 15	4.8 ± 0.1	5.0	-0.2	- 4
Sample 16	4.23 ± 0.06	4.7	-0.47	- 10
Average			-0.3 ± 0.2	- 6.4 ± 4.2

Difference = Capacitive immunosensor – Albumin BCG method

$$\% \text{ Difference} = \frac{\text{Capacitive immunosensor-Albumin BCG method}}{\text{Albumin BCG method}} \times 100$$

The figure shows a linear regression plot with y-axis labeled "Capacitive immunosensor ($\times 10^{-4}$ M)" ranging from 3.00 to 8.00, and x-axis labeled "Albumin BCG method ($\times 10^{-4}$ M)" ranging from 2.00 to 8.00. The equation shown is:

$$y = (0.97 \pm 0.1)\, x - (0.2 \pm 0.6)$$
$$R = 0.9827$$
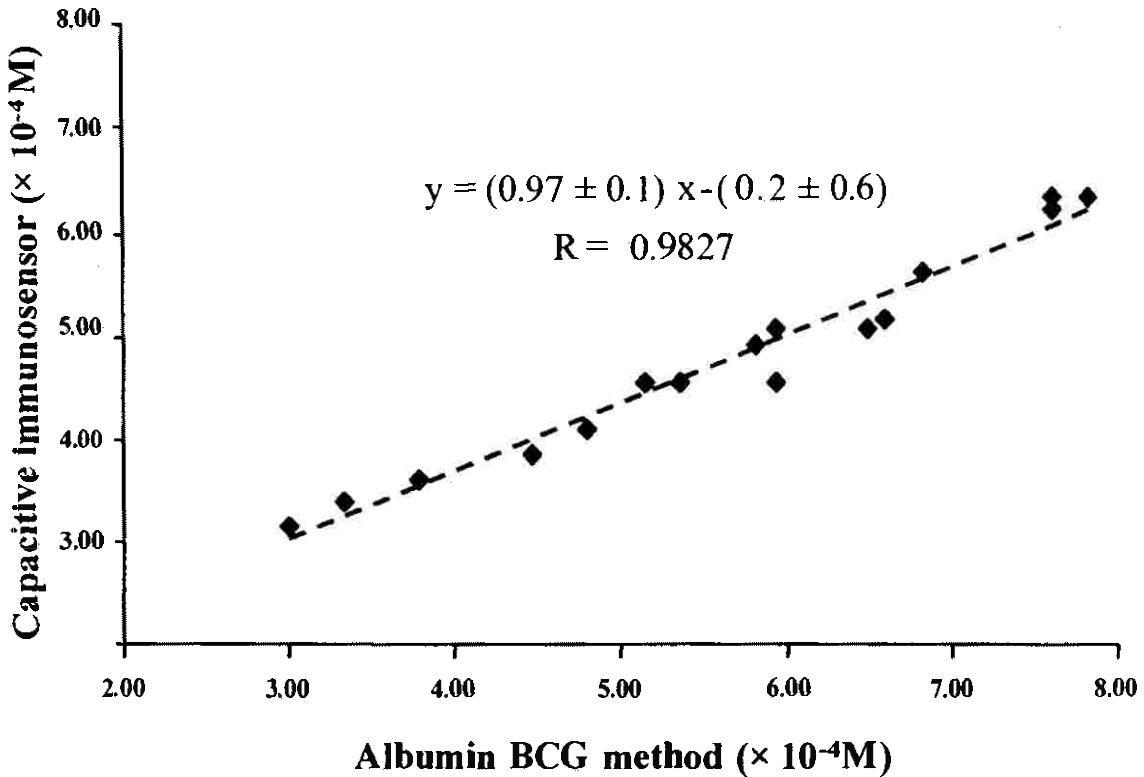
Figure 3.31 Linear regression line plotted between concentration of HSA obtained by capacitive immunosensor and Albumin BCG method.

It is not possible to apply a correction factor because of variation in difference between methods over the range of albumin value and the concentrations of α-and β globulin in patients ((Cafray *et al.*, 2000; Stokol *et al.*, 2001).

This study shows that thermally evaporated gold electrode can be used for the immobilization of anti-HSA and used as working electrode for the construction of capacitive immunosensor system with anti-HSA-HSA as an model study. The developed system was applied for the analysis of HSA in human serum samples. Concentrations of HSA determined by capacitive immunosensor system are lower than those obtained from Albumin BCG method. With a mass productive of the electrodes fabrication, these thin gold film can be used as disposable electrodes and could be apply to many class of biomolecules for biosensor construction.

CHAPTER4

CONCLUSIONS

Thin gold film electrodes were fabricated using sputtering and thermal evaporation techniques. These electrodes were tested in a label-free capacitive immunosensor system. Immobilization of biological molecules on the electrode surface was performed by self assembled monolayer (SAM) and electropolymerization of o-PD. Antibody to host cell protein (anti-HCP) and its antigen (HCP) was used as a model study to test the performance of sputtered gold electrodes and antibody to human serum albumin (anti-HSA) and its antigen (HSA) were used for thermally evaporated gold electrodes.

The electrodes fabricated by sputtering technique can be used for the immobilization of anti-HCP via SAM technique without any pretreatment steps. These electrodes were used as working electrodes for a capacitive immunosensor system to detect HCP. The capacitive measurement provided a linear dynamic range from 1.0×10^{-17} to 1.0×10^{-13} M with a limit of detection 8.0×10^{-18} M. The system can be reused up to 25 times. The capacitive immunosensor system was used to investigate the residual HCP impurities during purification processes and in final purified product of enzyme Lactate dehydrogenase (LDH) from *Escherichia coli (E. coli)* using immobilized metal affinity chromatography (IMAC). However, the concentrations HCP found in the purification process need to be analyzed further for their precision since the analysis of HCP in samples were only performed one time and anti-HCP can also bind to the other proteins (Eaton, 1995) which will give positive results, however, the concentrations of HCP in the samples are informative in order to investigate the trends for HCP releasing during purification process. The analytical performance of the developed system was compared to the other techniques as shown in Table 4.1. It can be seen that the capacitive immunosensor provides much better performance than Immunosrobent assay (Wan *et al.*, 2002) and Slot blot assay (Zhu *et al.*, 2005).

Thermal evaporation can also be used as an alternative technique for the fabrication of a thin film working electrode which are successfully used in capacitive immunosensor system with anti-HSA-HSA as a model study. AFM images of gold film electrode show good characteristic of surface properties. This electrode can be used without any surface pretreatment such as mechanical polishing and electrochemical treatment. Electropolymerization of o-PD can be used for anti-HSA immobilization via covalent coupling with glutaraldehyde. The modified electrodes, which is simple and rapid to prepare, when incorporated in a capacitive immunosensor system could provide high sensitivity and low detection limit (8.0×10^{-15}M). It is possible to apply this developed system for the analysis of HSA in other samples such as urine for the investigation of renal disease in diabetic patients. The normal concentration HSA in urine is about 2.9×10^{-7} M, whereas it can be up to 2.9 $\times 10^{-6}$ M in a heavy renal sick people (Sakti et $al.$, 2001). The electrode can be reused up to 30 times and this helps to reduce the cost of analysis. The developed system showed good performance for the determination of albumin in human serum samples. Table 4.2 shows the comparison of the analytical performance of the developed system to the other techniques for the determination of HSA. The capacitive immunosensor using thermally evaporated gold electrode provides wider linear range and lower detection limit when compared to the other capacitive immunosensor techniques which gold rod was employed (Hedström et $al.$, 2005; Wu et $al.$, 2005). This developed capacitive immunosensor system shows much better performance when compared to the other technique such as chemiluminescence (Aoyagi et $al.$, 2001), spectrofluorometric (Jiang et $al.$, 2004) and AOAO assay (Luo et $al.$, 1999).

On this basis, we suggest that the use of thin gold film electrodes fabricated by sputtering and thermal evaporation will provide an easy and low cost biosensor. Using sputtering technique, 100 electrodes can be fabricated at one time with 0.3 g of gold. The cost of each electrode is 3 Baht (include adhesion layer of chromium). The electrode immobilized with anti-HCP costs about 20 Baht. Since one electrode can be reused 25 times, the cost for each analysis is about 0.8 Bath. For thermal evaporation technique, 70 electrodes can be fabricated at one time with 0.4 g of gold. The fabrication cost of one electrode include the cost of chromium is about 5 Baht. Each electrodes immobilized with anti-HSA cost 29 Baht. One electrode can be

reused up to 30 times. Therefore, each analysis cost 0.97 Baht. Since both electrodes can be reused several times, the cost for each analysis is less than 1 Baht making it possible to use these electrodes as disposable. Moreover these electrodes could be applied to many classes of biological substance and mass production of this type of electrode is also a real possibility.

Table 4.1 Comparison of analytical performance for HCP analysis using difference techniques.

Analytical techniques	Analytical performance		References
	Linear dynamic range (ng mL^{-1})	Limit of detection (LOD) (ng mL^{-1})	
Immunoserbent assay	1-100	1 ng mL^{-1}	Wan *et al.*, 2002
Slot blot assay	61-1,562	6.1 ng mL^{-1}	Zhu *et al.*, 2005
Capacitive immunosensor	0.5 – 5,000	0.4 ng mL^{-1}	This work

Note: Molecular weight of HCP; 6-36 kDa (Zhu *et al.*, 2002); < 14 and > 100 kDa (Wan *et al.*, 2005) and 50 kDa (this work).

Table 4.2 Comparison of analytical performance for HSA analysis using difference techniques.

Analytical technique	Electrode type	Analytical performance		References
		Linear dynamic range (M)	Limit of detection (LOD) (M)	
Capacitive immunosensor	Gold rod	$2.7 \times 10^{-11} - 5.5 \times 10^{-8}$	2.4×10^{-11}	Wu et al., 2005
Capacitive imunosensor	Gold rod	$2.5 \times 10^{-11} - 2.5 \times 10^{-9}$	-	Hedström et al., 2005
Chemiluminescence	-	$0-1.5 \times 10^{-5}$	-	Aoyagi et al., 2001
Spectrofluorometric	-	$1.4 \times 10^{-5} - 5.1 \times 10^{-5}$	$.7 \times 10^{-9}$	Jiang et al., 2004
Albumin BCG method	-	$1.5 \times 10^{-4} - 1.1 \times 10^{-3}$	3.0×10^{-5}	Roche diagnostic, 2005
AOAO assay	-	$9.9 \times 10^{-9} - 5.9 \times 10^{-7}$	1.2×10^{-9}	Luo et al., 1999
Capacitive immunosensor	Thermally evaporated gold film	$1.0 \times 10^{-14} - 1.0 \times 10^{-9}$	8.0×10^{-15}	This work

References

Adilakshami, T. and Laine, R.O. 2002. Ribosomal protein S25 mRNA partners with MTF-1 and La to provide a p53-mediated mechanism for survival or death. *Journal of Biological Chemistry* 277:4147-51.

Aizawa, M. 1994. Immunosensors for clinical analysis. *Advances in Clinical Chemistry* **31**: 247-275.

Andersson, K., Hämäläinen, M. and Malmqvist, M. 1999. Identification an Optimization of Regeneration Conditions for Affinity-Based Biosensor Assays. A Multivariate Cocktail Approach. *Analytical Chemistry* **71**:2475-2481

Aoyagi, S., Iwata, T., Miyasaka, T., Sakai, K. 2001. Determination of human serum albumin by chemiluminescence immunoassay with luminal using a platinum-immobilized flow cell. *Analytica Chimica Acta* **436**: 103-108.

Bain, C.D. and Whitesides, G.M. 1988. Molecular-level control over surface order in self assembled monolayer films of thiols on gold. *Science* **24**: 62-63.

Bard, A.J. and Faulkner, L.R. 2001. Electrochemical methods; fundamentals and applications. New York, John Wiley & Sons, INC.

Bashar, S. A. (1998). Study of Indium Tin Oxide (ITO) for Novel Optoelectronic Devices Electronic Engineering London, KING'S COLLEGE LONDON, University of London. **Doctor of Philosophy**

Bechera, S and Raj, C.R. 2007. Self-assemble monolayer of thio-substiutued

nucleobases on gold electrode for the electroanalysis of NADH, ethanol and uric acid. *Sensor and Actuator B.* **128**: 31-38.

Berggren, C. and Johansson, G. 1997. Capacitance Measurements of Antibody-Antigen interaction in a flow system. *Analytical Chemistry* **69**; 3651-3657.

Berggren, C., Bjarnason, B. and Johansson, G. 1998. An immunological Interleukine 6 capacitive biosensor using perturbation with a potentiostatic step. *Biosensors and Bioelectronics* **13**: 1061-1068.

Bolanos-Garcia, V. M., Davies, O. R. 2006. Structural analysis and classification of native protein from E. colicommonly co-purified by immobilized metal affinity chromatography. *Biochimica et Biophysica Acta* **1760**: 1304-1313.

Bonal, C., Morel, J. P., Morel-Desrosiers, N.1996. Interactions between lanthanide cations and nitrate anions in water. Part I.—Effect of the ionic strength on the Gibbs energy, enthalpy and entropy of complexation of the neodymium cation *Journal of the Chemical Society, Faraday Transactions* 92, 4957- 4963.

Bontidean, I., Berggren, C., Johansson, G., Csoregi, E., Mattiasson, B., Lloyd, J. R., Jakeman, K. J. and Brown, N. L. 1998. Detection of heavy metal ions at femtomolar levels using protein-based biosensors. *Analytical Chemistry* **70**: 4162-4169.

Buck R.P. and Lindner, E. 1994. Recommendations for nomenclature of ion-selective electrodes (IUPAC Recommendations 1994). *Pure and Applied Chemistry.* **66**: 2527-2536.

Carfray, A., Patel, K., Whitaker, P., Garrick, P., Griffiths, G. J., Warwick, G. L. 2000. Albumin as an outcome measure in haemodialysis in patients: the effect of validation in assay method. *Nephrol Dial Transplant* **15**: 1819-1822.

Choi, J.-J., Kim, D.-Y., Park, G.-T. and Kim, H.-E. 2004. Effect of Electrode Configuration on Phase Retardation of PLZT Films Grown on Glass Substrate. *Communications of the American Ceramic Society* **87** (5): 950-952.

Choi, S., Choi, E. Y., Kim, D. J., Kim, J. H., Kim, T. S., Oh, S. W. 2004. A rapid, simple measurement of human albumin in whole blood osing fluorescence immunoassay (I). *Clinica Chimica Acta* **339**: 147-156.

Dai, Z. R., Pan, Z. W. and Wang, Z. L. 2003. Novel Nanostructures of Functional Oxides Synthesized by Thermal Evaporation. *Advanced Functional Materials* **13** (1): 9-24.

Doumas, B. T., Peters, T. 1997. Serum and urine albumin: a progress report on their measurement and clinical significance. *Clinical Chimica Acta* **258**: 3-20.

Eaton, L. C. 1995. Host cellcontaminant protein assay development for recombinant biopharmaceuticals. *Journal of Chromatography A* **705**: 105-114.

Engström, H. A., Andersson, P. O., Ohlson, S.2006. A label-free continuous total-internal-reflection-fluorescence-based immunosensor. *Analytical biochemistry* **357**: 159-166.

Eurachem Working Group, 1998. Fitness for Purpose of Analytical Methods: A Laboratory Guide to Method Validation and Related Topics Eurachem Guide, 1st English ed. 1.0. LGC (Teddington) Ltd.

Freudenberg, J., Schickfus, M. v. and Hunklinger, S. 2001. A SAW immunosensor for operation in liquid using a SiO$_2$ protective layer. *Sensors and Actuators B: Chemical* **76** (1-3): 147-151.

Fu, Y., Yuan, R., Tang, D., Chai, Y. and Xu, L. 2004. Study on the immobilization of anti-IgG on Au-colloid modified gold electrode via potentiometric immunosensor, cyclic voltammetry, and electrochemical impedance techniques. *Colloids and Surfaces B: Biointerfaces* **40**: 61-66.

Garjonyte, R. and Malinauskas, A. 1999. Amperometric glucose biosensor based on glucose oxidase immobilized in poly (o-phenylenediamine) layer. *Sensors and Actuators B: Chemical* **56** (1-2): 85-92.

Gebbert, A., Alvarez-Icaza, M., Stocklein, W. and Schmid, R.D. 1992. Real-time monitoring of immunochemical interactions with a tantalum capacitance flow-through cell. *Analytical Chemistry* **64**: 997-1003.

Gil, M, H., Sardinha, J.P., Vieira, M.T., Vivan, M., Costa, D., Rodrigues, C., Matysik, F.-M., Brett, O. 1999. Immobilization of glucose oxidase on thin-film gold electrodes produced by magnetron sputtering and their application in an electrochemical biosensor. *Biotechnology Techniques* **13**: 595-599.

Gizeli, E., Bender, F., Rasmusson, A., Saha, K,. Josse, F., Cernosek. 2003. Sensitivity of the acoustic waveguide biosensor to protein binding as a function of the wave guide properties. *Biosensors and Bioelectronic* **18**: 1399-1406.

Gobi, K. V., Iwasaka, H. and Miura, N. 2007. Self-assembled PEG monolayer based SPR immunosensor for label-free detection of insulin. *Biosensors and Bioelectronics* **22** (7):1382-1389.

Gobi, K. V., Tanaka, H., Shoyama, Y. and Miura, N. 2005. Highly sensitive regenerable immunosensor for label-free detection of 2,4-dichlorophenoxyacetic acid at ppb levels by using surface plasmon resonance imaging. *Sensors and Actuators B: Chemical* **111-112**: 562-571.

Guiducci, C., Stagni, C., Zuccheri,G., Bogliolo, A., Benini, L., Samor, B. and Riccò, B. 2004. DNA detection by integrable electronics. *Biosensors and Bioelectronics* **19**: 781–787.

Gustafasson, J. E. C.1976. Improve specificity of serum albumin dehtermination and estimation of "acute phase reactants" by use of the bromocresal green. *Clinical Chemistry* **22**: 616-622.

Hedström, M., Galaev, I. Yu. and Mattiasson, B. 2005. Continuous measurements of a binding reaction using a capacitive biosensor. *Biosensors and Bioelectronics* **21**: 41-48.

Halliwell, B. 1988. Albumin-an important extracellular antioxidant. *Biochmistry Pharmacology* **37**: 569-571.

Hock, B. 1997. Antibodies for immunosensors A review. *Analytica Chimica Acta* **347**, 177-186.

Hu, S.Q., Wu, Z.Y., Zhou, Y.M., Cao, Z.X., Shen, G.L. and Yu, R.Q. 2002. Capacitive immunosensor foe transferrin based on an o-aminobenzenthiol oligomer layer. *Analytical Chimica Acta* **458**: 297-304.

Janek, R.P., Fawcett, W.R. and Ulman, A.1997. Impedance spectroscopy of self-assembled monolayers on Au (III): evidence for complex double-layer

structure in aqueous at the potential of zero charge. *Journal of Physical Chemistry* **101**: 4550-4558.

Jedrzejewska-Szczerska, M., Bogdanowicz, R., Gnyba, M., Hypszer, R. and Kosmowski, B. B. 2008. Fiber-optic temperature sensor using low-coherence interferometry. *The European Physical Journal Special Topics* **154** (1): 107-111.

Jiang, D., Tang, J., Liu, B., Yang, P., Shen, X. and Kong, J. 2003. Covalently coupling the antibody on an amine-self-assembled gold surface to probe hyaluronan-binding protein with capacitance measurement. *Biosensors and Bioelectronics* **18**: 1183-1191.

Karalemas, I. D., Georgiou, C. A., Papastathopoulos. 2000. Construction of L-lysine biosensor by immobilizing lysine oxidase on a gold-poly (o-phenylenediamine) electrode. *Talanta* **53**: 391-402.

Kelly, P. J., Arnell, R. D. 2000. Magnetron sputtering: a review of recent developments and applications. *Vacuum* **56**: 159-172.

Lepesheva, G. I., Azeva, T. N., Knyukshto, V. N., Chashchin, V. L. and Usanov, S. A. 2000. A model of optical immunosensor for hemoproteins based on Langmuir–Blodgett films of FITC-labelled immunoglobulin G. *Sensors and Actuators B: Chemical* **68** (1-3): 27-33.

Liang, W.-B., Yuan, R., Chai, Y.-Q., Li, Y. and Zhuo, Y. 2008. A novel label-free voltammetric immunosensor for the detection of a-fetoprotein using functional titanium dioxide nanoparticles. *Electrochimica Acta* **53** (5): 2302-2308.

Limbut, W. 2006. Affinity Biosensor Using Electrochemical Detection Principle.

Doctoral Thesis of Philosophy in Chemistry Prince of Songkla University, Thailand.

Limbut, W., Kanatharana, P., Mattiasson, B., Asawatreratanakul, P. and Thavarungkul, P. 2006. A comparative study of capacitive immunosensors based on self-assembled monolayers formed thiourea, thioctic acid, and 3-mercaptopropionic acid. *Biosensors & Bioelectronics* **22**: 233-240.

Long, G and Winefordner, J.D. 1982. Limit of Detection. *Analytical Chemistry* **55**: 712A-724A.

Lund, J., Dong, J, Deng, Z., Mao, C., Parviz, B. A. 2006. Electrical conduction in 7 nm wires constructed on λ-DNA. *Nanotechnology* **17**: 2752-2757.

Luppa, P.B., Sokoll, L.J. and Chan, D.W. 2001. Review: Immunosensors-principles and applications to chemistry. *Clinica Chimica Acta* **314**: 1-26.

Miller, J.C. and Miller, J.N., 1993. Statistics for Analytical Chemistry, third edition. Simon & Schuster International Group, West Sussex.

Mirsky, V.M., Riepl, M. and Wolfbeis, O.S. 1997. Capacitive monitoring of protein immobilization and antigen/antibody reactions on monomolecular alkylthiol films on gold electrodes. *Biosensor and Bioelectronics* **12**: 977-989.

Miyoshi, N., Tuziuti, T., Yasui, K., Iida, Y., Shimizu, N., Riesz, P. and Sostaric, J. Z. 2008. Ultrasound-induced cytolysis of cancer cells is enhanced in the presence of micron-sized alumina particles. *Ultrasonics Sonochemistry* **15** (5): 881-890.

O'Regan, T. M., O'Riordan, L. J., Pravda, M., O'Sullivan, C. K. and Guilbault, G. G. 2002. Direct detection of myoglobin in whole blood using a disposable amperometric immunosensor. *Analytica Chimica Acta* **460** (2): 141-150.

Park, J., Kurosawa, S., Takai, M. and Ishihara, K. 2007. Antibody immobilization to phospholipid polymer layer on gold substrate of quartz crystal microbalance immunosensor. *Colloids and Surfaces B: Biointerfaces* **55** (2): 164-172.

Park, S-M. and Yoo, J-S. 2003. Electrochemical impedance spectroscopy for better electrochemical measurements. *Analytical Chemistry*, November 1:455A-461A.

Peter, T. 1996. All about albumin: Biochemistry, Genetics, and Medical Applications. San Diego, CA: Academic Press.

Pierson, J. F., Wiederkehr, D. and Billard, A. 2005. Reactive magnetron sputtering of copper, silver, and gold. *Thin Solid Films* **478** (1-2): 196-205.

Ramanaviciene, A. and Ramanavocous, A. 2004. Molecularly imprinted polypyrrole-based synthetic receptor for direct detection of bovine leukemia virus glycoproteins. *Biosensors and Bioelectronics* **20**: 1076-1082.

Rathore, A. S., Sobacke, S. E., Kocot, T. J., Morgan, D. R., Dufield, R. L., Mozier, N. M. 2003. Analysis of residual host cell proteins and DNA in process streams of a recombinant protein product expressed in *Escherichia coli* cells. *Journal of Pharmaceutical and Biomedical Analysis* **32**: 1199-1211.

Rehacek, V., Novotny, I., Tvarozek, V., Riepl, M., Hirsch, T., Mass, M., Schweiss,

R., Mirsky, V.M. Wolfbeis, O.S. 1998. ASDAM '98, 2nd International Conference on Advance Semiconductor Device and Microsystems, Smolenice Castle, Slovakia. 0-7 October.

Rickert, J., Göpel, W., Beck, W., Jung, G. and Heiduschka, P. 1996. A "mixed" self-assembled monolayer for an impedimetric immunosensor. *Biosensors & Bioelectronics* **11**: 757-768.

Sakti, S.P., Hauptmann, P., Zimmermann, B., Bühling, F., Ansorge, S. 2001. Disposable HAS QCM-immunosensor for practical measurement in liquid. *Sensors and Actuators B* **78**: 257-262.

Sangpour, P., Akhavan, O., Moshfegh, A. Z. and Roozbehi, M. 2007. Formation of gold nanoparticles in heat-treated reactive co-sputtered Au-SiO$_2$ thin films. *Applied Surface Science* **254** (1): 286-290.

Sharma, S.K., Sehgal, N. and Kumar, A. 2003. Biomolecules for development of biosensors and their applications. *Current Applied Physics* **3**: 307-316.

Stokol, T., Tarrant, J.M., Scarlett, J.M. 2001. 2001. Overestimation of Canine Albumin Concentration with Bromocresal green Method in Heparinized Plasma Samples. 2001. *Veterinary Clinical pathology* **30**: 170-177.

Spadavecchia, J., Manera, M. G., Quaranta, F., Siciliano, P., Rella, R. 2005. Surface plasmon resonance imaging of DNA based biosensors for potential applications in food analysis. *Biosensors and bioelectronics* **21**: 894-900.

Swartz, M.E. and Krull, I.S. 1997. Analytical method development and validation. New York, Marcel Dekker, Inc.

Tang, D., Yuan, R., Chai, Y., Fu, Y., Dai, J., Liu, Y. and Zhong, X. 2005. New amperometric and potentiometric immunosensors based on gold nanoparticles/tris(2,2'-bipyridyl)cobalt(III) multilayer films for hepatitis B surface antigen determinations. *Biosensors and Bioelectronics* **21**. 539–548.

Taverniers, I., Loose, M. D., and Bockstaele, E. V. 2004. Trends in quality in the analytical laboratory. II. Analytical method validation and quality assurance. *Trends in Analytical Chemistry* **23**: 535-552.

Thavarungkul, P., Dawan, S., Kanatharana, P. and Asawatreratanakul, P. 2007. Detecting penicillin G in milk with impedimetric label-free immunosensor. *Biosensors and Bioelectronics* **23**(5): 688-694.

Thévenot, D.R., Toth, K., Durst, R.A. and Wilson, G.S. 2001. Electrochemical biosensors: recommended definitions and classification. *Biosensors & Bioelectronics* **16**: 121-131.

Thévenot, D.R., Toth, K., Durst, R.A. and Wilso, G.S. 1999. Electrochemical biosensors: recommended definitions and classification. *Pure and Applied Chemistry* **77**: 2333-2348.

Townsend, P. D. 1976. Defect Formation by Multiphoton Absorption. *Physical Review Online Archive* **36** (14): 827-829.

Turner, A. P. F. Chen., B., Piletsky, S.1999. In vitro diagnostic in diabetes: meeting the challenge. *Clinical chemistry* **45** (9):1596-1601.

van der Merwe, P.A. 2000. Surface Plasmon Resonance. In Protein-Ligand interactions: A Practical Approach, 828 pp. Oxford University Press.

Wan, M., Wang, Y., Rabideau, S., Moreadith, R., Schrimsher, J., Conn, G. 2002. An enzyme-linked immunosorbent assay for host cell protein contaminants in recombinant PEGylated staphylokinase mutant SY161. *Journal of Pharmaceutical and Biomedical analysis* **2002**. 953-963.

Wang, J. 2000. *Analytical Electrochemitry* (2nd ed). New York: John, Wiley & Sons.

Wrobel, N. 2001. Optimization of Interfaces for Genosensors Based on Thiol Layers on Gold Films. Diploma Thesis of Chemie und Pharmazie der Universität Regensburg, Regensburg University, Regensburg.

Xu, F. 2006. Surface plasmon optical detection of β- lactamase binding to different Interfacial matrices combined with fiber optic absorbance spectroscopy for enzymatic activity assays. *Biointerphases* **1** (2): 73-81.

Xu, Q., Guo, R.-X., Wang, C.-Y. and Hu, X.-Y. 2007. Application of activated glassy carbon electrode for the detection of nuciferine in lotus leaves. *Talanta* **73** (2): 262-268.

Yagiuda, K., Hemmi, A., Ito, S. and Asano, Y. 1996. Development of a conductivity-based immunosensor for sensitive detection of methamphetamine (stimulant drug) in human urine. *Biosensors and Bioelectronics* **11**: 703-707.

Yang, D.F., Wilde, C.P. and Morin, M. 1996. Electrochemical desorption and adsorption of nonyl-mercaptan at gold sigle crystal electrode surface. *Langmuir* **12**: 6570-6577.

Yang, J., Sandhu, P., Liang, W., Xu, C.-Q. and Li, Y. 2007. Label-Free Fiber Optic

Biosensors With Enhanced Sensitivity. *Ieee Journal of Selected Topics in Quantum Electronics* **13** (6): 1991-1696.

Yang, Z., Gonzalez-Cortes, A., Jourquin, G., Vire, J.C., Kauffmann, J.M., Delplancke, J.L. 1995. Analytical application of self assembled monolayers on gold electrodes: Critical importance of surface pretreatment. *Biosensors and Bioelectronics* **10**, 789-795.

Yano, J. and Nagaoka, T. 1996. Ion pairing between dissolved poly(o-phenylenediamine) and halogenide ions. *Journal of Electroanalytical Chemistry* **410** (2): 213-217.

Yin, F. 2004. Capacitive sensors using electropolymerized o-phenylenediamine film dope with ion-pair complex as selective elements for the determination of pentoxyverine. Talanta 63: 641-646.

Yuan, R., Zhang, L., Li, Q., Chai, Y. and Cao, S. 2005. A label-free amperometric immunosenor based on multi-layer assembly of polymerized o-phenylenediamine and gold nanoparticles for determination of Japanese B encephalitis vaccine. *Analytica Chimica Acta* **531** (1): 1-5.

Yuan, R., Tang, D., Chai, Y., Zhong, X., Liu, Y. and Dai, J. 2004. Ultrasensitive potentiometric immunosensor based on SA and OCA techniques for immobilization of HBsAb with colloidal Au and polyvinyl butyral as matrixes. *Langmuir* **20**: 7240-7245.

Zhang L., Yuan, R., Huang, X., Chai, Y., Tang, D. and Cao, S. 2005. A new label-free amperometric immunosenor for rubella vaccine. *Anayticall Bioanayticall Chemistry* **381**: 1036-1040.

Zhang, S., Berguiga, L., Elezgaray, J., Roland, T., Faivre-Moskalenko, C., Argoul, F. 2007. Surface plasmon resonance characterization of thermally evaporated thin gold films. *Surface science* **xxx**: xxx-xxx.

Zhang, S., Dong, D., Gan, L., Liub, Z. and Huanga, C. 2001. Photoelectric response of a gold electrode modiÐed with self-assembled monolayers of pyrrolidinofullerenes. *New Journal of Chemistry* **25** (4): 606-610.

Zhu, D., Saul, A. J., Miles, A, P. 2005. A quantitative slot blot assay for host cell protein impurities in recombinant proteins expressed in E. coli. *Journal of Immunological Methods* **306**: 40-50.

Vitae

Name   Mr. Kosin Teeparuksapun

Student ID   4822007

Education Attainment

Degree	Name of Institution	Year of Graduation
Bachelor of Science (Chemistry)	Prince of Songkla University	2005

Scholarship Awards during Enrolment

1. The development and Promotion of Science and Technology Talents Project (DPST)

2. The Center for Innovation in Chemistry: Postgraduate Education and Research Program in Chemistry (PERCH-CIC), Commission on Higher Education, Ministry of Education.

List of Publications and Proceedings

Poster Presentations

1. Kosin Teeparuksapun, Apon Numnuam, Proespichaya Kanatharana and Panote Thavarungkul. "Comparative Study of Enzyme Reactor Column and Modified Enzyme Electrode for Glucose Biosensor". The International Conference on BioNanotechnology: A New Chapter of Life at Biothailand: Biotechnology Challenges in the 21st Century. The Queen Sirikit National Convention Center (QSNCC), Bangkok, Thailand. 2nd -5th November, 2005.

2. Kosin Teeparuksapun, Chongdee Thammakhet, Warakorn Limbut, Suchera Loyprasert, Proespichaya Kanatharana and Panote Thavarungkul. "PDMS microfluidic Chip for Amperometric glucose biosensor". The 5th PERCH-CIC Annual Scientific Congress (PERCH-CIC Congress V), Jomtien Palm Beach Resort, Pattaya, Thailand. 6th -9th May, 2007.